

1           **Ice, Cloud, and Land Elevation Satellite 2 (ICESat-2)**  
2  
3           **Algorithm Theoretical Basis Document (ATBD)**  
4                   **for**  
5           **Land - Vegetation Along-Track Products (ATL08)**

6  
7           **Contributions by Land/Vegetation SDT Team Members**  
8                   **and ICESat-2 Project Science Office**

9           **(Amy Neuenschwander, Katherine Pitts, Benjamin Jelley, John Robbins,**  
10           **Jonathan Markel, Sorin Popescu, Ross Nelson, David Harding, Dylan**  
11           **Pederson, Brad Klotz, and Ryan Sheridan)**

12  
13                   **ATBD prepared by**  
14                   **Amy Neuenschwander**

15  
16                           **01 July 2022**  
17           **(This ATBD Version corresponds to release 006 of the ICESat-2 ATL08**  
18                   **data)**

19  
20           **Content reviewed: technical approach, assumptions, scientific soundness,**  
21                   **maturity, scientific utility of the data product**

22  
23                   **This document may be cited as:**

24           Neuenschwander, A., K. Pitts, B. Jelley, J. Robbins, J. Markel, S. Popescu, R. Nelson,  
25           D. Harding, D. Pederson, B. Klotz, and R. Sheridan (2022). *Ice, Cloud, and Land*  
26           *Elevation Satellite (ICESat-2) Project Algorithm Theoretical Basis Document (ATBD) for*  
27           *Land - Vegetation Along-Track Products (ATL08), Version 6.* ICESat-2 Project, DOI:  
28           10.5067/8ANPSL1NN7YS.

29 **ATL08 algorithm and product change history**  
 30

ATBD Version	Change
2016 Nov	Product segment size changed from 250 signal photons to 100 m using five 20m segments from ATL03 (Sec 2)
2016 Nov	Filtered signal classification flag removed from classed_pc_flag (Sec 2.3.2)
2016 Nov	DRAGANN signal flag added (Sec 2.3.5)
2016 Nov	Do not report segment statistics if too few ground photons within segment (Sec 4.14 (3))
2016 Nov	Product parameters added: h_canopy_uncertainty, landsat_flag, d_flag, delta_time_beg, delta_time_end, night_flag, msw_flag (Sec 2)
2017 May	Revised region boundaries to be separated by continent (Sec 2)
2017 May	Alternative DRAGANN parameter calculation added (Sec 4.3.1)
2017 May	Set canopy flag = 0 when <i>L-km</i> segment is over Antarctica or Greenland regions (Sec <b>Error! Reference source not found.</b> (1))
2017 May	Change initial canopy filter search radius from 3 m to 15 m (Sec 4.8 (6))
2017 May	Product parameters removed: h_rel_ph, terrain_thresh
2017 May	Product parameters added: segment_id, segment_id_beg, segment_id_end, dem_flag, surf_type (Sec 2)
2017 July	Urban flag added (Sec 2.4.20)
2017 July	Dynamic point spread function added (Sec 4.10 (6))
2017 July	Methodology for processing <i>L-km</i> segments with buffer added (Sec 4.1 (2), Sec <b>Error! Reference source not found.</b> )
2017 July	Revised alternative DRAGANN methodology (see <del>bolded text</del> in Sec 4.3.1)
2017 July	Added post-DRAGANN filtering methodology (Sec 4.6)
2017 July	Updated SNR to be estimated from superset of ATL03 and DRAGANN found signal used for processing ATL08 (Sec 2.5.18)
2017 September	More details added to DRAGANN description (Sec 4.3), and corrections to DRAGANN implementation (Sec 3.1.1, Sec 4.3 (9))
2017 September	Added Appendix A - very detailed DRAGANN description
2017 September	Revised alternative DRAGANN methodology (see bolded text in Sec 4.3.1)
2017 September	Clarified SNR calculation (Sec 2.5.18, Sec 4.3 (18))
2017 September	Added cloud flag filtering option (Sec <b>Error! Reference source not found.</b> )

2017 September	Added top of canopy median surface filter (Sec 3.5 (a), Sec 4.9 (3), Sec 4.11 (1-3))
2017 September	Modified 500 canopy photon segment filter (Sec 3.5 (c), Sec 4.11 (6))
2017 November	Added solar_azimuth, solar_elevation, and n_seg_ph to Reference Data group; parameters were already in product (Sec 2.4)
2017 November	Specified number of ground photons threshold for relative canopy product calculations (Sec 4.15 (2)); no number of ground photons threshold for absolute canopy heights (Sec 4.15.1 (1))
2017 November	Changed the ATL03 signal used in superset from all ATL03 signal (signal_conf_ph flags 1-4) to the medium-high confidence flags (signal_conf_ph flags 3-4) (Sec 3.1, Sec 4.3 (17))
2017 November	Removed Date parameter from Table 2.4 since UTC date is in file metadata
2018 March	Clarified that cloud flag filtering option should be turned off by default (Sec <b>Error! Reference source not found.</b> )
2018 March	Changed h_diff_ref QA threshold from 10 m to 25 m (Table 5.2)
2018 March	Added absolute canopy height quartiles, canopy_h_quartile_abs ( <i>Later removed</i> )
2018 March	Removed psf_flag from main product; psf_flag will only be a QAQC alert (Sec 5.2)
2018 March	Added an Asmooth filter based on the reference DEM value (Sec 4.5 (4-5))
2018 March	Changed relief calculation to 95 <sup>th</sup> – 5 <sup>th</sup> signal photon heights. (Sec 4.5 (6))
2018 March	Adjusted the Asmooth smoothing methodology (Sec 4.5 (8))
2018 March	Recalculate the Asmooth surface after filtering outlying noise from signal, then detrend signal height data (Sec 4.6 (3-4))
2018 March	Added option to run alternative DRAGANN process again in high noise cases (Sec 4.3.3)
2018 March	Changed global land cover reference to MODIS Global Mosaics product (Sec 2.4.16)
2018 March	Adjusted the top of canopy median filter thresholds based on SNR (Sec 4.11 (1-2))
2018 March	Added a final photon classification QA check (Sec 4.13, Table 5.2)
2018 March	Added slope adjusted terrain parameters ( <i>Later removed</i> )
2018 June	Replaced slope adjusted terrain parameters with terrain best fit parameter (Sec 2.1.14, 4.14 (2.e))
2018 June	Clarified source for water mask (Sec 2.4.18)
2018 June	Clarified source for urban mask (Sec 2.4.20)

2018 June	Added expansion to the terrain_slope calculation (Sec 4.14)
2018 June	Removed canopy_d_quartile
2018 June	Removed canopy_quartile_heights and canopy_quartile_heights_abs, replaced with canopy_h_metrics (Secs 2.2.3, 4.15 (6), 4.15.1 (5))
2018 *** draft 1	Delta_time specified as mid-segment time, rather than mean segment time (Sec 2.4.7)
2018 *** draft 1	QA/QC products to be reported on a per orbit basis, rather than per region (Sec 5.2)
2018 *** draft 1	Added more detail to landsat_flag description (Sec <b>Error! Reference source not found.</b> )
2018 *** draft 1	Added psf_flag back into ATL08 product, as it is also needed for the QA product (Sec 2.5.12)
2018 *** draft 1	Specified that the sigma_h value reported here is the mean of the ATL03 reported sigma_h values (Sec 2.5.7)
2018 *** draft 1	Removed n_photons from all subgroups
2018 *** draft 1	Better defined the interpolation and smoothing methods used throughout: <ul style="list-style-type: none"> <li>• <b>Error! Reference source not found.</b> (4): Interpolation – nearest</li> <li>• 4.5 (5): Interpolation – PCHIP</li> <li>• 4.5 (8): Smoothing – moving average</li> <li>• 4.6 (3): Interpolation – PCHIP</li> <li>• 4.6 (3): Smoothing – moving average</li> <li>• 4.7 (10): Smoothing – moving average</li> <li>• 4.7 (11): Interpolation – linear</li> <li>• 4.7 (12): Smoothing – moving average</li> <li>• 4.7 (13): Interpolation – linear</li> <li>• 4.7 (14): Smoothing – moving average</li> <li>• 4.7 (15): Smoothing – Savitzky-Golay</li> <li>• 4.7 (16): Interpolation – linear</li> <li>• 4.7 (21): Interpolation – PCHIP</li> <li>• 4.9 (10): Interpolation – linear</li> <li>• 4.10 (all): Smoothing – moving average</li> <li>• 4.10 (6.b): Interpolation – linear</li> <li>• 4.11 (1.a): Interpolation – linear</li> <li>• 4.11 (1.c): Smoothing – lowess</li> <li>• 4.11 (4): Interpolation – PCHIP</li> <li>• 4.11 (7): Interpolation – PCHIP</li> <li>• 4.11 (9): Smoothing – moving average</li> <li>• 4.14 (2.e.i.1): Interpolation – linear</li> </ul>
2018 *** draft 1	Added ref_elev and ref_azimuth back in (it was mistakenly removed in a previous version; Secs 2.5.3, 2.5.4)
2018 *** draft 1	Clarified wording of h_canopy_quad definition (Sec 2.2.18)

2018 *** draft 1	Updated segment_snowcover description to match the ATL09 snow_ice parameter it references (Sec 2.4.19) and added product reference to Table 4.2
2018 *** draft 1	Added ph_ndx_beg (Sec 2.5.22); parameter was already on product
2018 *** draft 1	Added dem_removal_flag for QA purposes (Sec 2.4.13; Table 5.2)
2018 *** draft 2	Reformatted QA/QC trending and trigger alert list into a table for better clarification (Table 5.3)
2018 *** draft 2	Replaced n_photons in Table 5.2 with n_te_photons, n_ca_photons, and n_toc_photons
2018 *** draft 2	Removed beam_number from Table 2.5. Beam number and weak/strong designation within gtx group attributes.
2018 *** draft 2	Clarified calculation of h_te_best_fit (Sec 4.14 (2.e))
2018 *** draft 2	Changed h_canopy and h_canopy_abs to be 98 <sup>th</sup> percentile height (Table 2.2, Sec 2.2.5, Sec 2.2.6, Sec 4.15 (4), Sec 4.15.1 (3))
2018 *** draft 2	Separated h_canopy_metrics_abs from h_canopy_metrics (Table 2.2, Sec 2.2.3, Sec 4.15.1 (5))
2018 October	Removed 99 <sup>th</sup> percentile from h_canopy_metrics and h_canopy_metrics_abs (Table 2.2, Sec 2.2.3, Sec 2.2.4, Sec 4.15 (4), Sec 4.15.1 (5))
2018 December	Renamed and reworded Section 4.3.1 to better indicate that the DRAGANN preprocessing step is not optional
2018 December	Specified that DRAGANN should use along-track time, and added time rescaling step (Sec 4.3 (1 - 4))
2018 December	Added DRAGANN changes made to better capture sparse canopy in cases of low noise rates (Sec 4.3, Appendix A)
2018 December	Made corrections to DRAGANN description regarding the determination of the noise Gaussian (Sec 3.1.1, Sec 4.3)
2018 December	Removed h_median_canopy and h_median_canopy_abs, as they are equivalent to canopy_h_metrics(50) and canopy_h_metrics_abs(50) (Table 2.2, Sec 4.15 (5), Sec 4.15.1 (4))
2018 December	Removed the requirement that > 5% ground photons required to calculate relative canopy height parameters (Table 2.2, Sec 4.15 (2))
2018 December	Added canopy relative height confidence flag (canopy_rh_conf) based on the percentage of ground and canopy photons in a segment (Table 2.2, Sec 4.15 (2))
2018 December	Added ATL09 layer_flag to ATL08 output (Table 2.5, Table 4.2)
2019 February	Adjusted cloud filtering to be based on ATL09 backscatter analysis rather than cloud flags (Sec 4.1)

2019 March 5	Updated ATL09-based product descriptions reported on ATL08 product (Secs 2.5.13, 2.5.14, 2.5.15, 2.5.16)
2019 March 5	Updated cloud-based low signal filter methodology, and moved to first step of ATL08 processing (Sec 4.1)
2019 March 13	Replace canopy_closure with new landsat_perc parameter (Table 2.2, Sec <b>Error! Reference source not found.</b> )
2019 March 13	Change ATL08 product output regions to match ATL03 regions (Sec 2), but keep ATL08 regions internally and report in new parameter atl08_regions (Table 2.4, Sec 2.4.22)
2019 March 13	Add methodology for handling short ATL08 processing segments at the end of an ATL03 granule (Sec 4.2), and output distance the processing segment length is extended into new parameter last_seg_extend (Table 2.4, Sec 2.4.23)
2019 March 13	Add preprocessing step for removing atmospheric and ocean tide corrections from ATL03 heights ( <i>Later removed</i> )
2019 March 27	Remove preprocessing step for removing atmospheric and ocean tide corrections from ATL03 heights, since those values are now removed from the ATL03 photon heights.
2019 March 27	Replaced ATL03 region figure with corrected version (Figure 2.2)
2019 March 27	Specified that at least 50 classed photons are required to create the 100 m land and canopy products (Secs 2, 4.14(1), 4.15(1))
2019 March 27	Clarified that any non-extended segments would report a land_seg_extend value of 0 (Sec 4.2, Sec 2.4.23)
2019 April 30	Fixed the error in Eqn 1.4 for the sigma topo value
2019 May 13	Specified for cloud flag carry-over from ATL09 that ATL08 will report the highest cloud flag if an 08 segment straddles two 09 segments. (Section 2.5)
2019 May 13	Changed parameter cloud_flag_asr to cloud_flag_atm since the cloud_flag_asr is likely not to work over land due to varying surface reflectance (Sec, 2.5)
2019 May 13	Add ATL09 parameter cloud_fold_flag to the ATL08 data product for future qa/qc checks for low clouds. (Secs, 2.5)
2019 May 13	Clarification on the calculation of gradient for slope that feeds into the calculation of the point spread function (Sec 4.11)
2019 July 8	Changed Landsat canopy cover percentage to 3 % (from original value of 5%) (Section 4.4)
2019 July 8	Added a QA method for DRAGANN flags to help remove false positives (now Section 4.3.1)
2019 July 8	Set the window size to 9 rather than SmoothSize for the final ground finding step. (Section 4.11 and 4.12)
2019 July 8	Added a brightness flag to land segments. (Section 2.4.21)

2019 November 12	Added subset_te_flag to (Section 2.1) which indicate 100 m segments that are populated by less than 100 m worth of data
2019 November 12	Added subset_can_flag (section 2.2) which indicate 100 m segments that are populated by less than 100 m worth of data
2020 January 5	Clarified the interpolation of values (latitude, longitude, delta time) when the 100 m segments are populated by less than 100 m worth of data. (Section 2.4.3 and 2.4.4)
2020 January 13	Fine-tuned the methodology to improve ground finding by first histogramming the photons to improve detecting the ground in cases of dense canopy. (Section 4.8)
2020 January 13	Updated ATL08 HDF5 file organization figure in Section 2.1
2020 February 14	Added sentence to avoid ATL03 data having a degraded PPD flag to beginning of Section 4
2020 February 14	Added documentation for removing signal photons due to cloud contamination by checking the reference DEM to beginning of Section 4
2020 February 14	Added full saturation flag and near saturation flag from ATL03 to ATL08 data product to Section 2.
2020 February 14	Added statement to clarify handling of remaining geosegments that do not fit within a 100 m window at the end of a 10-km processing window in Section 4.2
2020 April 15	Added ph_h parameter to photon group on data structure. ph_h is the photon height above the interpolated ground surface.
2020 May 15	Added sat_flag which is derived from the ATL03 product. The saturation flag indicates that the ATL08 segment experienced some saturation which is often an indicator for water
2020 May 15	Canopy height metrics (relative and absolute heights) were expanded to every 5% ranging from 5 - 95%.
2020 May 15	The Landsat canopy cover check to determine whether the algorithm should search for both ground and canopy or just ground has been disabled. Now the ATL08 algorithm will search for both ground and canopy points everywhere.
2020 June 15	Corrected the calculation of the absolute canopy heights
2020 June 15	Changed the search radius for initial top of canopy determination (Section 4.9)
2020 September 1	Incorporate the quality_ph flag from ATL03 into the ATL08 workflow (beginning of Section 4)
2020 September 1	Added the calculation of Terrain photon rate (photon_rate_te) for each ATL08 segment to the land product (Section 2.1.16)

2020 September 1	Added the calculation of canopy photon rate (photon_rate_can) for each ATL08 segment to the land product (Section 2.2.26)
2020 September 1	Changed the k-d tree search radius for the top of canopy from 15 m to 100 m. Section 4.9.6
2020 September 15	Added new parameter for terrain heights (h_te_rh25) which represents the height of the 25% of ground cumulative distribution.
2021 March 15	Added terrain_best_fit_geosegment (h_te_best_fit_20m) parameter to the data product. 20 m estimate of best fit terrain height
2021 March 15	Added canopy_height_geosegment (h_canopy_20m) to the data product. 20 m estimate of relative canopy height
2021 March 15	Added latitude_20m to the data product.
2021 March 15	Added longitude_20m to the data product
2021 March 15	Updated the urban_flag parameter. Inclusion of the DLR Global Urban Footprint (GUF) as a potential indicator of man-made/built structures. Section 2.4.20
2021 March 15	Updated the Segment_landcover with Copernicus. Replace the MODIS landcover value with the landcover classification from the 100 m Copernicus landcover. Section 2.4.16
2021 March 15	Added the Segment_Woody_Vegetation_Fractional_cover. Inclusion of a woody vegetation fraction cover derived from the 2019 Copernicus fractional cover data products. Section 2.4.17
2021 March 15	Removed Landsat_perc (Landsat Percentage Calculation), Landsat_flag, and Canopy_flag from the ATL08 data product and from the algorithm. Removed all reference to Landsat from the ATBD.
<b>2021 September 1</b>	Added section 4.16 on quality control for the final products
<b>2021 September 1</b>	Change histogram height bin from 0.5 m to 1 m in section 4.7, step 3 and 8
<b>2021 November 1</b>	Added Final segment QA/QC Check for canopy photons that fall more than 150 m below the reference DEM. Section 4.16.1
<b>January 15, 2022</b>	Calculate number of background noise photons within canopy Section 2.2.26
<b>January 15, 2022</b>	Adjust canopy radiometry value by removing canopy noise photons from calculation Section 2.2.25
<b>January 15, 2022</b>	Add Final segment QA/QC check based on radiometric values. Section 4.16.2
<b>January 15, 2022</b>	Add Final segment QA/QC check to reassign noise photons mislabeled as canopy photons. Section 4.16.3



<b>15 April 2022</b>	Incorporate YAPC photon weights from ATL03 data product to ground finding approach. Section 4.7
<b>15 June 2022</b>	Modified the number of labeled photons required to report canopy or terrain heights within a segment for both the strong and weak beams. Section 2.2

31  
32

33 **Contents**

34 List of Tables..... 16

35 List of Figures..... 17

36 1 INTRODUCTION ..... 19

37 1.1. Background ..... 20

38 1.2 Photon Counting Lidar ..... 22

39 1.3 The ICESat-2 concept..... 23

40 1.4 Height Retrieval from ATLAS ..... 26

41 1.5 Accuracy Expected from ATLAS..... 28

42 1.6 Additional Potential Height Errors from ATLAS..... 30

43 1.7 Dense Canopy Cases ..... 30

44 1.8 Sparse Canopy Cases ..... 31

45 2. ATL08: DATA PRODUCT ..... 32

46 2.1 Subgroup: Land Parameters ..... 35

47 2.1.1 Georeferenced\_segment\_number\_beg..... 36

48 2.1.2 Georeferenced\_segment\_number\_end ..... 37

49 2.1.3 Segment\_terrain\_height\_mean..... 37

50 2.1.4 Segment\_terrain\_height\_med ..... 37

51 2.1.5 Segment\_terrain\_height\_min ..... 38

52 2.1.6 Segment\_terrain\_height\_max..... 38

53 2.1.7 Segment\_terrain\_height\_mode..... 38

54 2.1.8 Segment\_terrain\_height\_skew ..... 38

55 2.1.9 Segment\_number\_terrain\_photons..... 39

56 2.1.10 Segment height\_interp..... 39

57 2.1.11 Segment h\_te\_std..... 39

58 2.1.12 Segment\_terrain\_height\_uncertainty ..... 39

59 2.1.13 Segment\_terrain\_slope ..... 39

60	2.1.14	Segment_terrain_height_best_fit .....	40
61	2.1.15	Segment_terrain_height_25 .....	40
62	2.1.16	Subset_te_flag {1:5} .....	40
63	2.1.17	Segment Terrain Photon Rate .....	41
64	2.1.18	Terrain Best Fit GeoSegment {1:5} .....	41
65	2.2	Subgroup: Vegetation Parameters .....	41
66	2.2.1	Georeferenced_segment_number_beg .....	44
67	2.2.2	Georeferenced_segment_number_end .....	44
68	2.2.3	Canopy_height_metrics_abs .....	45
69	2.2.4	Canopy_height_metrics .....	45
70	2.2.5	Absolute_segment_canopy_height .....	46
71	2.2.6	Segment_canopy_height .....	46
72	2.2.7	canopy_height GeoSegment {1:5} .....	46
73	2.2.8	Absolute_segment_mean_canopy .....	47
74	2.2.9	Segment_mean_canopy .....	47
75	2.2.10	Segment_dif_canopy .....	47
76	2.2.11	Absolute_segment_min_canopy .....	47
77	2.2.12	Segment_min_canopy .....	47
78	2.2.13	Absolute_segment_max_canopy .....	48
79	2.2.14	Segment_max_canopy .....	48
80	2.2.15	Segment_canopy_height_uncertainty .....	48
81	2.2.16	Segment_canopy_openness .....	49
82	2.2.17	Segment_top_of_canopy_roughness .....	49
83	2.2.18	Segment_canopy_quadratic_height .....	49
84	2.2.19	Segment_number_canopy_photons .....	50
85	2.2.20	Segment_number_top_canopy_photons .....	50
86	2.2.21	Centroid_height .....	50

87	2.2.22	Segment_rel_canopy_conf .....	50
88	2.2.23	Subset_can_flag {1:5}.....	50
89	2.2.24	Segment Canopy Photon Rate .....	51
90	2.2.25	Segment Canopy Photon Rate Reduced .....	51
91	2.2.26	Segment Background Photons in Canopy .....	52
92	2.3	Subgroup: Photons.....	52
93	2.3.1	Indices_of_classed_photons.....	53
94	2.3.2	Photon_class.....	53
95	2.3.3	Georeferenced_segment_number .....	53
96	2.3.4	Photon Height.....	54
97	2.3.5	DRAGANN_flag.....	54
98	2.4	Subgroup: Reference data.....	54
99	2.4.1	Georeferenced_segment_number_beg.....	56
100	2.4.2	Georeferenced_segment_number_end .....	56
101	2.4.3	Segment_latitude .....	56
102	2.4.4	Geosegment_latitude{1:5} .....	57
103	2.4.5	Segment_longitude.....	57
104	2.4.6	Geosegment_longitude{1:5}.....	58
105	2.4.7	Delta_time .....	58
106	2.4.8	Delta_time_beg.....	58
107	2.4.9	Delta_time_end.....	58
108	2.4.10	Night_Flag .....	58
109	2.4.11	Segment_reference_DTM.....	58
110	2.4.12	Segment_reference_DEM_source .....	59
111	2.4.13	Segment_reference_DEM_removal_flag .....	59
112	2.4.14	Segment_terrain_difference .....	59
113	2.4.15	Segment_terrain flag .....	59

114	2.4.16	Segment_landcover .....	59
115	2.4.17	Segment_Woody Vegetation Fractional Cover .....	61
116	2.4.18	Segment_watermask .....	61
117	2.4.19	Segment_snowcover .....	61
118	2.4.20	Urban_flag .....	62
119	2.4.21	Surface Type .....	62
120	2.4.22	ATL08_region .....	62
121	2.4.23	Last_segment_extend .....	62
122	2.4.24	Brightness_flag.....	63
123	2.5	Subgroup: Beam data.....	63
124	2.5.1	Georeferenced_segment_number_beg.....	66
125	2.5.2	Georeferenced_segment_number_end .....	66
126	2.5.3	Beam_coelevation.....	66
127	2.5.4	Beam_azimuth.....	67
128	2.5.5	ATLAS_Pointing_Angle .....	67
129	2.5.6	Reference_ground_track.....	67
130	2.5.7	Sigma_h .....	67
131	2.5.8	Sigma_along.....	67
132	2.5.9	Sigma_across.....	68
133	2.5.10	Sigma_topo .....	68
134	2.5.11	Sigma_ATLAS_LAND .....	68
135	2.5.12	PSF_flag .....	68
136	2.5.13	Layer_flag .....	68
137	2.5.14	Cloud_flag_atm .....	69
138	2.5.15	MSW.....	69
139	2.5.16	Cloud Fold Flag .....	69
140	2.5.17	Computed_Apparent_Surface_Reflectance .....	69

141	2.5.18	Signal_to_Noise_Ratio .....	70
142	2.5.19	Solar_Azimuth .....	70
143	2.5.20	Solar_Elevation .....	70
144	2.5.21	Number_of_segment_photons .....	70
145	2.5.22	Photon_Index_Begin .....	70
146	2.5.23	Saturation Flag.....	70
147	3	ALGORITHM METHODOLOGY.....	72
148	3.1	Noise Filtering.....	72
149	3.1.1	DRAGANN .....	73
150	3.2	Surface Finding.....	77
151	3.2.1	De-trending the Signal Photons.....	79
152	3.2.2	Canopy Determination .....	79
153	3.2.3	Variable Window Determination.....	80
154	3.2.4	Compute descriptive statistics.....	81
155	3.2.5	Ground Finding Filter (Iterative median filtering) .....	83
156	3.3	Top of Canopy Finding Filter .....	84
157	3.4	Classifying the Photons .....	85
158	3.5	Refining the Photon Labels.....	85
159	3.6	Canopy Height Determination .....	90
160	3.7	Link Scale for Data products.....	90
161	4.	ALGORITHM IMPLEMENTATION .....	91
162	4.1	Cloud based filtering .....	94
163	4.2	Preparing ATL03 data for input to ATL08 algorithm .....	96
164	4.3	Noise filtering via DRAGANN.....	98
165	4.3.1	DRAGANN Quality Assurance.....	100
166	4.3.2	Preprocessing to dynamically determine a DRAGANN parameter .....	102
167	4.3.3	Iterative DRAGANN processing.....	105

168	4.4	Compute Filtering Window .....	105
169	4.5	De-trend Data .....	106
170	4.6	Filter outlier noise from signal .....	108
171	4.7	Finding the initial ground estimate .....	109
172	4.8	Find the top of the canopy .....	112
173	4.9	Compute statistics on de-trended (Asmooth) data.....	112
174	4.10	Refine Ground Estimates.....	113
175	4.11	Canopy Photon Filtering.....	115
176	4.12	Compute individual Canopy Heights.....	117
177	4.13	Final photon classification QA check .....	118
178	4.14	Compute segment parameters for the Land Products .....	118
179	4.15	Compute segment parameters for the Canopy Products .....	121
180	4.15.1	Canopy Products calculated with absolute heights .....	123
181	4.16	Segment Quality Check.....	123
182	4.17	Record final product without buffer .....	125
183	5	DATA PRODUCT VALIDATION STRATEGY.....	126
184	5.1	Validation Data .....	126
185	5.2	Internal QC Monitoring .....	129
186	6	REFERENCES .....	135
187			

188 **List of Tables**

189 Table 2.1. Summary table of land parameters on ATL08.....35

190 Table 2.2. Summary table of canopy parameters on ATL08.....42

191 Table 2.3. Summary table for photon parameters for the ATL08 product.....53

192 Table 2.4. Summary table for reference parameters for the ATL08 product.....54

193 Table 2.5. Summary table for beam parameters for the ATL08 product.....64

194 Table 3.1. Standard deviation ranges utilized to qualify the spread of photons within  
195 moving window.....82

196 Table 4.1. Input parameters to ATL08 classification algorithm.....92

197 Table 4.2. Additional external parameters referenced in ATL08 product. ....93

198 Table 5.1. Airborne lidar data vertical height (Z accuracy) requirements for  
199 validation data. .... 126

200 Table 5.2. ATL08 parameter monitoring..... 129

201 Table 5.3. QA/QC trending and triggers. .... 133

202



203	<b>List of Figures</b>	
204	Figure 1.1. Various modalities of lidar detection. Adapted from Harding, 2009.....	23
205	Figure 1.2. Schematic of 6-beam configuration for ICESat-2 mission. The laser	
206	energy will be split into 3 laser beam pairs – each pair having a weak spot (1X) and a	
207	strong spot (4X). .....	25
208	Figure 1.3. Illustration of off-nadir pointing scenarios. Over land (green regions) in	
209	the mid-latitudes, ICESat-2 will be pointed away from the repeat ground tracks to	
210	increase the density of measurements over terrestrial surfaces. ....	26
211	Figure 1.4. Illustration of the point spread function, also referred to as Znoise, for a	
212	series of photons about a surface.....	28
213	Figure 2.1. HDF5 data structure for ATL08 products.....	33
214	Figure 2.2. ATL03 granule regions; graphic from ATL03 ATBD (Neumann et al.). ....	34
215	Figure 2.3. ATL08 product regions.....	35
216	Figure 2.4. Illustration of canopy photons (red dots) interaction in a vegetated area.	
217	Relative canopy heights, $H_i$ , are computed by differencing the canopy photon height	
218	from an interpolated terrain surface. ....	42
219	Figure 3.1. Combination of noise filtering algorithms to create a superset of input	
220	data for surface finding algorithms. ....	73
221	Figure 3.2. Histogram of the number of photons within a search radius. This	
222	histogram is used to determine the threshold for the DRAGANN approach.....	75
223	Figure 3.3. Output from DRAGANN filtering. Signal photons are shown as blue. ....	77
224	Figure 3.4. Flowchart of overall surface finding method. ....	78
225	Figure 3.5. Plot of Signal Photons (black) from 2014 MABEL flight over Alaska and	
226	de-trended photons (red). ....	79
227	Figure 3.6. Shape Parameter for variable window size. ....	81
228	Figure 3.7. Illustration of the standard deviations calculated for each moving	
229	window to identify the amount of spread of signal photons within a given window.	
230	.....	83
231	Figure 3.8. Three iterations of the ground finding concept for $L$ -km segments with	
232	canopy. ....	84

233	Figure 3.9. Example of the intermediate ground and top of canopy surfaces	
234	calculated from MABEL flight data over Alaska during July 2014.....	87
235	Figure 3.10. Example of classified photons from MABEL data collected in Alaska	
236	2014. Red photons are photons classified as terrain. Green photons are classified as	
237	top of canopy. Canopy photons (shown as blue) are considered as photons lying	
238	between the terrain surface and top of canopy.....	88
239	Figure 3.11. Example of classified photons from MABEL data collected in Alaska	
240	2014. Red photons are photons classified as terrain. Green photons are classified as	
241	top of canopy. Canopy photons (shown as blue) are considered as photons lying	
242	between the terrain surface and top of canopy.....	89
243	Figure 3.12. Example of classified photons from MABEL data collected in Alaska	
244	2014. Red photons are photons classified as terrain. Green photons are classified as	
245	top of canopy. Canopy photons (shown as blue) are considered as photons lying	
246	between the terrain surface and top of canopy.....	89
247	Figure 5.1. Example of <i>L-km</i> segment classifications and interpolated ground	
248	surface.....	132
249		

## 250 1 INTRODUCTION

251 This document describes the theoretical basis and implementation of the  
252 processing algorithms and data parameters for Level 3 land and vegetation heights  
253 for the non-polar regions of the Earth. The ATL08 product contains heights for both  
254 terrain and canopy in the along-track direction as well as other descriptive  
255 parameters derived from the measurements. At the most basic level, a derived surface  
256 height from the ATLAS instrument at a given time is provided relative to the WGS-84  
257 ellipsoid. Height estimates from ATL08 can be compared with other geodetic data and  
258 used as input to higher-level ICESat-2 products, namely ATL13 and ATL18. ATL13  
259 will provide estimates of inland water-related heights and associated descriptive  
260 parameters. ATL18 will consist of gridded maps for terrain and canopy features.

261 The ATL08 product will provide estimates of terrain heights, canopy heights,  
262 and canopy cover at fine spatial scales in the along-track direction. Along-track is  
263 defined as the direction of travel of the ICESat-2 satellite in the velocity vector.  
264 Parameters for the terrain and canopy will be provided at a fixed step-size of 100 m  
265 along the ground track referred to as a segment. A fixed segment size of 100 m was  
266 chosen to provide continuity of data parameters on the ATL08 data product. From an  
267 analysis perspective, it is difficult and cumbersome to attempt to relate canopy cover  
268 over variable lengths. Furthermore, a segment size of 100 m will facilitate a simpler  
269 combination of along-track data to create the gridded products.

270 We anticipate that the signal returned from the weak beam will be sufficiently  
271 weak and may prohibit the determination of both a terrain and canopy segment  
272 height, particularly over areas of dense vegetation. However, in more arid regions we  
273 anticipate producing a terrain height for both the weak and strong beams.

274 In this document, section 1 provides a background of lidar in the ecosystem  
275 community as well as describing photon counting systems and how they differ from  
276 discrete return lidar systems. Section 2 provides an overview of the Land and  
277 Vegetation parameters and how they are defined on the data product. Section 3  
278 describes the basic methodology that will be used to derive the parameters for ATL08.

279 Section 4 describes the processing steps, input data, and procedure to derive the data  
280 parameters. Section 5 will describe the test data and specific tests that NASA's  
281 implementation of the algorithm should pass in order to determine a successful  
282 implementation of the algorithm.

283

### 284 ***1.1. Background***

285 The Earth's land surface is a complex mosaic of geomorphic units and land  
286 cover types resulting in large variations in terrain height, slope, roughness, vegetation  
287 height and reflectance, often with the variations occurring over very small spatial  
288 scales. Documentation of these landscape properties is a first step in understanding  
289 the interplay between the formative processes and response to changing conditions.  
290 Characterization of the landscape is also necessary to establish boundary conditions  
291 for models which are sensitive to these properties, such as predictive models of  
292 atmospheric change that depend on land-atmosphere interactions. Topography, or  
293 land surface height, is an important component for many height applications, both to  
294 the scientific and commercial sectors. The most accurate global terrain product was  
295 produced by the Shuttle Radar Topography Mission (SRTM) launched in 2000;  
296 however, elevation data are limited to non-polar regions. The accuracy of SRTM  
297 derived elevations range from 5 – 10 m, depending upon the amount of topography  
298 and vegetation cover over a particular area. ICESat-2 will provide a global distribution  
299 of geodetic measurements (of both the terrain surface and relative canopy heights)  
300 which will provide a significant benefit to society through a variety of applications  
301 including sea level change monitoring, forest structural mapping and biomass  
302 estimation, and improved global digital terrain models.

303 In addition to producing a global terrain product, monitoring the amount and  
304 distribution of above ground vegetation and carbon pools enables improved  
305 characterization of the global carbon budget. Forests play a significant role in the  
306 terrestrial carbon cycle as carbon pools. Events, such as management activities  
307 (Krankina et al. 2012) and disturbances can release carbon stored in forest above

308 ground biomass (AGB) into the atmosphere as carbon dioxide, a greenhouse gas that  
309 contributes to climate change (Ahmed et al. 2013). While carbon stocks in nations  
310 with continuous national forest inventories (NFIs) are known, complications with NFI  
311 carbon stock estimates exist, including: (1) ground-based inventory measurements  
312 are time consuming, expensive, and difficult to collect at large-scales (Houghton  
313 2005; Ahmed et al. 2013); (2) asynchronously collected data; (3) extended time  
314 between repeat measurements (Houghton 2005); and (4) the lack of information on  
315 the spatial distribution of forest AGB, required for monitoring sources and sinks of  
316 carbon (Houghton 2005). Airborne lidar has been used for small studies to capture  
317 canopy height and in those studies canopy height variation for multiple forest types  
318 is measured to approximately 7 m standard deviation (Hall et al., 2011).

319 Although the spatial extent and changes to forests can be mapped with existing  
320 satellite remote sensing data, the lack of information on forest vertical structure and  
321 biomass limits the knowledge of biomass/biomass change within the global carbon  
322 budget. Based on the global carbon budget for 2015 (Quere et al., 2015), the largest  
323 remaining uncertainties about the Earth's carbon budget are in its terrestrial  
324 components, the global residual terrestrial carbon sink, estimated at  $3.0 \pm 0.8$   
325 GtC/year for the last decade (2005-2014). Similarly, carbon emissions from land-use  
326 changes, including deforestation, afforestation, logging, forest degradation and  
327 shifting cultivation are estimated at  $0.9 \pm 0.5$  GtC /year. By providing information on  
328 vegetation canopy height globally with a higher spatial resolution than previously  
329 afforded by other spaceborne sensors, the ICESat-2 mission can contribute  
330 significantly to reducing uncertainties associated with forest vegetation carbon.

331 Although ICESat-2 is not positioned to provide global biomass estimates due  
332 to its profiling configuration and somewhat limited detection capabilities, it is  
333 anticipated that the data products for vegetation will be complementary to ongoing  
334 biomass and vegetation mapping efforts. Synergistic use of ICESat-2 data with other  
335 space-based mapping systems is one solution for extended use of ICESat-2 data.  
336 Possibilities include NASA's Global Ecosystems Dynamics Investigation (GEDI) lidar

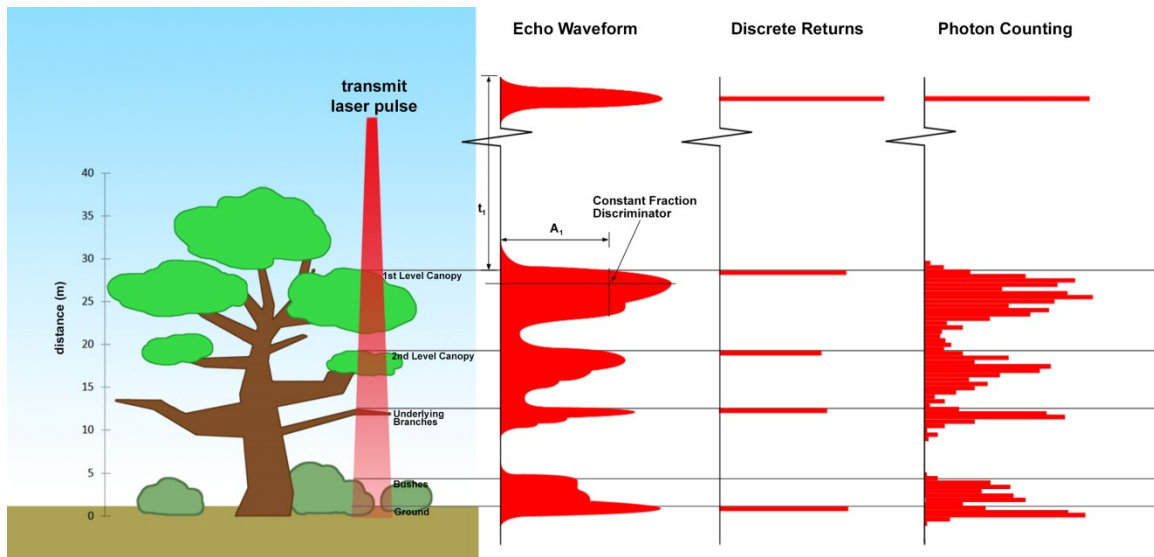
337 planned to fly onboard the International Space Station (ISS) or imaging sensors, such  
338 as Landsat 8, or NASA/ISRO –NISAR radar mission.

339

## 340 **1.2 Photon Counting Lidar**

341 Rather than using an analog, full waveform system similar to what was utilized  
342 on the ICESat/GLAS mission, ICESat-2 will employ a photon counting lidar. Photon  
343 counting lidar has been used successfully for ranging for several decades in both the  
344 science and defense communities. Photon counting lidar systems operate on the  
345 concept that a low power laser pulse is transmitted and the detectors used are  
346 sensitive at the single photon level. Due to this type of detector, any returned photon  
347 whether from the reflected signal or solar background can trigger an event within the  
348 detector. A discussion regarding discriminating between signal and background noise  
349 photons is discussed later in this document. A question of interest to the ecosystem  
350 community is to understand where within the canopy is the photon likely to be  
351 reflected. Figure 1.1 is an example of three different laser detector modalities: full  
352 waveform, discrete return, and photon counting. Full waveform sensors record the  
353 entire temporal profile of the reflected laser energy through the canopy. In contrast,  
354 discrete return systems have timing hardware that record the time when the  
355 amplitude of the reflected signal energy exceeds a certain threshold amount. A photon  
356 counting system, however, will record the arrival time associated with a single  
357 photon detection that can occur anywhere within the vertical distribution of the  
358 reflected signal. If a photon counting lidar system were to dwell over a surface for a  
359 significant number of shots (i.e. hundreds or more), the vertical distribution of the  
360 reflected photons will resemble a full waveform. Thus, while an individual photon  
361 could be reflected from anywhere within the vertical canopy, the probability  
362 distribution function (PDF) of that reflected photon would be the full waveform.  
363 Furthermore, the probability of detecting the top of the tree is not as great as  
364 detecting reflective surfaces positioned deeper into the canopy where the bulk of  
365 leaves and branches are located. As one might imagine, the PDF will differ according

366 to canopy structure and vegetation physiology. For example, the PDF of a conifer tree  
367 will look different than broadleaf trees.



368

369 Figure 1.1. Various modalities of lidar detection. Adapted from Harding, 2009.

370 A cautionary note, the photon counting PDF that is illustrated in Figure 1.1 is  
371 merely an illustration if enough photons (i.e. hundreds of photons or more) were to  
372 be reflected from a target. In reality, due to the spacecraft speed, ATLAS will record 0  
373 – 4 photons per transmit laser pulse over vegetation.

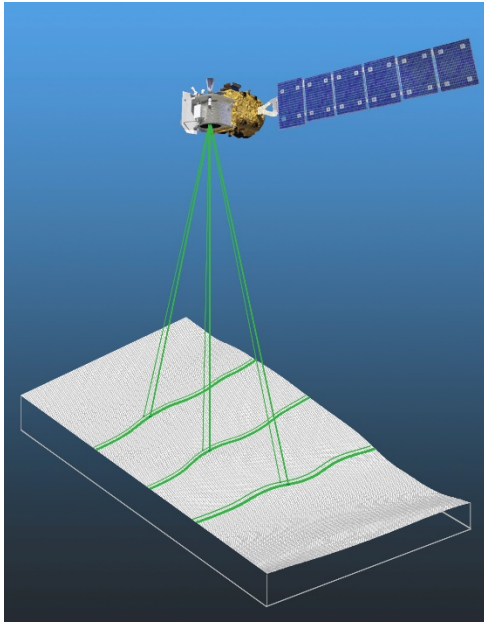
374

### 375 1.3 The ICESat-2 concept

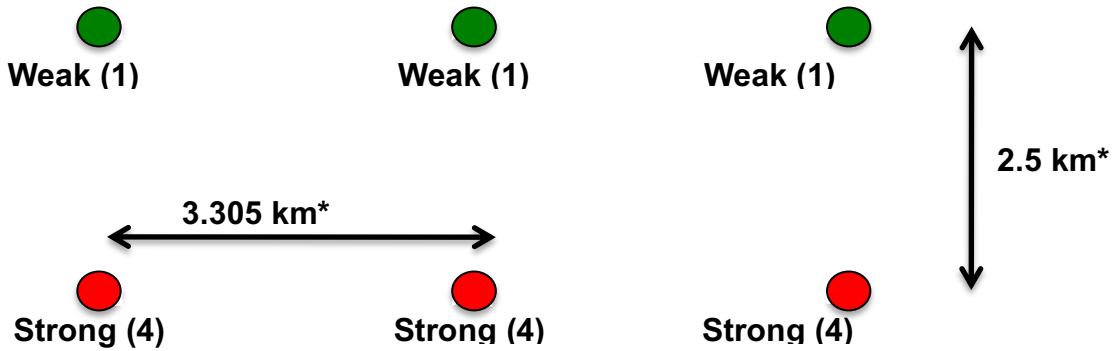
376 The Advanced Topographic Laser Altimeter System (ATLAS) instrument  
377 designed for ICESat-2 will utilize a different technology than the GLAS instrument  
378 used for ICESat. Instead of using a high-energy, single-beam laser and digitizing the  
379 entire temporal profile of returned laser energy, ATLAS will use a multi-beam,  
380 micropulse laser (sometimes referred to as photon-counting). The travel time of each  
381 detected photon is used to determine a range to the surface which, when combined  
382 with satellite attitude and pointing information, can be geolocated into a unique XYZ  
383 location on or near the Earth's surface. For more information on how the photons  
384 from ICESat-2 are geolocated, refer to ATL03 ATBD. The XYZ positions from ATLAS

385 are subsequently used to derive surface and vegetation properties. The ATLAS  
386 instrument will operate at 532 nm in the green range of the electromagnetic (EM)  
387 spectrum and will have a laser repetition rate of 10 kHz. The combination of the laser  
388 repetition rate and satellite velocity will result in one outgoing laser pulse  
389 approximately every 70 cm on the Earth's surface and each spot on the surface is ~13  
390 m in diameter. Each transmitted laser pulse is split by a diffractive optical element in  
391 ATLAS to generate six individual beams, arranged in three pairs (Figure 1.2). The  
392 beams within each pair have different transmit energies ('weak' and 'strong', with an  
393 energy ratio of approximately 1:4) to compensate for varying surface reflectance. The  
394 beam pairs are separated by ~3.3 km in the across-track direction and the strong and  
395 weak beams are separated by ~2.5 km in the along-track direction. As ICESat-2 moves  
396 along its orbit, the ATLAS beams describe six tracks on the Earth's surface; the array  
397 is rotated slightly with respect to the satellite's flight direction so that tracks for the  
398 fore and aft beams in each column produce pairs of tracks – each separated by  
399 approximately 90 m.





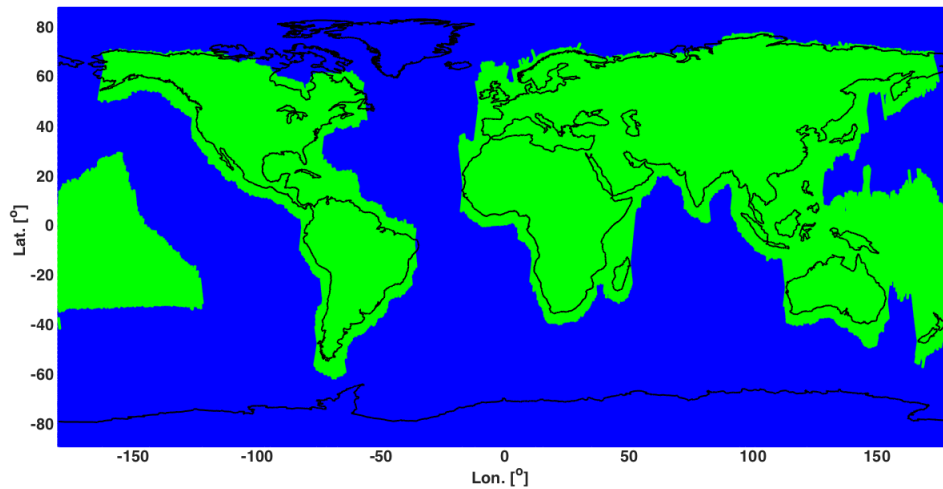
400



401

402 Figure 1.2. Schematic of 6-beam configuration for ICESat-2 mission. The laser energy will  
 403 be split into 3 laser beam pairs – each pair having a weak spot (1X) and a strong spot (4X).

404 The motivation behind this multi-beam design is its capability to compute  
 405 cross-track slopes on a per-orbit basis, which contributes to an improved  
 406 understanding of ice dynamics. Previously, slope measurements of the terrain were  
 407 determined via repeat-track and crossover analysis. The laser beam configuration as  
 408 proposed for ICESat-2 is also beneficial for terrestrial ecosystems compared to GLAS  
 409 as it enables a denser spatial sampling in the non-polar regions. To achieve a spatial  
 410 sampling goal of no more than 2 km between equatorial ground tracks, ICESat-2 will  
 411 be off-nadir pointed a maximum of 1.8 degrees from the reference ground track  
 412 during the entire mission.



413

414 Figure 1.3. Illustration of off-nadir pointing scenarios. Over land (green regions) in the  
 415 mid-latitudes, ICESat-2 will be pointed away from the repeat ground tracks to increase the  
 416 density of measurements over terrestrial surfaces.

417 ICESat-2 is designed to densely sample the Earth’s surface, permitting  
 418 scientists to measure and quantitatively characterize vegetation across vast  
 419 expanses, e.g., nations, continents, globally. ICESat-2 will acquire synoptic  
 420 measurements of vegetation canopy height, density, the vertical distribution of  
 421 photosynthetically active material, leading to improved estimates of forest biomass,  
 422 carbon, and volume. In addition, the orbital density, i.e., the number of orbits per unit  
 423 area, at the end of the three year mission will facilitate the production of gridded  
 424 global products. ICESat-2 will provide the means by which an accurate “snapshot” of  
 425 global biomass and carbon may be constructed for the mission period.

426

#### 427 **1.4 Height Retrieval from ATLAS**

428 Light from the ATLAS lasers reaches the earth’s surface as flat disks of down-  
 429 traveling photons approximately 50 cm in vertical extent and spread over  
 430 approximately 14 m horizontally. Upon hitting the earth’s surface, the photons are  
 431 reflected and scattered in every direction and a handful of photons return to the

432 ATLAS telescope's focal plane. The number of photon events per laser pulse is a  
433 function of outgoing laser energy, surface reflectance, solar conditions, and scattering  
434 and attenuation in the atmosphere. For highly reflective surfaces (such as land ice)  
435 and clear skies, approximately 10 signal photons from a single strong beam are  
436 expected to be recorded by the ATLAS instrument for a given transmit laser pulse.  
437 Over vegetated land where the surface reflectance is considerably less than snow or  
438 ice surfaces, we expect to see fewer returned photons from the surface. Whereas  
439 snow and ice surfaces have high reflectance at 532 nm (typical Lambertian  
440 reflectance between 0.8 and 0.98 (Martino, GSFC internal report, 2010)), canopy and  
441 terrain surfaces have much lower reflectance (typically around 0.3 for soil and 0.1 for  
442 vegetation) at 532 nm. As a consequence we expect to see 1/3 to 1/9 as many photons  
443 returned from terrestrial surfaces as from ice and snow surfaces. For vegetated  
444 surfaces, the number of reflected signal photon events per transmitted laser pulse is  
445 estimated to range between 0 to 4 photons.

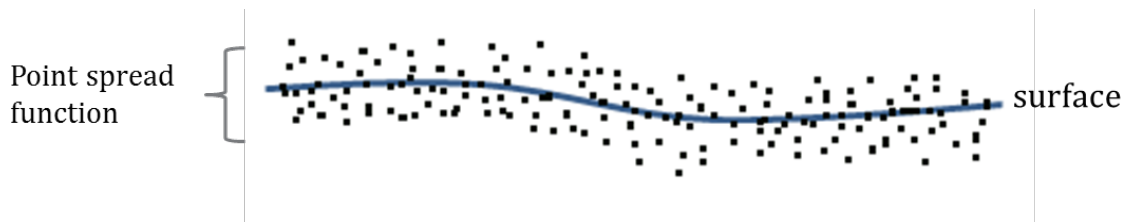
446 The time measured from the detected photon events are used to compute a  
447 range, or distance, from the satellite. Combined with the precise pointing and attitude  
448 information about the satellite, the range can be geolocated into a XYZ point (known  
449 as a geolocated photon) above the WGS-84 reference ellipsoid. In addition to  
450 recording photons from the reflected signal, the ATLAS instrument will detect  
451 background photons from sunlight which are continually entering the telescope. A  
452 primary objective of the ICESat-2 data processing software is to correctly  
453 discriminate between signal photons and background photons. Some of this  
454 processing occurs at the ATL03 level and some of it also occurs within the software  
455 for ATL08. At ATL03, this discrimination is done through a series of three steps of  
456 progressively finer resolution with some processing occurring onboard the satellite  
457 prior to downlink of the raw data. The ATL03 data product produces a classification  
458 between signal and background (i.e. noise) photons, and further discussion on that  
459 classification process can be read in the ATL03 ATBD. In addition, not all geophysical  
460 corrections (e.g. ocean tide) are applied to the position of the individual geolocated  
461 photons at the ATL03 level, but they are provided on the ATL03 data product if there

462 exists a need to apply them. Thus, in general, all of the heights processed in the ATL08  
463 algorithm consists of the ATL03 heights with respect to the WGS-84 ellipsoid, with  
464 geophysical corrections applied, as specified in Chapter 6 of the ATL03 ATBD.

465

### 466 **1.5 Accuracy Expected from ATLAS**

467 There are a variety of elements that contribute to the elevation accuracy that  
468 are expected from ATLAS and the derived data products. Elevation accuracy is a  
469 composite of ranging precision of the instrument, radial orbital uncertainty,  
470 geolocation knowledge, forward scattering in the atmosphere, and tropospheric path  
471 delay uncertainty. The ranging precision seen by ATLAS will be a function of the laser  
472 pulse width, the surface area potentially illuminated by the laser, and uncertainty in  
473 the timing electronics. The requirement on radial orbital uncertainty is specified to  
474 be less than 4 cm and tropospheric path delay uncertainty is estimated to be 3 cm. In  
475 the case of ATLAS, the ranging precision for flat surfaces, is expected to have a  
476 standard deviation of approximately 25 cm. The composite of each of the errors can  
477 also be thought of as the spread of photons about a surface (see Figure 1.4) and is  
478 referred to as the point spread function or Znoise.



479

480 Figure 1.4. Illustration of the point spread function, also referred to as Znoise, for a series  
481 of photons about a surface.

482 The estimates of  $\sigma_{orbit}$ ,  $\sigma_{troposphere}$ ,  $\sigma_{forwardscattering}$ ,  $\sigma_{pointing}$ , and  $\sigma_{timing}$   
483 for a photon will be represented on the ATL03 data product as the final geolocated  
484 accuracy in the X, Y, and Z (or height) direction. In reality, these parameters have  
485 different temporal and spatial scales, however until ICESat-2 is on orbit, it is uncertain  
486 how these parameters will vary over time. As such, Equation 1.1 may change once the

487 temporal aspects of these parameters are better understood. For a preliminary  
 488 quantification of the uncertainties, Equation 1.1 is valid to incorporate the instrument  
 489 related factors.

$$490 \quad \sigma_Z = \sqrt{\sigma_{Orbit}^2 + \sigma_{trop}^2 + \sigma_{forwardscattering}^2 + \sigma_{pointing}^2 + \sigma_{timing}^2} \quad \text{Eqn. 1.1}$$

491

492 Although  $\sigma_Z$  on the ATL03 product represents the best understanding of the  
 493 uncertainty for each geolocated photon, it does not incorporate the uncertainty  
 494 associated with local slope of the topography. The slope component to the geolocation  
 495 uncertainty is a function of both the geolocation knowledge of the pointing (which is  
 496 required to be less than 6.5 m) multiplied by the tangent of the surface slope. In a case  
 497 of flat topography ( $\leq 1$  degree slope),  $\sigma_Z \leq 25$  cm, whereas in the case of a 10 degree  
 498 surface slope,  $\sigma_Z = 119$  cm. The uncertainty associated with the local slope will be  
 499 combined with  $\sigma_Z$  to produce the term  $\sigma_{AtlasLand}$ .

$$500 \quad \sigma_{AtlasLand} = \sqrt{\sigma_Z^2 + \sigma_{topo}^2} \quad \text{Eqn. 1.2}$$

$$501 \quad \sigma_{topo} = \sigma_{topo} = \sqrt{(6.5 \tan(\theta_{surface\ slope}))^2} \quad \text{Eqn. 1.3}$$

502 Ultimately, the uncertainty that will be reported on the data product ATL08  
 503 will include the  $\sigma_{AtlasLand}$  term and the local rms values of heights computed within  
 504 each data parameter segment. For example, calculations of terrain height will be  
 505 made on photons classified as terrain photons (this process is described in the  
 506 following sections). The uncertainty of the terrain height for a segment is described  
 507 in Equation 1.4, where the root mean square term of  $\sigma_{AtlasLand}$  and rms of terrain  
 508 heights are normalized by the number of terrain photons for that given segment.

$$509 \quad \sigma_{ATL08\ segment} = \sqrt{\sigma_{AtlasLand}^2 + \sigma_{Zrms\ segment\ class}^2} \quad \text{Eqn. 1.4}$$

510

511 **1.6 Additional Potential Height Errors from ATLAS**

512 Some additional potential height errors in the ATL08 terrain and vegetation  
513 product can come from a variety of sources including:

514 a. Vertical sampling error. ATLAS height estimates are based on a  
515 random sampling of the surface height distribution. Photons may  
516 be reflected from anywhere within the PDF of the reflecting surface;  
517 more specifically, anywhere from within the canopy. A detailed  
518 look at the potential effect of vertical sampling error is provided in  
519 Neuenschwander and Magruder (2016).

520 b. Background noise. Random noise photons are mixed with the  
521 signal photons so classified photons will include random outliers.

522 c. Complex topography. The along-track product may not always  
523 represent complex surfaces, particularly if the density of ground  
524 photons does not support an accurate representation.

525 d. Vegetation. Dense vegetation may preclude reflected photon  
526 events from reaching the underlying ground surface. An incorrect  
527 estimation of the underlying ground surface will subsequently lead  
528 to an incorrect canopy height determination.

529 e. Misidentified photons. The product from ATL03 combined with  
530 additional noise filtering may not identify the correct photons as  
531 signal photons.

532

533 **1.7 Dense Canopy Cases**

534 Although the height accuracy produced from ICESat-2 is anticipated to be  
535 superior to other global height products (e.g. SRTM), for certain biomes photon  
536 counting lidar data as it will be collected by the ATLAS instrument present a challenge  
537 for extracting both the terrain and canopy heights, particularly for areas of dense

538 vegetation. Due to the relatively low laser power, we anticipate that the along-track  
539 signal from ATLAS may lose ground signal under dense forest (e.g. >96% canopy  
540 closure) and in situations where cloud cover obscures the terrestrial signal. In areas  
541 having dense vegetation, it is likely that only a handful of photons will be returned  
542 from the ground surface with the majority of reflections occurring from the canopy.  
543 A possible source of error can occur with both the canopy height estimates and the  
544 terrain heights if the vegetation is particularly dense and the ground photons were  
545 not correctly identified.

546

### 547 **1.8 Sparse Canopy Cases**

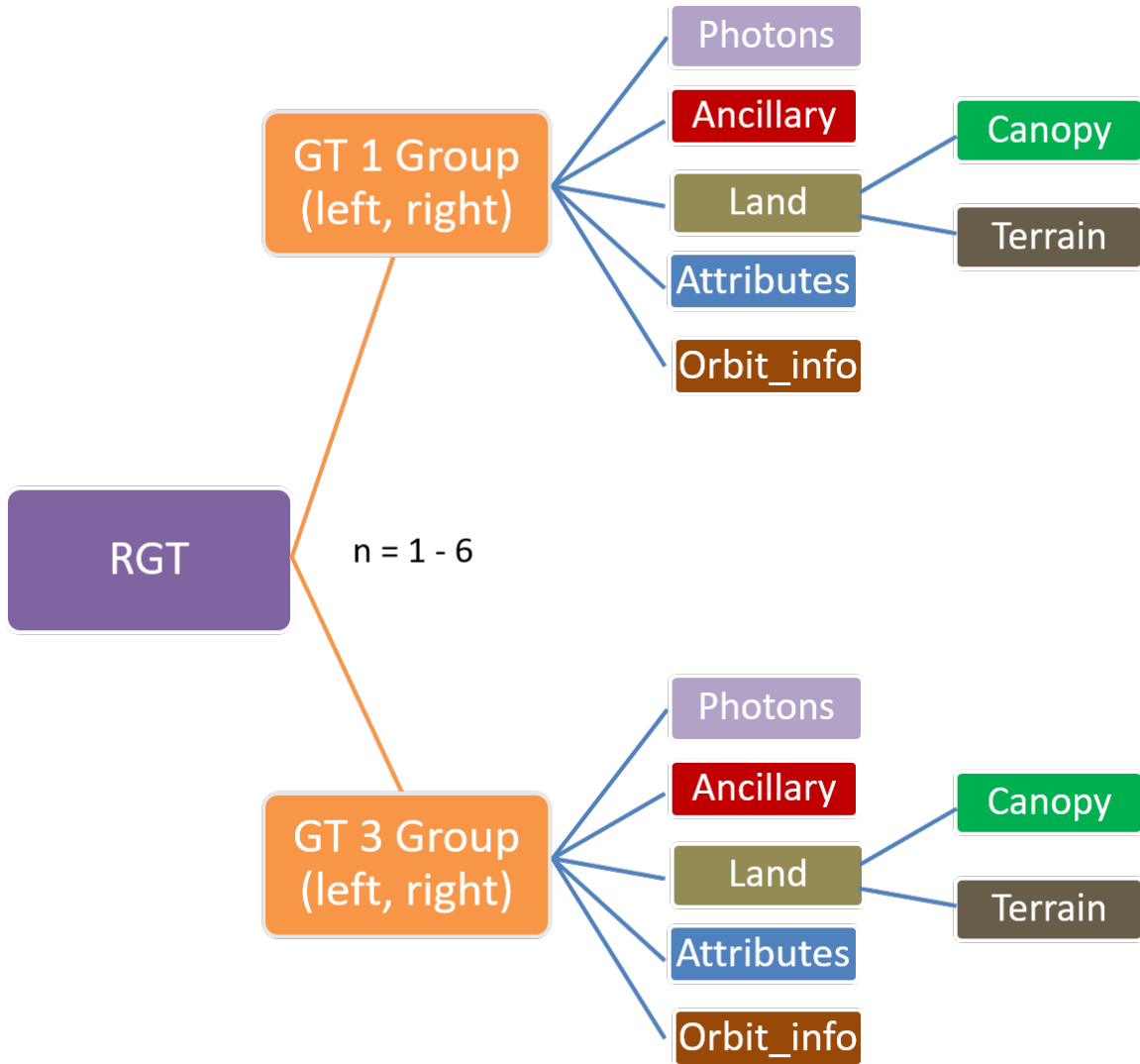
548 Conversely, sparse canopy cases also pose a challenge to vegetation height  
549 retrievals. In these cases, expected reflected photon events from sparse trees or  
550 shrubs may be difficult to discriminate between solar background noise photons. The  
551 algorithms being developed for ATL08 operate under the assumption that signal  
552 photons are close together and noise photons will be more isolated in nature. Thus,  
553 signal (in this case canopy) photons may be incorrectly identified as solar background  
554 noise on the data product. Due to the nature of the photon counting processing,  
555 canopy photons identified in areas that have extremely low canopy cover <15% will  
556 be filtered out and reassigned as noise photons.

557

## 558 2. ATL08: DATA PRODUCT

559 The ATL08 product will provide estimates of terrain height, canopy height,  
560 and canopy cover at fine spatial scales in the along-track direction. In accordance with  
561 the HDF-driven structure of the ICESat-2 products, the ATL08 product will  
562 characterize each of the six Ground Tracks (GT) associated with each Reference  
563 Ground Track (RGT) for each cycle and orbit number. Each ground track group has a  
564 distinct beam number, distance from the reference track, and transmit energy  
565 strength, and all beams will be processed independently using the same sequence of  
566 steps described within ATL08. Each ground track group (GT) on the ATL08 product  
567 contains subgroups for land and canopy heights segments as well as beam and  
568 reference parameters useful in the ATL08 processing. In addition, the labeled photons  
569 that are used to determine the data parameters will be indexed back to the ATL03  
570 products such that they are available for further, independent analysis. A layout of  
571 the ATL08 HDF product is shown in Figure 2.1. The six GTs are numbered from left to  
572 right, regardless of satellite orientation.





573

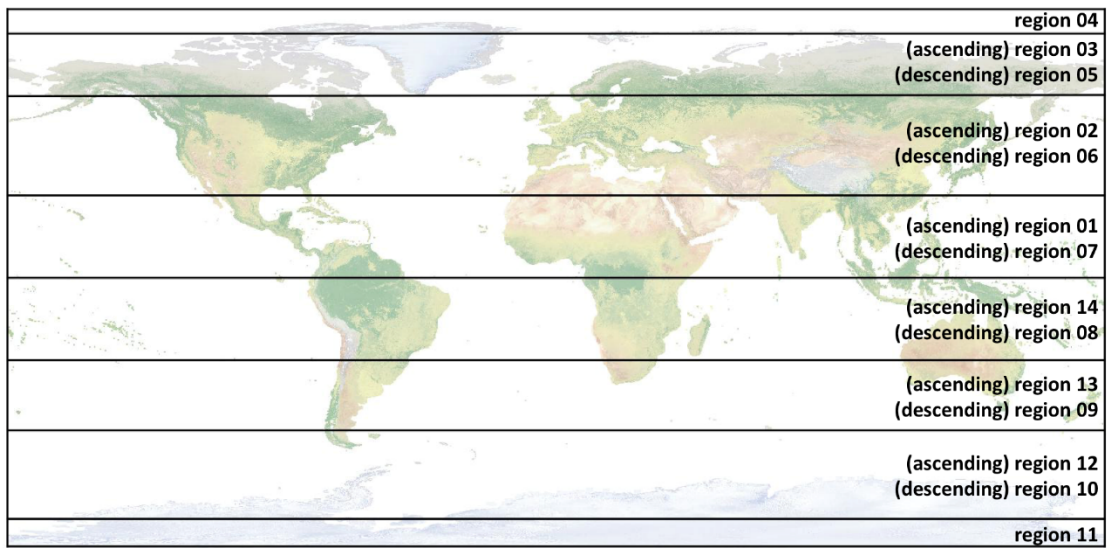
574 Figure 2.1. HDF5 data structure for ATL08 products

575

576 For each data parameter, terrain surface elevation and canopy heights will be  
 577 provided at a fixed segment size of 100 meters along the ground track. Based on the  
 578 satellite velocity and the expected number of reflected photons for land surfaces, each  
 579 segment should have more than 100 signal photons, but in some instances there may  
 580 be less than 100 signal photons per segment. If a segment has less than 50 classed  
 581 (i.e., labeled by ATL08 as ground, canopy, or top of canopy) photons we feel this  
 582 would not accurately represent the surface. Thus, an invalid value will be reported in

583 all height fields. In the event that there are more than 50 classed photons, but a terrain  
 584 height cannot be determined due to an insufficient number of ground photons, (e.g.  
 585 lack of photons penetrating through dense canopy), the only reported terrain height  
 586 will be the interpolated surface height.

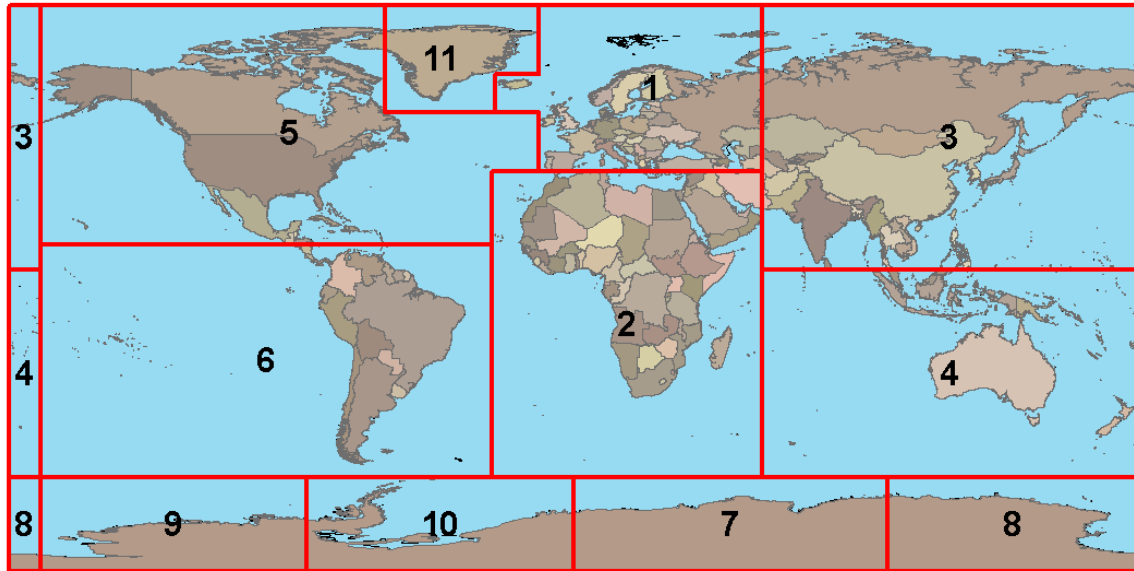
587 The ATL08 product will be produced per granule based on the ATL03 defined  
 588 regions (see Figure 2.2). Thus, the ATL08 file/name convention scheme will match  
 589 the file/naming convention for ATL03 –in attempt for reducing complexity to allow  
 590 users to examine both data products.



591

592 Figure 2.2. ATL03 granule regions; graphic from ATL03 ATBD (Neumann et al.).

593 The ATL08 product additionally has its own internal regions, which are  
 594 roughly assigned by continent, as shown by Figure 2.3. For the regions covering  
 595 Antarctica (regions 7, 8, 9, 10) and Greenland (region 11), the ATL08 algorithm will  
 596 assume that no canopy is present. These internal ATL08 regions will be noted in the  
 597 ATL08 product (see parameter atl08\_region in Section 2.4.22). Note that the regions  
 598 for each ICESat-2 product are not the same.



599

600 Figure 2.3. ATL08 product regions.

601

602 **2.1 Subgroup: Land Parameters**

603 ATL08 terrain height parameters are defined in terms of the absolute height  
 604 above the reference ellipsoid.

605 Table 2.1. Summary table of land parameters on ATL08.

Group	Data type	Description	Source
<b>segment_id_beg</b>	Integer	First along-track segment_id number in 100-m segment	ATL03
<b>segment_id_end</b>	Integer	Last along-track segment_id number in 100-m segment	ATL03
<b>h_te_mean</b>	Float	Mean terrain height for segment	computed
<b>h_te_median</b>	Float	Median terrain height for segment	computed
<b>h_te_min</b>	Float	Minimum terrain height for segment	computed
<b>h_te_max</b>	Float	Maximum terrain height for segment	computed
<b>h_te_mode</b>	Float	Mode of terrain height for segment	computed
<b>h_te_skew</b>	Float	Skew of terrain height for segment	computed

<b>n_te_photons</b>	Integer	Number of ground photons in segment	computed
<b>h_te_interp</b>	Float	Interpolated terrain surface height at mid-point of segment	computed
<b>h_te_std</b>	Float	Standard deviation of ground heights about the interpolated ground surface	computed
<b>h_te_uncertainty</b>	Float	Uncertainty of ground height estimates. Includes all known uncertainties such as geolocation, pointing angle, timing, radial orbit errors, etc.	computed from Equation 1.4
<b>terrain_slope</b>	Float	Slope of terrain within segment	computed
<b>h_te_best_fit</b>	Float	Best fit terrain elevation at the 100 m segment mid-point location	computed
<b>h_te_best_fit_20m</b>	Float	Best fit terrain elevation at the 20 m geosegment mid-point location	computed
<b>h_te_rh25</b>	float	The relative height from classified canopy photons are sorted into a cumulative distribution, and the height associated with the 98% height above the h_te_bestfit for that segment is reported.	computed
<b>subset_te_flag</b>	Integer	Quality flag indicating the terrain photons populating the 100 m segment statistics are derived from less than 100 m worth of photons	computed
<b>photon_rate_te</b>	Float	Calculated photon rate for ground photons within each segment	computed

606

### 607 2.1.1 Georeferenced\_segment\_number\_beg

608 (parameter = segment\_id\_beg). The first along-track segment\_id in each 100-m  
609 segment. Each 100-m segment consists of five sequential 20-m segments provided  
610 from the ATL03 product, which are labeled as segment\_id. The segment\_id is a seven  
611 digit number that uniquely identifies each along track segment, and is written at the  
612 along-track geolocation segment rate (i.e. ~20m along track). The four digit RGT

613 number can be combined with the seven digit segment\_id number to uniquely define  
614 any along-track segment number. Values are sequential, with 0000001 referring to  
615 the first segment after the equatorial crossing of the ascending node.

#### 616 **2.1.2** Georeferenced\_segment\_number\_end

617 (parameter = segment\_id\_end). The last along-track segment\_id in each 100-m  
618 segment. Each 100-m segment consists of five sequential 20-m segments provided  
619 from the ATL03 product, which are labeled as segment\_id. The segment\_id is a seven  
620 digit number that uniquely identifies each along track segment, and is written at the  
621 along-track geolocation segment rate (i.e. ~20m along track). The four digit RGT  
622 number can be combined with the seven digit segment\_id number to uniquely define  
623 any along-track segment number. Values are sequential, with 0000001 referring to  
624 the first segment after the equatorial crossing of the ascending node.

#### 625 **2.1.3** Segment\_terrain\_height\_mean

626 (parameter = h\_te\_mean). Estimated mean of the terrain height above the  
627 reference ellipsoid derived from classified ground photons within the 100 m segment.  
628 If a terrain height cannot be directly determined within the segment (i.e. there are not  
629 a sufficient number of ground photons), only the interpolated terrain height will be  
630 reported. Required input data is classified point cloud (i.e. photons labeled as either  
631 canopy or ground in the ATL08 processing). This parameter will be derived from only  
632 classified ground photons.

#### 633 **2.1.4** Segment\_terrain\_height\_med

634 (parameter = h\_te\_median). Median terrain height above the reference  
635 ellipsoid derived from the classified ground photons within the 100 m segment. If  
636 there are not a sufficient number of ground photons, an invalid value will be reported  
637 –no interpolation will be done. Required input data is classified point cloud (i.e.  
638 photons labeled as either canopy or ground in the ATL08 processing). This parameter  
639 will be derived from only classified ground photons.

640           **2.1.5** Segment\_terrain\_height\_min

641           (parameter = h\_te\_min). Minimum terrain height above the reference ellipsoid  
642 derived from the classified ground photons within the 100 m segment. If there are  
643 not a sufficient number of ground photons, an invalid value will be reported –no  
644 interpolation will be done. Required input data is classified point cloud (i.e. photons  
645 labeled as either canopy or ground in the ATL08 processing). This parameter will be  
646 derived from only classified ground photons.

647           **2.1.6** Segment\_terrain\_height\_max

648           (parameter = h\_te\_max). Maximum terrain height above the reference  
649 ellipsoid derived from the classified ground photons within the 100 m segment. If  
650 there are not a sufficient number of ground photons, an invalid value will be reported  
651 –no interpolation will be done. Required input data is classified point cloud (i.e.  
652 photons labeled as either canopy or ground in the ATL08 processing). This parameter  
653 will be derived from only classified ground photons.

654           **2.1.7** Segment\_terrain\_height\_mode

655           (parameter = h\_te\_mode). Mode of the classified ground photon heights above  
656 the reference ellipsoid within the 100 m segment. If there are not a sufficient number  
657 of ground photons, an invalid value will be reported –no interpolation will be done.  
658 Required input data is classified point cloud (i.e. photons labeled as either canopy or  
659 ground in the ATL08 processing). This parameter will be derived from only classified  
660 ground photons.

661           **2.1.8** Segment\_terrain\_height\_skew

662           (parameter = h\_te\_skew). The skew of the classified ground photons within the  
663 100 m segment. If there are not a sufficient number of ground photons, an invalid  
664 value will be reported –no interpolation will be done. Required input data is classified  
665 point cloud (i.e. photons labeled as either canopy or ground in the ATL08 processing).  
666 This parameter will be derived from only classified ground photons.

667       **2.1.9** Segment\_number\_terrain\_photons  
668           (parameter = n\_te\_photons). Number of terrain photons identified in segment.

669       **2.1.10** Segment height\_interp  
670           (parameter = h\_te\_interp). Interpolated terrain surface height above the  
671 reference ellipsoid from ATL08 processing at the mid-point of each segment. This  
672 interpolated surface is the FINALGROUND estimate (described in section 4.9).

673       **2.1.11** Segment h\_te\_std  
674           (parameter = h\_te\_std). Standard deviations of terrain points about the  
675 interpolated ground surface within the segment. Provides an indication of surface  
676 roughness.

677       **2.1.12** Segment\_terrain\_height\_uncertainty  
678           (parameter = h\_te\_uncertainty). Uncertainty of the mean terrain height for the  
679 segment. This uncertainty incorporates all systematic uncertainties (e.g. timing,  
680 orbits, geolocation, etc.) as well as uncertainty from errors of identified photons. This  
681 parameter is described in Section 1, Equation 1.4. If there are not a sufficient number  
682 of ground photons, an invalid value will be reported –no interpolation will be done.  
683 Required input data is classified point cloud (i.e. photons labeled as either canopy or  
684 ground in the ATL08 processing). This parameter will be derived from only classified  
685 ground photons. The  $\sigma_{segmentclass}$  term in Equation 1.4 represents the standard  
686 deviation of the terrain height residuals about the FINALGROUND estimate.

687       **2.1.13** Segment\_terrain\_slope  
688           (parameter = terrain\_slope). Slope of terrain within each segment. Slope is  
689 computed from a linear fit of the terrain photons. It estimates the rise [m] in relief  
690 over each segment [100 m]; e.g., if the slope value is 0.04, there is a 4 m rise over the  
691 100 m segment. Required input data are the classified terrain photons.





718 inform the user that, in this example, the 100 m estimate are being derived from only  
719 40 m worth of data.

#### 720 **2.1.17 Segment Terrain Photon Rate**

721 (parameter = photon\_rate\_te). This value indicates the terrain photon rate  
722 within each ATL08 segment. This value is calculated as the total number of terrain  
723 photons divided by the total number of laser shots within each ATL08 segment. The  
724 number of laser shots is defined as the number of unique Delta\_Time values within  
725 each segment.

#### 726 **2.1.18 Terrain Best Fit GeoSegment {1:5}**

727 (parameter = h\_te\_best\_fit\_20m). The best fit terrain elevation at the mid-point  
728 location of each 20 m geosegment. The mid-segment terrain elevation is determined  
729 by selecting the best of three fits – linear, 3<sup>rd</sup> order and 4<sup>th</sup> order polynomials – to the  
730 terrain photons and interpolating the elevation at each 20 m along a 100 m segment.  
731 For the linear fit, a slope correction and weighting is applied to each ground photon  
732 based on the distance to the slope height at the center of the segment. For segments  
733 that do not have a sufficient number of photons, an invalid (or fill) value will be  
734 reported. Each 20 m geo-segment shall have 10 signal photons as a minimum number  
735 to be used for calculations and a minimum of 3 terrain photons are required to  
736 estimate a height.

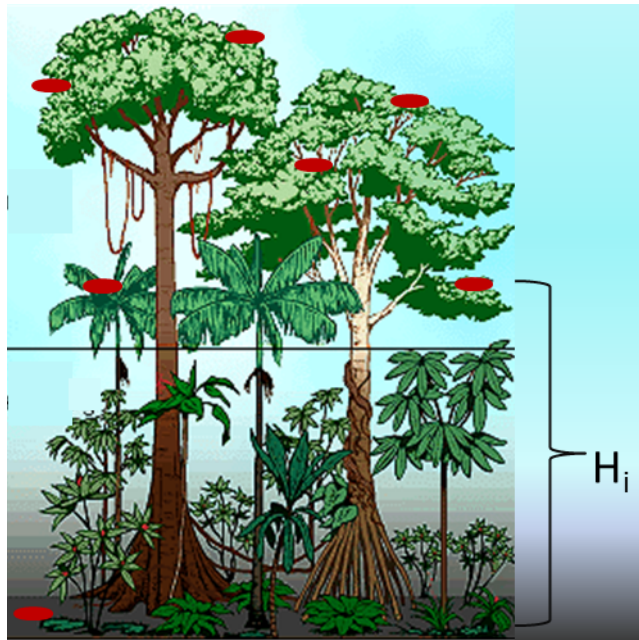
737

### 738 **2.2 Subgroup: Vegetation Parameters**

739 Canopy parameters will be reported on the ATL08 data product in terms of both  
740 the absolute height above the reference ellipsoid as well as the relative height above  
741 an estimated ground. The relative canopy height,  $H_i$ , is computed as the height from  
742 an identified canopy photon minus the interpolated ground surface for the same  
743 horizontal geolocation (see Figure 2.3). Thus, each identified signal photon above an  
744 interpolated surface (including a buffer distance based on the instrument point  
745 spread function) is by default considered a canopy photon. For strong beams, canopy

746 parameters will only be computed for segments where more than 10 of the at least  
 747 50 labeled signal photons are labeled as canopy photons. For weak beams, canopy  
 748 parameters will only be computed for segments having at least 30 signal photons with  
 749 6 of them being labeled as canopy photons.

750



751

752 Figure 2.4. Illustration of canopy photons (red dots) interaction in a vegetated area.  
 753 Relative canopy heights,  $H_i$ , are computed by differencing the canopy photon height from  
 754 an interpolated terrain surface.

755 Table 2.2. Summary table of canopy parameters on ATL08.

Group	Data type	Description	Source
<b>segment_id_beg</b>	Integer	First along-track segment_id number in 100-m segment	ATL03
<b>segment_id_end</b>	Integer	Last along-track segment_id number in 100-m segment	ATL03
<b>canopy_h_metrics_abs</b>	Float	Absolute (H##) canopy height metrics calculated at the following percentiles: 5, 10, 15, 20, 25, 30, 35, 40, 45, 50, 55, 60, 65, 70, 75, 80, 85, 90, 95.	computed
<b>canopy_h_metrics</b>	Float	Relative (RH##) canopy height metrics calculated at the following percentiles:	computed

---

		5, 10, 15, 20, 25, 30, 35, 40, 45, 50, 55, 60, 65, 70, 75, 80, 85, 90, 95.	
<b>h_canopy_abs</b>	Float	98% height of all the individual absolute canopy heights (height above WGS84 ellipsoid) for segment.	computed
<b>h_canopy</b>	Float	98% height of all the individual relative canopy heights (height above terrain) for segment.	computed
<b>h_canopy_20m</b>	Float	98% height of all the individual relative canopy heights (height above terrain) for 20m geosegment.	
<b>h_mean_canopy_abs</b>	Float	Mean of individual absolute canopy heights within segment	computed
<b>h_mean_canopy</b>	Float	Mean of individual relative canopy heights within segment	computed
<b>h_dif_canopy</b>	Float	Difference between h_canopy and canopy_h_metrics(50)	computed
<b>h_min_canopy_abs</b>	Float	Minimum of individual absolute canopy heights within segment	computed
<b>h_min_canopy</b>	Float	Minimum of individual relative canopy heights within segment	computed
<b>h_max_canopy_abs</b>	Float	Maximum of individual absolute canopy heights within segment. Should be equivalent to H100	computed
<b>h_max_canopy</b>	Float	Maximum of individual relative canopy heights within segment. Should be equivalent to RH100	computed
<b>h_canopy_uncertainty</b>	Float	Uncertainty of the relative canopy height (h_canopy)	computed
<b>canopy_openness</b>	Float	STD of relative heights for all photons classified as canopy photons within the segment to provide inference of canopy openness	computed
<b>toc_roughness</b>	Float	STD of relative heights of all photons classified as top of canopy within the segment	computed
<b>h_canopy_quad</b>	Float	Quadratic mean canopy height	computed
<b>n_ca_photons</b>	Integer4	Number of canopy photons within 100 m segment	computed
<b>n_toc_photons</b>	Integer4	Number of top of canopy photons within 100 m segment	computed
<b>centroid_height</b>	Float	Absolute height above reference ellipsoid associated with the centroid of all signal photons	computed
<b>canopy_rh_conf</b>	Integer	Canopy relative height confidence flag based on percentage of ground and canopy photons within a segment: 0	computed

---

---

<b>subset_can_flag</b>	Integer	(<5% canopy), 1 (>5% canopy, <5% ground), 2 (>5% canopy, >5% ground) Quality flag indicating the canopy photons populating the 100 m segment statistics are derived from less than 100 m worth of photons	computed
<b>photon_rate_can</b>	Float	Photon rate of canopy photons within each 100 m segment	computed
<b>photon_rate_can_nr</b>	Float	Noise removed photon canopy rate within each 100 m segment	computed
<b>can_noise</b>	integer	Number of noise photons calculated that fall within the canopy height for each 100 m segment based on ATL03 background rate parameters	computed

---

756

757       **2.2.1 Georeferenced\_segment\_number\_beg**

758           (parameter = segment\_id\_beg). The first along-track segment\_id in each 100-m  
759 segment. Each 100-m segment consists of five sequential 20-m segments provided  
760 from the ATL03 product, which are labeled as segment\_id. The segment\_id is a seven  
761 digit number that uniquely identifies each along track segment, and is written at the  
762 along-track geolocation segment rate (i.e. ~20m along track). The four digit RGT  
763 number can be combined with the seven digit segment\_id number to uniquely define  
764 any along-track segment number. Values are sequential, with 0000001 referring to  
765 the first segment after the equatorial crossing of the ascending node.

766       **2.2.2 Georeferenced\_segment\_number\_end**

767           (parameter = segment\_id\_end). The last along-track segment\_id in each 100-m  
768 segment. Each 100-m segment consists of five sequential 20-m segments provided  
769 from the ATL03 product, which are labeled as segment\_id. The segment\_id is a seven  
770 digit number that uniquely identifies each along track segment, and is written at the  
771 along-track geolocation segment rate (i.e. ~20m along track). The four digit RGT  
772 number can be combined with the seven digit segment\_id number to uniquely define  
773 any along-track segment number. Values are sequential, with 0000001 referring to  
774 the first segment after the equatorial crossing of the ascending node.

775           **2.2.3 Canopy\_height\_metrics\_abs**

776           (parameter = canopy\_h\_metrics\_abs). The absolute height metrics (H##) of  
777 classified canopy photons (labels 2 and 3) above the ellipsoid. The height metrics are  
778 sorted based on a cumulative distribution and calculated at the following percentiles:  
779 10, 15, 20, 25, 30, 35, 40, 45, 50, 55, 60, 65, 70, 75, 80, 85, 90, 95. These height metrics  
780 are often used in the literature to characterize vertical structure of vegetation. One  
781 important distinction of these canopy height metrics compared to those derived from  
782 other lidar systems (e.g., LVIS or GEDI) is that the ICESat-2 canopy height metrics are  
783 heights above the ground surface. These metrics do not include the ground photons.  
784 Required input data are the relative canopy heights of all canopy photons above the  
785 estimated terrain surface and the mid-segment elevation. The absolute canopy  
786 heights metrics are determined by adding the relative canopy height metric to the  
787 best-fit terrain (h\_te\_bestfit). For cases where the h\_te\_bestfit is invalid, the  
788 cumulative distribution will be calculated for the absolute canopy heights (not the  
789 relative canopy heights) and those cumulative heights will be reported.

790

791           **2.2.4 Canopy\_height\_metrics**

792           (parameter = canopy\_h\_metrics). Relative height metrics above the estimated  
793 terrain surface (RH##) of classified canopy photons (labels 2 and 3). The height  
794 metrics are sorted based on a cumulative distribution and calculated at the following  
795 percentiles: 10, 15, 20, 25, 30, 35, 40, 45, 50, 55, 60, 65, 70, 75, 80, 85, 90, 95. These  
796 height metrics are often used in the literature to characterize vertical structure of  
797 vegetation. One important distinction of these canopy height metrics compared to  
798 those derived from other lidar systems (e.g., LVIS or GEDI) is that the ICESat-2 canopy  
799 height metrics are heights above the ground surface. These metrics do not include the  
800 ground photons. Required input data are relative canopy heights above the estimated  
801 terrain surface for all canopy photons.

802           **2.2.5 Absolute\_segment\_canopy\_height**

803           (parameter = h\_canopy\_abs). The absolute 98% height of classified canopy  
804 photon heights (labels 2 and 3) above the ellipsoid. The relative height from classified  
805 canopy photons are sorted into a cumulative distribution, and the height associated  
806 with the 98% height above the h\_te\_bestfit for that segment is reported. For cases  
807 where the h\_te\_bestfit is invalid, the cumulative distribution will be calculated for the  
808 absolute canopy heights and the 98% absolute height will be reported.

809           **2.2.6 Segment\_canopy\_height**

810           (parameter = h\_canopy). The relative 98% height of classified canopy photon  
811 heights (labels 2 and 3) above the estimated terrain surface. Relative canopy heights  
812 have been computed by differencing the canopy photon height from the estimated  
813 terrain surface in the ATL08 processing. The relative canopy heights are sorted into  
814 a cumulative distribution, and the height associated with the 98% height is reported.

815           **2.2.7 canopy\_height GeoSegment {1:5}**

816           (parameter = h\_canopy\_20m). The relative 98% height of classified canopy  
817 photon heights (labels 2 and 3) above the estimated terrain surface in each 20 m  
818 geosegment. Relative canopy heights have been computed by differencing the canopy  
819 photon height from the estimated terrain surface in the ATL08 processing. The  
820 relative canopy heights are sorted into a cumulative distribution, and the height  
821 associated with the 98% height is reported. For segments that do not have a sufficient  
822 number of photons, an invalid (or fill) value will be reported. Each 20 m geo-segment  
823 shall have 10 signal photons as a minimum number to be used for calculations and a  
824 minimum of 3 canopy photons are required to estimate a height.

825

826

827           **2.2.8** Absolute\_segment\_mean\_canopy

828           (parameter = h\_mean\_canopy\_abs). The absolute mean canopy height for the  
829 segment. relative canopy heights are the photons heights for canopy photons (labels  
830 2 and 3) above the estimated terrain surface. These relative heights are averaged and  
831 then added to h\_te\_bestfit.

832           **2.2.9** Segment\_mean\_canopy

833           (parameter = h\_mean\_canopy). The mean canopy height for the segment.  
834 Relative canopy heights have been computed by differencing the canopy photon  
835 height (labels 2 and 3) from the estimated terrain surface in the ATL08 processing.  
836 These heights are averaged.

837           **2.2.10** Segment\_dif\_canopy

838           (parameter = h\_dif\_canopy). Difference between h\_canopy and  
839 canopy\_h\_metrics(50). This parameter is one metric used to describe the vertical  
840 distribution of the canopy within the segment.

841           **2.2.11** Absolute\_segment\_min\_canopy

842           (parameter = h\_min\_canopy\_abs). The minimum absolute canopy height for  
843 the segment. Relative canopy heights are the photons heights for canopy photons  
844 (labels 2 and 3) above the estimated terrain surface. Required input data is classified  
845 point cloud (i.e. photons labeled as either canopy or ground in the ATL08 processing).  
846 The minimum relative canopy height for each segment is added to h\_te\_bestfit and  
847 reported as the absolute minimum canopy height.

848           **2.2.12** Segment\_min\_canopy

849           (parameter = h\_min\_canopy). The minimum relative canopy height for the  
850 segment. Canopy heights are the photons heights for canopy photons (labels 2 and 3)  
851 differenced from the estimated terrain surface. Required input data is classified point  
852 cloud (i.e. photons labeled as either canopy or ground in the ATL08 processing).

853           **2.2.13 Absolute\_segment\_max\_canopy**

854           (parameter = h\_max\_canopy\_abs). The maximum absolute canopy height for  
855 the segment. This parameter is equivalent to H100 metric reported in the literature.  
856 This parameter, however, has the potential for error as random solar background  
857 noise may not have been fully rejected. It is recommended that h\_canopy or  
858 h\_canopy\_abs (i.e., the 98% canopy height) be considered as the top of canopy  
859 measurement. Required input data is classified point cloud (i.e. photons labeled as  
860 either canopy or ground in the ATL08 processing). The absolute max canopy height  
861 is the maximum relative canopy height added to h\_te\_bestfit.

862           **2.2.14 Segment\_max\_canopy**

863           (parameter = h\_max\_canopy). The maximum relative canopy height for the  
864 segment. Canopy heights are the photons heights for canopy photons (labels 2 and 3)  
865 differenced from the estimated terrain surface. This product is equivalent to RH100  
866 metric reported in the literature. This parameter, however, has the potential for error  
867 as random solar background noise may not have been fully rejected. It is  
868 recommended that h\_canopy or h\_canopy\_abs (i.e., the 98% canopy height) be  
869 considered as the top of canopy measurement. Required input data is classified point  
870 cloud (i.e. photons labeled as either canopy or ground in the ATL08 processing).

871           **2.2.15 Segment\_canopy\_height\_uncertainty**

872           (parameter = h\_canopy\_uncertainty). Uncertainty of the relative canopy  
873 height for the segment. This uncertainty incorporates all systematic uncertainties  
874 (e.g. timing, orbits, geolocation, etc.) as well as uncertainty from errors of identified  
875 photons. This parameter is described in Section 1, Equation 1.4. If there are not a  
876 sufficient number of ground photons, an invalid value will be reported –no  
877 interpolation will be done. In the case for canopy height uncertainty, the parameter  
878  $\sigma_{segmentclass}$  is comprised of both the terrain uncertainty within the segment but also  
879 the top of canopy residuals. Required input data is classified point cloud (i.e. photons  
880 labeled as either top of canopy or ground in the ATL08 processing). This parameter



881 will be derived from only classified top of canopy photons, label = 3. The canopy  
 882 height uncertainty is derived from Equation 1.4, shown below as Equation 1.5,  
 883 represents the standard deviation of the terrain points and the standard deviation of  
 884 the top of canopy height photons.

$$885 \quad \sigma_{ATL08_{segment\_ch}} = \frac{\sqrt{\sigma_{AtlasLand}^2 + \sigma_{Zrms_{segment\_terrain}}^2 + \sigma_{Zrms_{segment\_toc}}^2}}{n_{photons_{segment\_terrain}} + n_{photons_{segment\_toc}}} \quad \text{Eqn 1.5}$$

886

### 887 **2.2.16 Segment\_canopy\_openness**

888 (parameter = canopy\_openness). Standard deviation of relative canopy  
 889 heights within each segment. This parameter will potentially provide an indicator of  
 890 canopy openness (label = 2 and 3) as a greater standard deviation of heights indicates  
 891 greater penetration of the laser energy into the canopy. Required input data is  
 892 classified point cloud (i.e. photons labeled as either canopy or ground in the ATL08  
 893 processing).

### 894 **2.2.17 Segment\_top\_of\_canopy\_roughness**

895 (parameter = toc\_roughness). Standard deviation of relative top of canopy  
 896 heights (label = 3) within each segment. This parameter will potentially provide an  
 897 indicator of canopy variability. Required input data is classified point cloud (i.e.  
 898 photons labeled as the top of the canopy in the ATL08 processing).

### 899 **2.2.18 Segment\_canopy\_quadratic\_height**

900 (parameter = h\_canopy\_quad). The quadratic mean relative height of relative  
 901 canopy heights. The quadratic mean height is computed as:

$$902 \quad qmh = \sqrt{\sum_{i=1}^{n_{ca\_photons}} \frac{h_i^2}{n_{ca\_photons}}}$$

903           **2.2.19 Segment\_number\_canopy\_photons**

904           (parameter = n\_ca\_photons). Number of canopy photons (label = 2) within  
905 each segment. Required input data is classified point cloud (i.e. photons labeled as  
906 either canopy or ground in the ATL08 processing). This parameter does not include  
907 the top of canopy photons. To determine the total number of canopy photons, add  
908 n\_ca\_photons to n\_toc\_photons within each segment.

909           **2.2.20 Segment\_number\_top\_canopy\_photons**

910           (parameter = n\_toc\_photons). Number of top of canopy photons (label = 3)  
911 within each segment. Required input data is classified point cloud (i.e. photons  
912 labeled as top of canopy in the ATL08 processing). To determine the total number of  
913 canopy photons, add n\_ca\_photons to n\_toc\_photons within each segment.

914           **2.2.21 Centroid\_height**

915           (parameter = centroid\_height). Optical centroid of all photons classified as  
916 either canopy or ground points (label = 1 2 or 3) within a segment. The heights used  
917 in this calculation are absolute heights above the reference ellipsoid. This parameter  
918 is equivalent to the centroid height produced on ICESat GLA14.

919           **2.2.22 Segment\_rel\_canopy\_conf**

920           (parameter = canopy\_rh\_conf). Canopy relative height confidence flag based  
921 on percentage of ground photons and percentage of canopy photons (label 2 and 3),  
922 relative to the total classified (ground and canopy, label = 1 2 and 3) photons within  
923 a segment: 0 (<5% canopy), 1 (>5% canopy and <5% ground), 2 (>5% canopy and  
924 >5% ground). This is a measure based on the quantity, not the quality, of the  
925 classified photons in each segment.

926           **2.2.23 Subset\_can\_flag {1:5}**

927           (parameter = subset\_can\_flag). This flag indicates the distribution of identified  
928 canopy photons (label 2 and 3) within each 100 m. The purpose of this flag is to  
929 provide the user with an indication whether the photons contributing to the canopy

930 height estimates are evenly distributed or only partially distributed (i.e. due to cloud  
931 cover or signal attenuation). A 100 m ATL08 segment is comprised of 5 geo-segments.  
932 subset\_can\_flags:

933 -1: no data within geosegment available for analysis

934 0: indicates no canopy photons within geosegment

935 1: indicates canopy photons within geosegment

936 For example, a 100 m ATL08 segment might have the following  
937 subset\_can\_flags: {-1 -1 -1 1 1} which would translate that no photons (canopy or  
938 ground) were available for processing in the first three geosegments. Geosegment 4  
939 and 5 had valid labeled canopy photons. Again, the motivation behind this flag is to  
940 inform the user that, in this example, the 100 m estimate are being derived from only  
941 40 m worth of data.

#### 942 **2.2.24 Segment Canopy Photon Rate**

943 (parameter = photon\_rate\_can). This value indicates the canopy photon rate  
944 within each ATL08 segment. This value is calculated as the total number of canopy  
945 photons (label =2 and 3) divided by the total number of unique laser shots within  
946 each ATL08 segment. The number of laser shots is defined as the number of unique  
947 Delta\_Time values within each segment.

#### 948 **2.2.25 Segment Canopy Photon Rate Reduced**

949 (parameter = photon\_rate\_can\_nr). This value indicates the canopy photon rate  
950 within each ATL08 segment where the background noise photons have been removed  
951 from the calculation. This value is calculated as the total number of canopy photons  
952 (label =2 and 3) minus the canopy noise count (can\_noise) divided by the total  
953 number of unique laser shots within each ATL08 segment. The number of laser shots  
954 is defined as the number of **unique** Delta\_Time values within each segment.

955           **2.2.26 Segment Background Photons in Canopy**

956           (parameter = can\_noise). This value represents the number of background  
957 photons that occur within the canopy height span of the 100 m ATL08 segment. Using  
958 the parameters from the ATL03 bckgrd\_atlas subgroup (bckgrd\_counts\_reduced) and  
959 (bckgrd\_in\_height\_reduced) we calculate the background noise rate (counts/m). The  
960 background noise rate is averaged across the ATL08 and finally multiplied by the  
961 ATL08 relative canopy height\_(h\_canopy).

962           Pseudocode for background noise photon removal

```
963           bcr = ATL03[gt + '/bckgrd_atlas/bckgrd_counts_reduced']
964           bihr = ATL03[gt + '/bckgrd_atlas/bckgrd_int_height_reduced']
965 # Calculate the Background Count Error Rate
966           rate = bcr / bihr
967
968 # Append the error rate from the 'Background Atlas' bins to the ATL03 Photon Level
969           ph_rate = rate[inds]
970
971 # Aggregate the error rate to the ATL08 rate by calculating the mean ph_rate
972           f08_rate = mean(ph_rate)
973
974 # Multiply the photon error rate at the ATL08 level to the h_max_canopy
975           canopy_noise_count = (f08_rate) * h_canopy
976
```

977           **2.3 Subgroup: Photons**

978           The subgroup for photons contains the classified photons that were used to  
979 generate the parameters within the land or canopy subgroups. Each photon that is  
980 identified as being likely signal will be classified as: 0 = noise, 1 = ground, 2 = canopy,

981 or 3 = top of canopy. The index values for each classified photon will be provided such  
 982 that they can be extracted from the ATL03 data product for independent evaluation.

983 Table 2.3. Summary table for photon parameters for the ATL08 product.

Group	Data Type	Description	Source
<b>classified_PC_idx</b>	Float	Indices of photons tracking back to ATL03 that surface finding software identified and used within the creation of the data products.	ATL03
<b>classified_PC_flag</b>	Integer	Classification flag for each photon as either noise, ground, canopy, or top of canopy.	computed
<b>ph_segment_id</b>	Integer	Georeferenced bin number (20-m) associated with each photon	ATL03
<b>ph_h</b>	Float	Height of photon above interpolated ground surface	computed
<b>d_flag</b>	Integer	Flag indicating whether DRAGANN labeled the photon as noise or signal	computed

984

985 **2.3.1 Indices\_of\_classed\_photons**

986 (parameter = `classified_PC_idx`). Indices of photons tracking back to ATL03 that  
 987 surface finding software identified and used within the creation of the data products  
 988 for a given segment.

989 **2.3.2 Photon\_class**

990 (parameter = `classified_PC_flag`). Classification flags for a given segment. 0 =  
 991 noise, 1 = ground, 2 = canopy, 3 = top of canopy. The final ground and canopy  
 992 classification are flags 1-3. The full canopy is the combination of flags 2 and 3.

993 **2.3.3 Georeferenced\_segment\_number**

994 (parameter = `ph_segment_id`). The `segment_id` associated with every photon in  
 995 each 100-m segment. Each 100-m segment consists of five sequential 20-m segments

996 provided from the ATL03 product, which are labeled as `segment_id`. The `segment_id`  
 997 is a seven digit number that uniquely identifies each along track segment, and is  
 998 written at the along-track geolocation segment rate (i.e. ~20m along track). The four  
 999 digit RGT number can be combined with the seven digit `segment_id` number to  
 1000 uniquely define any along-track segment number. Values are sequential, with  
 1001 0000001 referring to the first segment after the equatorial crossing of the ascending  
 1002 node.

1003 **2.3.4 Photon Height**

1004 (parameter = `ph_h`). Height of the photon above the interpolated ground  
 1005 surface at the location of the photon.

1006 **2.3.5 DRAGANN\_flag**

1007 (parameter = `d_flag`). Flag indicating the labeling of DRAGANN noise filtering for  
 1008 a given photon. 0 = noise, 1=signal.

1009

1010 **2.4 Subgroup: Reference data**

1011 The reference data subgroup contains parameters and information that are  
 1012 useful for determining the terrain and canopy heights that are reported on the  
 1013 product. In addition to position and timing information, these parameters include the  
 1014 reference DEM height, reference landcover type, and flags indicating water or snow.

1015 Table 2.4. Summary table for reference parameters for the ATL08 product.

Group	Data Type	Description	Source
<b>segment_id_beg</b>	Integer	First along-track <code>segment_id</code> number in 100-m segment	ATL03
<b>segment_id_end</b>	Integer	Last along-track <code>segment_id</code> number in 100-m segment	ATL03
<b>latitude</b>	Float	Center latitude of signal photons within each segment	ATL03

<b>longitude</b>	Float	Center longitude of signal photons within each segment	ATL03
<b>delta_time</b>	Float	Mid-segment GPS time in seconds past an epoch. The epoch is provided in the metadata at the file level	ATL03
<b>delta_time_beg</b>	Float	Delta time of the first photon in the segment	ATL03
<b>delta_time_end</b>	Float	Delta time of the last photon in the segment	ATL03
<b>night_flag</b>	Integer	Flag indicating whether the measurements were acquired during night time conditions	computed
<b>dem_h</b>	Float4	Reference DEM elevation	external
<b>dem_flag</b>		Source of reference DEM	external
<b>dem_removal_flag</b>	Integer	Quality check flag to indicate > 20% photons removed due to large distance from dem_h	computed
<b>h_dif_ref</b>	Float4	Difference between h_te_median and dem_h	computed
<b>terrain_flg</b>	Integer	Terrain flag quality check to indicate a deviation from the reference DTM	computed
<b>segment_landcover</b>	Integer4	Reference landcover for segment derived from best global landcover product available	external
<b>segment_watermask</b>	Integer4	Water mask indicating inland water produced from best sources available	external
<b>segment_snowcover</b>	Integer4	Daily snow cover mask derived from best sources	external
<b>urban_flag</b>	Integer	Flag indicating segment is located in an urban area	external
<b>surf_type</b>	Integer1	Flags describing surface types: 0=not type, 1=is type. Order of array is land, ocean, sea ice, land ice, inland water.	ATL03
<b>atl08_region</b>	Integer	ATL08 region(s) encompassed by ATL03 granule being processed	computed
<b>last_seg_extend</b>	Float	The distance (km) that the last ATL08 processing segment in a file is either extended or overlapped with	computed

---

		the previous ATL08 processing segment	
<b>brightness_flag</b>	Integer	Flag indicating that the ground surface is bright (e.g. snow-covered or other bright surfaces)	computed

---

1016

1017       **2.4.1** Georeferenced\_segment\_number\_beg

1018           (parameter = segment\_id\_beg). The first along-track segment\_id in each 100-m  
 1019 segment. Each 100-m segment consists of five sequential 20-m segments provided  
 1020 from the ATL03 product, which are labeled as segment\_id. The segment\_id is a seven  
 1021 digit number that uniquely identifies each along track segment, and is written at the  
 1022 along-track geolocation segment rate (i.e. ~20m along track). The four digit RGT  
 1023 number can be combined with the seven digit segment\_id number to uniquely define  
 1024 any along-track segment number. Values are sequential, with 0000001 referring to  
 1025 the first segment after the equatorial crossing of the ascending node.

1026       **2.4.2** Georeferenced\_segment\_number\_end

1027           (parameter = segment\_id\_end). The last along-track segment\_id in each 100-m  
 1028 segment. Each 100-m segment consists of five sequential 20-m segments provided  
 1029 from the ATL03 product, which are labeled as segment\_id. The segment\_id is a seven  
 1030 digit number that uniquely identifies each along track segment, and is written at the  
 1031 along-track geolocation segment rate (i.e. ~20m along track). The four digit RGT  
 1032 number can be combined with the seven digit segment\_id number to uniquely define  
 1033 any along-track segment number. Values are sequential, with 0000001 referring to  
 1034 the first segment after the equatorial crossing of the ascending node.

1035       **2.4.3** Segment\_latitude

1036           (parameter = latitude). Center latitude of signal photons within each segment.  
 1037 Each 100 m segment consists of 5 20m ATL03 geosegments. In most cases, there will  
 1038 be signal photons in each of the 5 geosegments necessary for calculating a latitude  
 1039 value. For instances where the 100 m ATL08 is not fully populated with photons (e.g.



1040 photons drop out due to clouds or signal attenuation), the latitude will be interpolated  
1041 to the mid-point of the 100 m segment. To implement this interpolation, we confirm  
1042 that each 100 m segment is comprised of at least 3 unique ATL03 geosegments IDs,  
1043 indicating that data is available near the mid-point of the land segment. If less than 3  
1044 ATL03 segments are available, the coordinate is interpolated based on the ratio of  
1045 delta time at the centermost ATL03 segment and that of the centermost photon, thus  
1046 applying the centermost photon's coordinates to represent the land segment with a  
1047 slight adjustment. In some instances, the latitude and longitude will require  
1048 extrapolation to estimate a mid-100 m segment location. It is possible that in these  
1049 extremely rare cases, the latitude and longitude could not represent the true center  
1050 of the 100 m segment. We encourage the user to investigate the parameters  
1051 `segment_te_flag` and `segment_can_flag` which provide information as to the number  
1052 and distribution of signal photons within each 100 m segment.

#### 1053 **2.4.4** `Geosegment_latitude{1:5}`

1054 (parameter = `latitude_20m`). Interpolated center latitude of each 20 m  
1055 geosegment.

#### 1056 **2.4.5** `Segment_longitude`

1057 (parameter = `longitude`). Center longitude of signal photons within each  
1058 segment. Each 100 m segment consists of 5 20m geosegments. In most cases, there  
1059 will be signal photons in each of the 5 geosegments necessary for calculating a  
1060 longitude value. For instances where the 100 m ATL08 is not fully populated with  
1061 photons (e.g. photons drop out due to clouds or signal attenuation), the latitude will  
1062 be interpolated to the mid-point of the 100 m segment. To implement this  
1063 interpolation, we confirm that each 100 m segment is comprised of at least 3 unique  
1064 ATL03 geosegments IDs, indicating that data is available near the mid-point of the  
1065 land segment. If less than 3 ATL03 segments are available, the coordinate is  
1066 interpolated based on the ratio of delta time at the centermost ATL03 segment and  
1067 that of the centermost photon, thus applying the centermost photon's coordinates to  
1068 represent the land segment with a slight adjustment. In some instances, the latitude

1069 and longitude will require extrapolation to estimate a mid-100 m segment location. It  
1070 is possible that in these extremely rare cases, the latitude and longitude could not  
1071 represent the true center of the 100 m segment. We encourage the user to investigate  
1072 the parameters `segment_te_flag` and `segment_can_flag` which provide information as to  
1073 the number and distribution of signal photons within each 100 m segment.

#### 1074 **2.4.6** `Geosegment_longitude{1:5}`

1075 (parameter = `longitude_20m`). Interpolated center longitude of each 20 m  
1076 geosegment.

1077

#### 1078 **2.4.7** `Delta_time`

1079 (parameter = `delta_time`). Mid-segment GPS time for the segment in seconds  
1080 past an epoch. The epoch is listed in the metadata at the file level.

#### 1081 **2.4.8** `Delta_time_beg`

1082 (parameter = `delta_time_beg`). Delta time for the first photon in the segment  
1083 in seconds past an epoch. The epoch is listed in the metadata at the file level.

#### 1084 **2.4.9** `Delta_time_end`

1085 (parameter = `delta_time_end`). Delta time for the last photon in the segment  
1086 in seconds past an epoch. The epoch is listed in the metadata at the file level.

#### 1087 **2.4.10** `Night_Flag`

1088 (parameter = `night_flag`). Flag indicating the data were acquired in night  
1089 conditions: 0 = day, 1 = night. Night flag is set when solar elevation is below 0.0  
1090 degrees.

#### 1091 **2.4.11** `Segment_reference_DTM`

1092 (parameter = `dem_h`). Reference terrain height value for segment determined  
1093 by the “best” DEM available based on data location. All heights in ICESat-2 are

1094 referenced to the WGS 84 ellipsoid unless clearly noted otherwise. DEM is taken from  
1095 a variety of ancillary data sources: MERIT, GIMP, GMTED, MSS. The DEM source flag  
1096 indicates which source was used.

#### 1097 **2.4.12** Segment\_reference\_DEM\_source

1098 (parameter = dem\_flag). Indicates source of the reference DEM height. Values:  
1099 0=None, 1=GIMP, 2=GMTED, 3=MSS, 4=MERIT.

#### 1100 **2.4.13** Segment\_reference\_DEM\_removal\_flag

1101 (parameter = dem\_removal\_flag). Quality check flag to indicate > 20%  
1102 classified photons removed from land segment due to large distance from dem\_h.

#### 1103 **2.4.14** Segment\_terrain\_difference

1104 (parameter = h\_dif\_ref). Difference between h\_te\_median and dem\_h. Since the  
1105 mean terrain height is more sensitive to outliers, the median terrain height will be  
1106 evaluated against the reference DEM. This parameter will be used as an internal data  
1107 quality check with the notion being that if the difference exceeds a threshold (TBD) a  
1108 terrain quality flag (terrain\_flg) will be triggered.

#### 1109 **2.4.15** Segment\_terrain flag

1110 (parameter = terrain\_flg). Terrain flag to indicate confidence in the derived  
1111 terrain height estimate. If h\_dif\_ref exceeds a threshold (TBD) the terrain\_flg  
1112 parameter will be set to 1. Otherwise, it is 0.

#### 1113 **2.4.16** Segment\_landcover

1114 (parameter = segment\_landcover). Updating the segment landcover with the  
1115 2019 Copernicus Landcover 100 m discrete landcover product which incorporates 23  
1116 discrete landcover classes which follow the UN-FAO's Land Cover Classification  
1117 System. The ATL08 landcover segment will be the Copernicus Landcover value at the  
1118 segment latitude/longitude. <https://land.copernicus.eu/global/products/lc>  
1119 (<https://doi.org/10.5281/zenodo.3939050>).

<b>Map Code</b>	<b>Landcover Class</b>	<b>Definition according to UN LCCS</b>
0	No data	
111	Closed forest, evergreen needle leaf	Tree canopy >70%, almost all needle leaf trees remain green all year. Canopy is never without green foliage
113	Closed forest, deciduous needle leaf	Tree canopy >70%, consists of seasonal needle leaf communities with an annual cycle of leaf-on and leaf-off periods.
112	Closed forest, evergreen broad leaf	Tree canopy >70%, almost all broadleaf trees remain green year round. Canopy is never without green foliage
114	Closed forest, deciduous broad leaf	Tree canopy >70%, consists of seasonal broad leaf communities with an annual cycle of leaf-on and leaf-off periods.
115	Closed forest, mixed	Closed forest, mix of types
116	Closed forest, unknown	Closed forest, not matching any of the other definitions
121	Open forest, evergreen needle leaf	Top layer- trees 15-70% and second layer mixed of shrubs and grassland, almost all needle leaf trees remain green all year. Canopy is never without green foliage
123	Open forest, deciduous needle leaf	Top layer- trees 15-70% and second layer mixed of shrubs and grassland, consists of seasonal needle leaf tree communities with an annual cycle of leaf-on and leaf-off
122	Open forest, evergreen broad leaf	Top layer- trees 15-70% and second layer mixed of shrubs and grassland, almost all broad leaf trees remain green all year. Canopy is never without green foliage
124	Open forest, deciduous broad leaf	Top layer- trees 15-70% and second layer mixed of shrubs and grassland, consists of seasonal broad leaf tree communities with an annual cycle of leaf-on and leaf-off
125	Open forest, mixed	Open forest, mix of types
126	Open forest, unknown	Open forest, not matching any of the other definitions
20	Shrubs	Woody perennial plants with persistent and woody stems and without a main stem being less than 5m. The shrub foliage can be either evergreen or deciduous.
30	Herbaceous	Plants without persistent stems or shoots above ground and lacking firm structure. Tree and shrub cover is less than 10%
90	Herbaceous Wetland	Lands with a permanent mixture of water and herbaceous or woody vegetation. The vegetation can be present in salt, brackish, or fresh water.
100	Moss and lichen	Moss and lichen
60	Bare/sparse vegetation	Lands with exposed soil, sand, or rocks and never has more than 10% vegetation cover during any time of the year
40	Cultivated and managed vegetation/agriculture	Lands covered with temporary crops followed by harvest and a bare soil period.

50	Urban/built up	Land covered by buildings or other man-made structures
70	Snow and ice	Land under snow or ice throughout the year
80	Permanent water bodies	Lakes, reservoirs, and rivers. Can be either fresh or salt-water bodies
200	Open sea	Oceans, seas. Can be either fresh or salt-water bodies.

1120

1121

1122

1123        **2.4.17 Segment\_Woody Vegetation Fractional Cover**

1124            (parameter = segment\_cover). Woody vegetation fractional cover derived  
1125 from the 2019 Copernicus 100 m shrub and forest fractional cover data products. The  
1126 woody cover fractional cover is the simple addition of the forest fractional cover with  
1127 the shrub fractional cover. The ATL08 woody vegetation fractional cover value shall  
1128 be the pixel value at the segment latitude/longitude. The Copernicus data products  
1129 can be found at <https://lcviewer.vito.be/download>

1130        **2.4.18 Segment\_watermask**

1131            (parameter = segment\_watermask). Water mask (i.e., flag) indicating inland  
1132 water as referenced from the Global Raster Water Mask at 250 m spatial resolution  
1133 (Carroll et al, 2009; available online at <http://glcf.umd.edu/data/watermask/>). 0 =  
1134 no water; 1 = water.

1135        **2.4.19 Segment\_snowcover**

1136            (parameter = segment\_snowcover). Daily snowcover mask (i.e., flag)  
1137 indicating a likely presence of snow or ice within each segment produced from best  
1138 available source used for reference. The snow mask will be the same snow mask as  
1139 used for ATL09 Atmospheric Products: NOAA snow-ice flag. 0=ice free water;  
1140 1=snow free land; 2=snow; 3=ice.

#### 1141       **2.4.20 Urban\_flag**

1142           (parameter = urban\_flag). Segment estimated urban cover flag as derived  
1143 from the Global Urban Footprint (GUF) data product. GUF is a global mapping of  
1144 urban areas derived from the TerraSAR-X and TanDEM-X satellites. The GUF maps  
1145 at a resolution of ~12 m (0.4 arcseconds). Due to differences in resolution, the  
1146 ATL08 GUF value is set based upon a 4x4 block of pixels about the 100 m segment  
1147 latitude/longitude . If ANY of the pixels the GUF pixels are labeled as urban, the  
1148 ATL08 GUF value is set to urban. The GUF urban flag is set as -1 = undetermined, 0 =  
1149 not urban, 1 = urban. The GUF data are available from DLR  
1150 [https://www.dlr.de/eoc/en/desktopdefault.aspx/tabid-9628/16557\\_read-40454/](https://www.dlr.de/eoc/en/desktopdefault.aspx/tabid-9628/16557_read-40454/)

#### 1151       **2.4.21 Surface Type**

1152           (parameter = surf\_type). The surface type for a given segment is determined at  
1153 the major frame rate (every 200 shots, or ~140 meters along-track) and is a two-  
1154 dimensional array surf\_type(n, nsurf), where n is the major frame number, and nsurf  
1155 is the number of possible surface types such that surf\_type(n, isurf) is set to 0 or 1  
1156 indicating if surface type isurf is present (1) or not (0), where isurf = 1 to 5 (land,  
1157 ocean, sea ice, land ice, and inland water) respectively.

#### 1158       **2.4.22 ATL08\_region**

1159           (parameter = atl08\_region). The ATL08 regions that encompass the ATL03  
1160 granule being processed through the ATL08 algorithm. The ATL08 regions are shown  
1161 by Figure 2.3.

#### 1162       **2.4.23 Last\_segment\_extend**

1163           (parameter = last\_seg\_extend). The distance (km) that the last ATL08 10 km  
1164 processing segment is either extended beyond 10 km or uses data from the previous  
1165 10 km processing segment to allow for enough data for processing the ATL03 photons  
1166 through the ATL08 algorithm. If the last portion of an ATL03 granule being processed  
1167 would result in a segment with less than 3.4 km (170 geosegments) worth of data,

1168 that last portion is added to the previous 10 km processing window to be processed  
1169 together as one extended ATL08 processing segment. The resulting last\_seg\_extend  
1170 value would be a positive value of distance beyond 10 km that the ATL08 processing  
1171 segment was extended by. If the last ATL08 processing segment would be less than  
1172 10 km but greater than 3.4 km, a portion extending from the start of current ATL08  
1173 processing segment backwards into the previous ATL08 processing segment would  
1174 be added to the current ATL08 processing segment to make it 10 km in length. The  
1175 distance of this backward data gathering would be reported in last\_seg\_extend as a  
1176 negative distance value. Only new 100 m ATL08 segment products generated from  
1177 this backward extension would be reported. All other segments that are not extended  
1178 will report a last\_seg\_extend value of 0.

#### 1179 **2.4.24** Brightness\_flag

1180 (parameter = brightness\_flag). Based upon the classification of the photons  
1181 within each 100 m, this parameter flags ATL08 segments where the mean number of  
1182 ground photons per shot exceed a value of 3. This calculation can be made as the total  
1183 number of ground photons divided by the number of ATLAS shots within the 100 m  
1184 segment. A value of 0 = indicates non-bright surface, value of 1 indicates bright  
1185 surface, and a value of 2 indicates “undetermined” due to clouds or other factors. The  
1186 brightness is computed initially on the 10 km processing segment. If the ground  
1187 surface is determined to be bright for the entire 10 km segment, the brightness is then  
1188 calculated at the 100 m segment size.

1189

### 1190 **2.5 Subgroup: Beam data**

1191 The subgroup for beam data contains basic information on the geometry and  
1192 pointing accuracy for each beam.

1193

1194 Table 2.5. Summary table for beam parameters for the ATL08 product.

<b>Group</b>	<b>Data Type</b>	<b>Units</b>	<b>Description</b>	<b>Source</b>
<b>segment_id_beg</b>	Integer		First along-track segment_id number in 100-m segment	ATL03
<b>segment_id_end</b>	Integer		Last along-track segment_id number in 100-m segment	ATL03
<b>ref_elev</b>	Float		Elevation of the unit pointing vector for the reference photon in the local ENU frame in radians. The angle is measured from East-North plane and positive towards up	ATL03
<b>ref_azimuth</b>	Float		Azimuth of the unit pointing vector for the reference photon in the ENU frame in radians. The angle is measured from North and positive toward East.	ATL03
<b>atlas_pa</b>	Float		Off nadir pointing angle of the spacecraft	ATL03
<b>rgt</b>	Integer		The reference ground track (RGT) is the track on the earth at which the vector bisecting laser beams 3 and 4 is pointed during repeat operations	ATL03
<b>sigma_h</b>	Float		Total vertical uncertainty due to PPD and POD	ATL03
<b>sigma_along</b>	Float		Total along-track uncertainty due to PPD and POD knowledge	ATL03
<b>sigma_across</b>	Float		Total cross-track uncertainty due to PPD and POD knowledge	ATL03
<b>sigma_topo</b>	Float		Uncertainty of the geolocation knowledge due to local topography (Equation 1.3)	computed



<b>sigma_atlas_land</b>	Float	Total uncertainty that includes sigma_h plus the geolocation uncertainty due to local slope Equation 1.2	computed
<b>psf_flag</b>	integer	Flag indicating sigma_atlas_land (aka PSF) as computed in Equation 1.2 exceeds a value of 1m.	computed
<b>layer_flag</b>	Integer	Cloud flag indicating presence of clouds or blowing snow	ATL09
<b>cloud_flag_atm</b>	Integer	Cloud confidence flag from ATL09 indicating clear skies	ATL09
<b>msw_flag</b>	Integer	Multiple scattering warning product produced on ATL09	ATL09
<b>cloud_fold_flag</b>	integer	Cloud flag to indicate potential of high clouds that have “folded” into the lower range bins	ATL09
<b>asr</b>	Float	Apparent surface reflectance	ATL09
<b>snr</b>	Float	Background signal to noise level	Computed
<b>solar_azimuth</b>	Float	The azimuth (in degrees) of the sun position vector from the reference photon bounce point position in the local ENU frame. The angle is measured from North and is positive towards East.	ATL03g
<b>solar_elevation</b>	Float	The elevation of the sun position vector from the reference photon bounce point position in the local ENU frame. The angle is measured from the East-North plane and is positive Up.	ATL03g
<b>n_seg_ph</b>	Integer	Number of photons within each land segment	computed

<b>ph_ndx_beg</b>	Integer	Photon index begin	computed
<b>sat_flag</b>	Integer	Flag derived from full_sat_fract and near_sat_fract on the ATL03 data product	computed

1195

1196       **2.5.1** Georeferenced\_segment\_number\_beg

1197           (parameter = segment\_id\_beg). The first along-track segment\_id in each 100-m  
1198 segment. Each 100-m segment consists of five sequential 20-m segments provided  
1199 from the ATL03 product, which are labeled as segment\_id. The segment\_id is a seven  
1200 digit number that uniquely identifies each along track segment, and is written at the  
1201 along-track geolocation segment rate (i.e. ~20m along track). The four digit RGT  
1202 number can be combined with the seven digit segment\_id number to uniquely define  
1203 any along-track segment number. Values are sequential, with 0000001 referring to  
1204 the first segment after the equatorial crossing of the ascending node.

1205       **2.5.2** Georeferenced\_segment\_number\_end

1206           (parameter = segment\_id\_end). The last along-track segment\_id in each 100-m  
1207 segment. Each 100-m segment consists of five sequential 20-m segments provided  
1208 from the ATL03 product, which are labeled as segment\_id. The segment\_id is a seven  
1209 digit number that uniquely identifies each along track segment, and is written at the  
1210 along-track geolocation segment rate (i.e. ~20m along track). The four digit RGT  
1211 number can be combined with the seven digit segment\_id number to uniquely define  
1212 any along-track segment number. Values are sequential, with 0000001 referring to  
1213 the first segment after the equatorial crossing of the ascending node.

1214       **2.5.3** Beam\_coelevation

1215           (parameter = ref\_elev). Elevation of the unit pointing vector for the reference  
1216 photon in the local ENU frame in radians. The angle is measured from East-North  
1217 plane and positive towards up.

1218       **2.5.4** Beam\_azimuth

1219           (parameter = ref\_azimuth). Azimuth of the unit pointing vector for the  
1220 reference photon in the ENU frame in radians. The angle is measured from North and  
1221 positive toward East.

1222       **2.5.5** ATLAS\_Pointing\_Angle

1223           (parameter = atlas\_pa). Off nadir pointing angle (in radians) of the satellite to  
1224 increase spatial sampling in the non-polar regions.

1225       **2.5.6** Reference\_ground\_track

1226           (parameter = rgt). The reference ground track (RGT) is the track on the earth  
1227 at which the vector bisecting laser beams 3 and 4 (or GT2L and GT2R) is pointed  
1228 during repeat operations. Each RGT spans the part of an orbit between two ascending  
1229 equator crossings and are numbered sequentially. The ICESat-2 mission has 1387  
1230 RGTs, numbered from 0001xx to 1387xx. The last two digits refer to the cycle number.

1231       **2.5.7** Sigma\_h

1232           (parameter = sigma\_h). Total vertical uncertainty due to PPD (Precise Pointing  
1233 Determination), POD (Precise Orbit Determination), and geolocation errors.  
1234 Specifically, this parameter includes radial orbit error,  $\sigma_{orbit}$ , tropospheric errors,  
1235  $\sigma_{Trop}$ , forward scattering errors,  $\sigma_{forwardscattering}$ , instrument timing errors,  $\sigma_{timing}$ ,  
1236 and off-nadir pointing geolocation errors. The component parameters are pulled  
1237 from ATL03 and ATL09. Sigma\_h is the root sum of squares of these terms as detailed  
1238 in Equation 1.1. The sigma\_h reported here is the mean of the sigma\_h values reported  
1239 within the five ATL03 geosegments that are used to create the 100 m ATL08 segment.

1240       **2.5.8** Sigma\_along

1241           (parameter = sigma\_along). Total along-track uncertainty due to PPD and POD  
1242 knowledge. This parameter is pulled from ATL03.

1243        **2.5.9** Sigma\_across

1244            (parameter = sigma\_across). Total cross-track uncertainty due to PPD and  
1245    POD knowledge. This parameter is pulled from ATL03.

1246        **2.5.10** Sigma\_topo

1247            (parameter = sigma\_topo). Uncertainty in the geolocation due to local surface  
1248    slope as described in Equation 1.3. The local slope is multiplied by the 6.5 m  
1249    geolocation uncertainty factor that will be used to determine the geolocation  
1250    uncertainty. The geolocation error will be computed from a 100 m sample due to the  
1251    local slope calculation at that scale.

1252        **2.5.11** Sigma\_ATLAS\_LAND

1253            (parameter = sigma\_atlas\_land). Total vertical geolocation error due to  
1254    ranging, and local surface slope. The parameter is computed for ATL08 as described  
1255    in Equation 1.2. The geolocation error will be computed from a 100 m sample due to  
1256    the local slope calculation at that scale.

1257        **2.5.12** PSF\_flag

1258            (parameter = psf\_flag). Flag indicating that the point spread function  
1259    (computed as sigma\_atlas\_land) has exceeded 1m.

1260        **2.5.13** Layer\_flag

1261            (parameter = layer\_flag). Flag is a combination of multiple ATL09 flags and  
1262    takes daytime/nighttime into consideration. A value of 1 means clouds or blowing  
1263    snow is likely present. A value of 0 indicates the likely absence of clouds or blowing  
1264    snow. If no ATL09 product is available for an ATL08 segment, an invalid value will be  
1265    reported. Since the cloud flags from the ATL09 product are reported at an along-track  
1266    distance of 250 m, we will report the highest value of the ATL09 flags at the ATL08  
1267    resolution (100 m). Thus, if a 100 m ATL08 segment straddles two values from  
1268    ATL09, the highest cloud flag value will be reported on ATL08. This reporting strategy  
1269    holds for all the cloud flags reported on ATL08.

1270        **2.5.14** Cloud\_flag\_atm

1271        (parameter = cloud\_flag\_atm). Cloud confidence flag from ATL09 that indicates  
1272 the number of cloud or aerosol layers identified in each 25Hz atmospheric profile. If  
1273 the flag is greater than 0, aerosols or clouds could be present.

1274        **2.5.15** MSW

1275        (parameter = msw\_flag). Multiple scattering warning flag with values from -1 to  
1276 5 as computed in the ATL09 atmospheric processing and delivered on the ATL09 data  
1277 product. If no ATL09 product is available for an ATL08 segment, an invalid value will  
1278 be reported. MSW flags:

1279                                -1 = signal to noise ratio too low to determine presence of  
1280                                cloud or blowing snow

1281                                0 = no\_scattering

1282                                1 = clouds at > 3 km

1283                                2 = clouds at 1-3 km

1284                                3 = clouds at < 1 km

1285                                4 = blowing snow at < 0.5 optical depth

1286                                5 = blowing snow at >= 0.5 optical depth

1287        **2.5.16** Cloud Fold Flag

1288        (parameter = cloud\_fold\_flag). Clouds occurring higher than 14 to 15 km in the  
1289 atmosphere will be folded down into the lower portion of the atmospheric profile.

1290        **2.5.17** Computed\_Apparent\_Surface\_Reflectance

1291        (parameter = asr). Apparent surface reflectance computed in the ATL09  
1292 atmospheric processing and delivered on the ATL09 data product. If no ATL09  
1293 product is available for an ATL08 segment, an invalid value will be reported.

1294        **2.5.18** Signal\_to\_Noise\_Ratio

1295            (parameter = snr). The Signal to Noise Ratio of geolocated photons as  
1296 determined by the ratio of the superset of ATL03 signal and DRAGANN found signal  
1297 photons used for processing the ATL08 segments to the background photons (i.e.,  
1298 noise) within the same ATL08 segments.

1299        **2.5.19** Solar\_Azimuth

1300            (parameter = solar\_azimuth). The azimuth (in degrees) of the sun position  
1301 vector from the reference photon bounce point position in the local ENU frame. The  
1302 angle is measured from North and is positive towards East.

1303        **2.5.20** Solar\_Elevation

1304            (parameter = solar\_elevation). The elevation of the sun position vector from  
1305 the reference photon bounce point position in the local ENU frame. The angle is  
1306 measured from the East-North plane and is positive up.

1307        **2.5.21** Number\_of\_segment\_photons

1308            (parameter = n\_seg\_ph). Number of photons in each land segment.

1309        **2.5.22** Photon\_Index\_Begin

1310            (parameter = ph\_ndx\_beg). Index (1-based) within the photon-rate data of  
1311 the first photon within this each land segment.

1312        **2.5.23** Saturation Flag

1313            (parameter = sat\_flag) Saturation flag derived from the ATL03 saturation  
1314 flags full\_sat\_frac. The saturation flags on the ATL03 data product (full\_sat\_frac)  
1315 are the percentage of photons determined to be saturated within each geosegment.  
1316 For the ATL08 saturation flag, a value of 0 will indicate no saturation. A value of 1  
1317 will indicate the average of all 5 geosegment full\_sat\_frac values was over 0.2. This  
1318 value of 1 is an indication of standing water or saturated soils. If an ATL08 segment  
1319 is not fully populated with 5 values for full\_sat\_frac, a value of -1 will be set.

1320        sat\_flag:     -1 indicates not enough valid data to make determination  
1321                        0 indicates no saturation in ATL08 segment  
1322                        1 indicates saturation in ATL08 segment  
1323  
1324  
1325  
1326

## 1327 3 ALGORITHM METHODOLOGY

1328 For the ecosystem community, identification of the ground and canopy surface  
1329 is by far the most critical task, as meeting the science objective of determining global  
1330 canopy heights hinges upon the ability to detect both the canopy surface and the  
1331 underlying topography. Since a space-based photon counting laser mapping system  
1332 is a relatively new instrument technology for mapping the Earth's surface, the  
1333 software to accurately identify and extract both the canopy surface and ground  
1334 surface is described here. The methodology adopted for ATL08 establishes a  
1335 framework to potentially accept multiple approaches for capturing both the upper  
1336 and lower surface of signal photons. One method used is an iterative filtering of  
1337 photons in the along-track direction. This method has been found to preserve the  
1338 topography and capture canopy photons, while rejecting noise photons. An advantage  
1339 of this methodology is that it is self-parameterizing, robust, and works in all  
1340 ecosystems if sufficient photons from both the canopy and ground are available. For  
1341 processing purposes, along-track data signal photons are parsed into  $L$ -km segment  
1342 of the orbit which is recommended to be 10 km in length.

1343

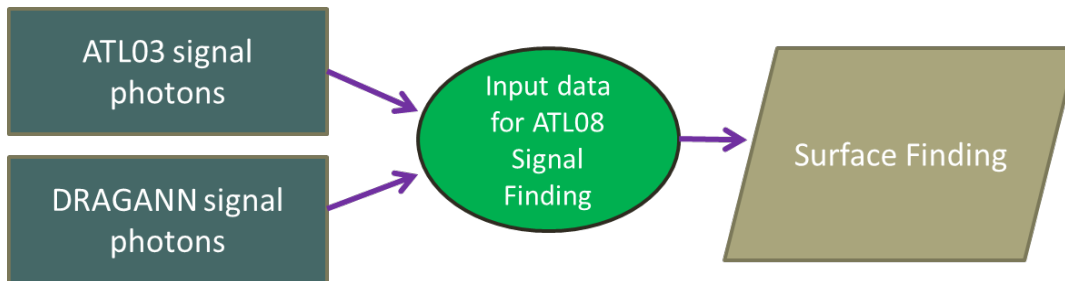
### 1344 3.1 Noise Filtering

1345 Solar background noise is a significant challenge in the analysis of photon  
1346 counting laser data. Range measurement data created from photon counting lidar  
1347 detectors typically contain far higher noise levels than the more common photon  
1348 integrating detectors available commercially in the presence of passive, solar  
1349 background photons. Given the higher detection sensitivity for photon counting  
1350 devices, a background photon has a greater probability of triggering a detection event  
1351 over traditional integral measurements and may sometimes dominate the dataset.  
1352 Solar background noise is a function of the surface reflectance, topography, solar  
1353 elevation, and atmospheric conditions. Prior to running the surface finding  
1354 algorithms used for ATL08 data products, the superset of output from the GSFC  
1355 medium-high confidence classed photons (ATL03 signal\_conf\_ph: flags 3-4) and the



1356 output from DRAGANN will be considered as the input data set. ATL03 input data  
1357 requirements include the latitude, longitude, height, segment delta time, segment ID,  
1358 and a preliminary signal classification for each photon. The motivation behind  
1359 combining the results from two different noise filtering methods is to ensure that all  
1360 of the potential signal photons for land surfaces will be provided as input to the  
1361 surface finding software. The description of the methodology for the ATL03  
1362 classification is described separately in the ATL03 ATBD. The methodology behind  
1363 DRAGANN is described in the following section.

1364



1365

1366 Figure 3.1. Combination of noise filtering algorithms to create a superset of input data for  
1367 surface finding algorithms.

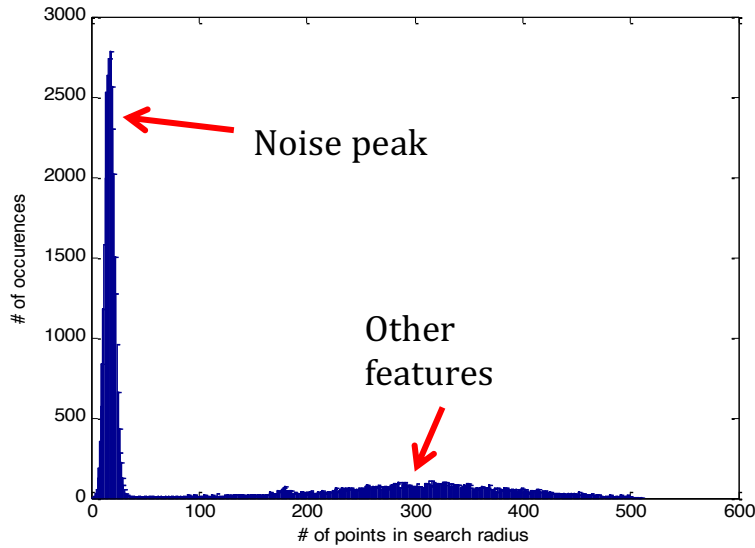
1368

### 1369 **3.1.1 DRAGANN**

1370 The Differential, Regressive, and Gaussian Adaptive Nearest Neighbor  
1371 (DRAGANN) filtering technique was developed to identify and remove noise photons  
1372 from the photon counting data point cloud. DRAGANN utilizes the basic premise that  
1373 signal photons will be closer in space than random noise photons. The first step of the  
1374 filtering is to implement an adaptive nearest neighbor search. By using an adaptive  
1375 method, different thresholds can be applied to account for variable amounts of  
1376 background noise and changing surface reflectance along the data profile. This search  
1377 finds an effective radius by computing the probability of finding P number of points  
1378 within a search area. For MABEL and mATLAS, P=20 points within the search area



1408



1409

1410 Figure 3.2. Histogram of the number of photons within a search radius. This histogram is  
1411 used to determine the threshold for the DRAGANN approach.

1412

1413 Once the radius has been computed, DRAGANN counts the number of points  
1414 within the radius for each point and histograms that set of values. The distribution of  
1415 the number of points, Figure 3.2, reveals two distinct peaks; a noise peak and a signal  
1416 peak. The motivation of DRAGANN is to isolate the signal photons by determining a  
1417 threshold based on the number of photons within the search radius. The noise peak  
1418 is characterized as having a large number of occurrences of photons with just a few  
1419 neighboring photons within the search radius. The signal photons comprise the broad  
1420 second peak. The first step in determining the threshold between the noise and signal  
1421 is to implement Gaussian fitting to the number of photons distribution (i.e., the  
1422 distribution shown in Figure 3.2). The Gaussian function has the form

1423

1424 
$$g(x) = ae^{-\frac{(x-b)^2}{2c^2}}$$
 Eqn. 3.3

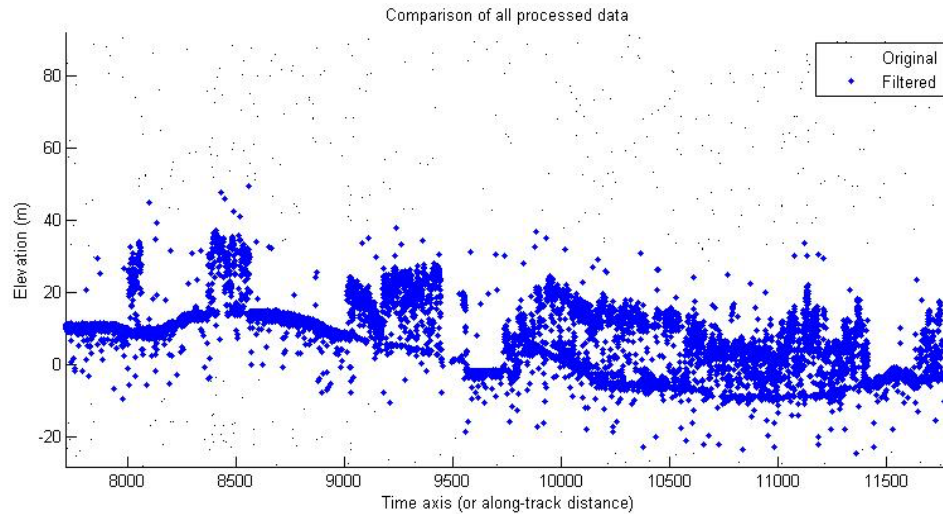
1425

1426 where  $a$  is the amplitude of the peak,  $b$  is the center of the peak, and  $c$  is the standard  
1427 deviation of the curve. A first derivative sign crossing method is one option to identify  
1428 peaks within the distribution.

1429         To determine the noise and signal Gaussians, up to ten Gaussian curves are fit  
1430 to the histogram using an iterative process of fitting and subtracting the max-  
1431 amplitude peak component from the histogram until all peaks have been extracted.  
1432 Then, the potential Gaussians pass through a rejection process to eliminate those with  
1433 poor statistical fits or other apparent errors (Goshtasby and O'Neill, 1994; Chauve et  
1434 al. 2008). A Gaussian with an amplitude less than  $1/5$  of the previous Gaussian and  
1435 within two standard deviations of the previous Gaussian should be rejected. Once the  
1436 errant Gaussians are rejected, the final two remaining are assumed to represent the  
1437 noise and signal. These are separated based on the remaining two Gaussian  
1438 components within the histogram using the logic that the leftmost Gaussian is noise  
1439 (low neighbor counts) and the other is signal (high neighbor counts).

1440         The intersection of these two Gaussians (noise and signal) determines a data  
1441 threshold value. The threshold value is the parameter used to distinguish between  
1442 noise points and signal points when the point cloud is re-evaluated for surface finding.  
1443 In the event that only one curve passes the rejection process, the threshold is set at  
1444  $1 \sigma$  above the center of the noise peak.

1445         An example of the noise filtered product from DRAGANN is shown in Figure  
1446 3.3. The signal photons identified in this process will be combined with the coarse  
1447 signal finding output available on the ATL03 data product.



1448

1449 Figure 3.3. Output from DRAGANN filtering. Signal photons are shown as blue.

1450 Figure 3.3 provides an example of along-track (profiling) height data collected  
 1451 in September 2012 from the MABEL (ICESat-2 simulator) over vegetation in North  
 1452 Carolina. The photons have been filtered such that the signal photons returned from  
 1453 vegetation and the ground surface are remaining. Noise photons that are adjacent to  
 1454 the signal photons are also retained in the input dataset; however, these should be  
 1455 classified as noise photons during the surface finding process. It is possible that some  
 1456 additional outlying noise may be retained during the DRAGANN process when noise  
 1457 photons are densely grouped, and these photons should be filtered out before the  
 1458 surface finding process. Estimates of the ground surface and canopy height can then  
 1459 be derived from the signal photons.

1460

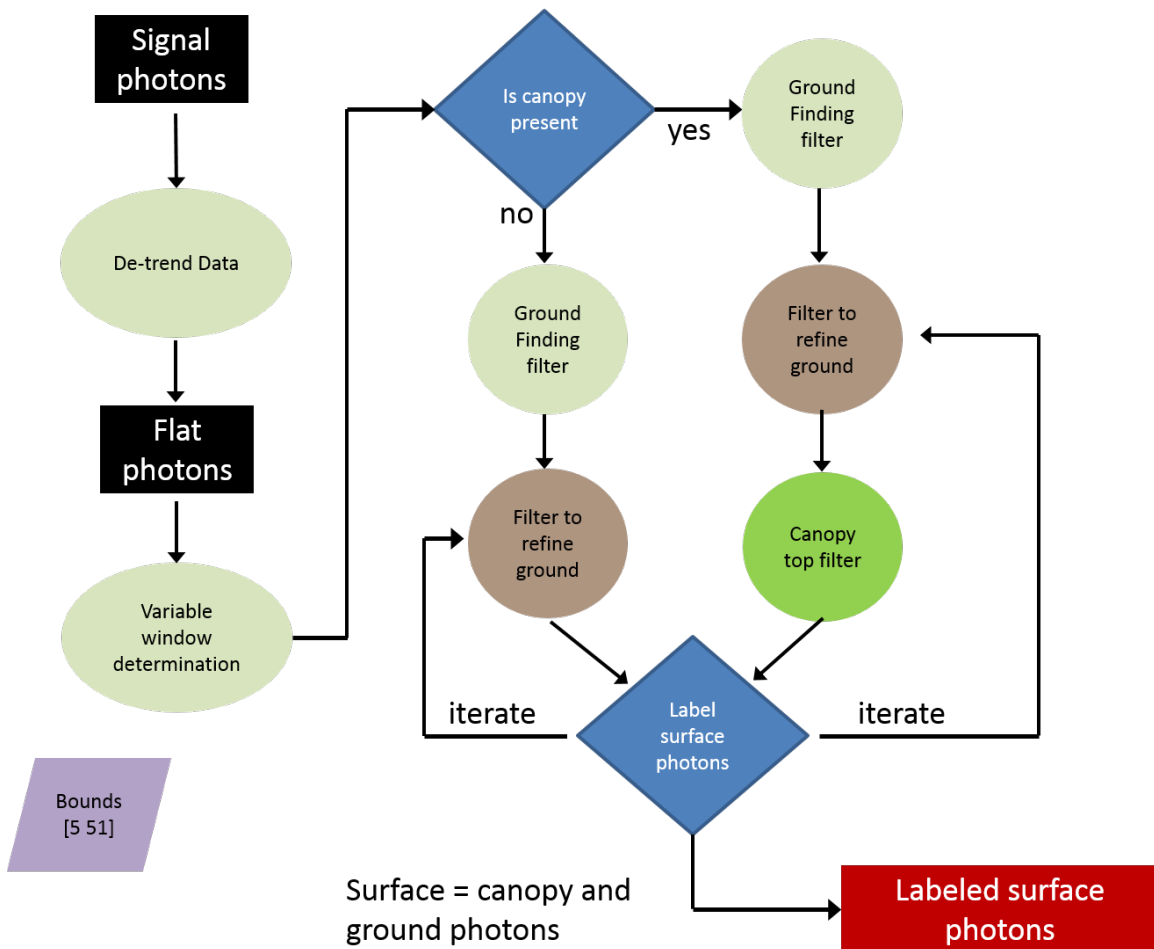
### 1461 **3.2 Surface Finding**

1462 Once the signal photons have been determined, the objective is to find the  
 1463 ground and canopy photons from within the point cloud. With the expectation that  
 1464 one algorithm may not work everywhere for all biomes, we are employing a  
 1465 framework that will allow us to combine the solutions of multiple algorithms into one  
 1466 final composite solution for the ground surface. The composite ground surface  
 1467 solution will then be utilized to classify the individual photons as ground, canopy, top

1468 of canopy, or noise. Currently, the framework described here utilizes one algorithm  
1469 for finding the ground surface and canopy surface. Additional methods, however,  
1470 could be integrated into the framework at a later time. Figure 3.4 below describes the  
1471 framework.

1472

1473



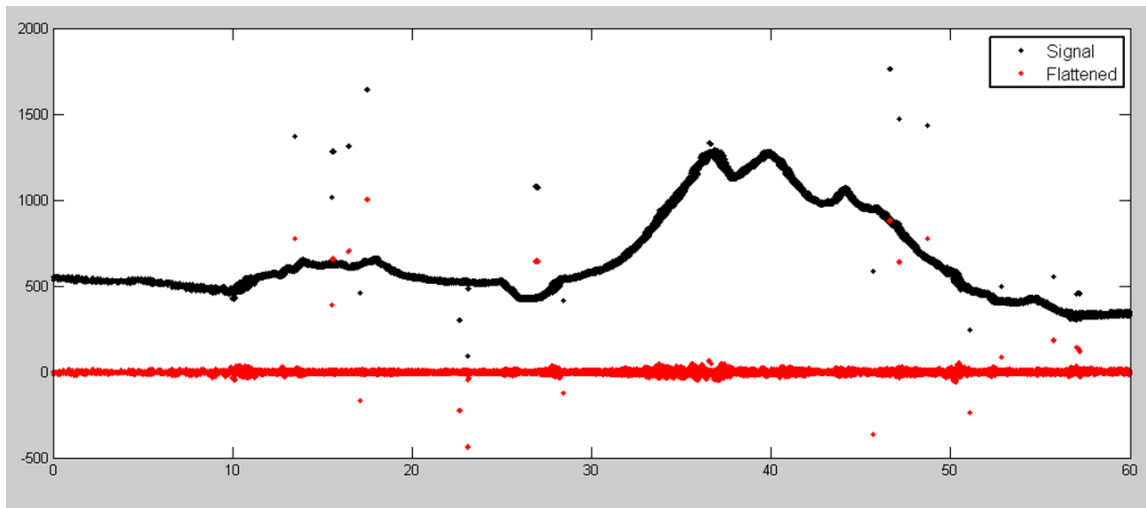
1474

1475 Figure 3.4. Flowchart of overall surface finding method.

1476

1477           **3.2.1 De-trending the Signal Photons**

1478           An important step in the success of the surface finding algorithm is to remove  
1479 the effect of topography on the input data, thus improving the performance of the  
1480 algorithm. This is done by de-trending the input signal photons by subtracting a  
1481 heavily smoothed “surface” that is derived from the input data. Essentially, this is a  
1482 low pass filter of the original data and most of the analysis to detect the canopy and  
1483 ground will subsequently be implemented on the high pass data. The amount of  
1484 smoothing that is implemented in order to derive this first surface is dependent upon  
1485 the relief. For segments where the relief is high, the smoothing window size is  
1486 decreased so topography isn’t over-filtered.



1487  
1488 Figure 3.5. Plot of Signal Photons (black) from 2014 MABEL flight over Alaska and de-  
1489 trended photons (red).

1490  
1491           **3.2.2 Canopy Determination**

1492           A key factor in the success of the surface finding algorithm is for the software  
1493 to automatically **account for the presence of canopy** along a given  $L$ -km segment.  
1494 Due to the large volume of data, this process has to occur in an automated fashion,  
1495 allowing the correct methodology for extracting the surface to be applied to the data.  
1496 In the absence of canopy, the iterative filtering approach to finding ground works

1497 extremely well, but if canopy does exist, we need to accommodate for that fact when  
1498 we are trying to recover the ground surface.

1499 For ATL08 product regions over Antarctica (regions 7, 8, 9, 10) and Greenland  
1500 (region 11), the algorithm will assume only ground photons (canopy flag = 0) (see  
1501 Figure 2.2).

1502

### 1503 3.2.3 Variable Window Determination

1504 The method for generating a best estimated terrain surface will vary depending  
1505 upon whether canopy is present. *L-km segments* without canopy are much easier to  
1506 analyze because the ground photons are usually continuous. *L-km segments* with  
1507 canopy, however, require more scrutiny as the number of signal photons from ground  
1508 are fewer due to occlusion by the vegetation.

1509 There are some common elements for finding the terrain surface for both cases  
1510 (canopy/no canopy) and with both methods. In both cases, we will use a variable  
1511 windowing span to compute statistics as well as filter and smooth the data. For  
1512 clarification, the window size is variable for each *L-km segment*, but it is constant  
1513 within the *L-km segment*. For the surface finding algorithm, we will employ a  
1514 Savitzky-Golay smoothing/median filtering method. Using this filter, we compute a  
1515 variable smoothing parameter (or window size). It is important to bound the filter  
1516 appropriately as the output from the median filter can lose fidelity if the scan is over-  
1517 filtered.

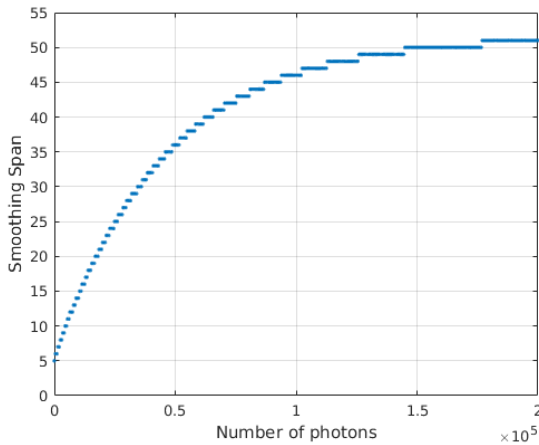
1518 We have developed an empirically-determined shape function, bound between  
1519 [5 51], that sets the window size (*Sspan*) based on the number of photons within each  
1520 *L-km segment*.

$$1521 \quad Sspan = \text{ceil}[5 + 46 * (1 - e^{-a*length})] \quad \text{Eqn. 3.4}$$

$$1522 \quad a = \frac{\log\left(1 - \frac{21}{51-5}\right)}{-28114} \approx 21 \times 10^{-6} \quad \text{Eqn. 3.5}$$



1523 where  $a$  is the shape parameter and length is the total number of photons in the  $L$ -km  
1524 segment. The shape parameter,  $a$ , was determined using data collected by MABEL and  
1525 is shown in Figure 3.6. It is possible that the model of the shape function, or the  
1526 filtering bounds, will need to be adjusted once ICESat-2/ATLAS is on orbit and  
1527 collecting data.



1528

1529 Figure 3.6. Shape Parameter for variable window size.

1530

### 1531 3.2.4 Compute descriptive statistics

1532 To help characterize the input data and initialize some of the parameters used  
1533 in the algorithm, we employ a moving window to compute descriptive statistics on  
1534 the de-trended data. The moving window's width is the smoothing span function  
1535 computed in Equation 5 and the window slides  $\frac{1}{4}$  of its size to allow of overlap  
1536 between windows. By moving the window with a large overlap helps to ensure that  
1537 the approximate ground location is returned. The statistics computed for each  
1538 window step include:

- 1539 • Mean height
- 1540 • Min height
- 1541 • Max height
- 1542 • Standard deviation of heights

1543

1544           Dependent upon the amount of vegetation within each window, the estimated  
1545 ground height is estimated using different statistics. A standard deviation of the  
1546 photon elevations computed within each moving window are used to classify the  
1547 vertical spread of photons as belonging to one of four classes with increasing amounts  
1548 of variation: open, canopy level 1, canopy level 2, canopy level 3. The canopy indices  
1549 are defined in Table 3.1.

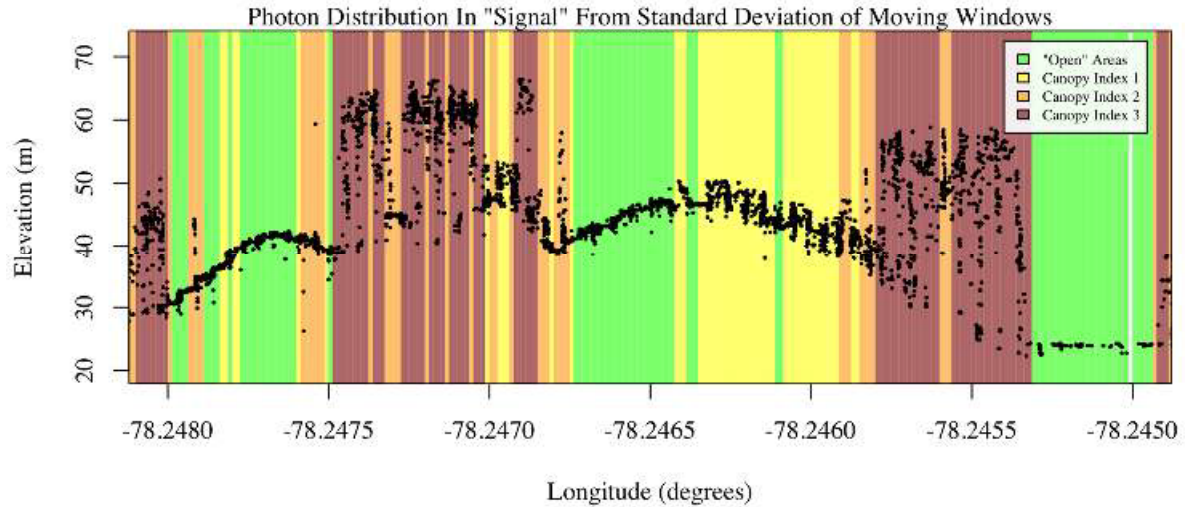
1550

1551 Table 3.1. Standard deviation ranges utilized to qualify the spread of photons within  
1552 moving window.

Name	Definition	Lower Limit	Upper Limit
Open	Areas with little or no spread in signal photons determined due to low standard deviation	N/A	Photons falling within 1 <sup>st</sup> quartile of Standard deviation
Canopy Level 1	Areas with small spread in signal photons	1 <sup>st</sup> quartile	Median
Canopy Level 2	Areas with a medium amount of spread	Median	3 <sup>rd</sup> quartile
Canopy Level 3	Areas with high amount of spread in signal photons	3 <sup>rd</sup> quartile	N/A

1553

1554



1555

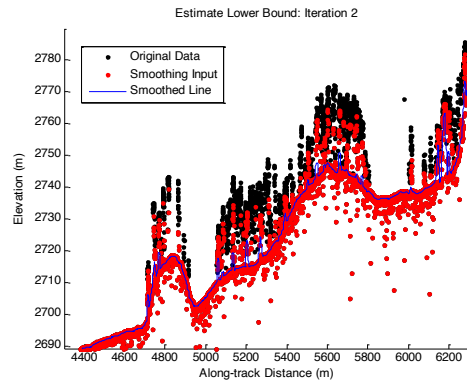
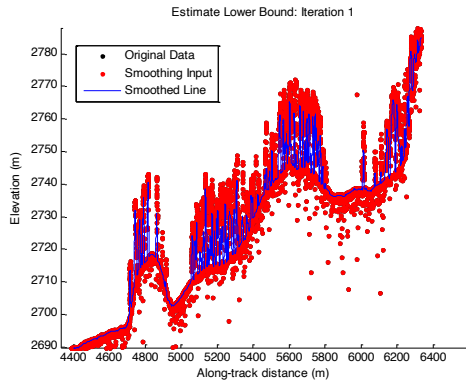
1556 Figure 3.7. Illustration of the standard deviations calculated for each moving window to  
 1557 identify the amount of spread of signal photons within a given window.

1558

### 1559 **3.2.5 Ground Finding Filter (Iterative median filtering)**

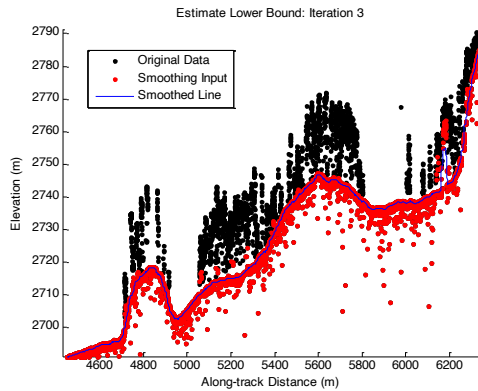
1560 A combination of an iterative median filtering and smoothing filter approach  
 1561 will be employed to derive the output solution of both the ground and canopy  
 1562 surfaces. The input to this process is the set of de-trended photons. Finding the  
 1563 ground in the presence of canopy often poses a challenge because often there are  
 1564 fewer ground photons underneath the canopy. The algorithm adopted here uses an  
 1565 iterative median filtering approach to retain/eliminate photons for ground finding in  
 1566 the presence of canopy. When canopy exists, a smoothed line will lay somewhere  
 1567 between the canopy top and the ground. This fact is used to iteratively label points  
 1568 above the smoothed line as canopy. The process is repeated five times to eliminate  
 1569 canopy points that fall above the estimated surface as well as noise points that fall  
 1570 below the ground surface. An example of iterative median filtering is shown in Figure  
 1571 3.8. The final median filtered line is the preliminary surface estimate. A limitation of  
 1572 this approach, however, is in cases of dense vegetation and few photons reaching the  
 1573 ground surface. In these instances, the output of the median filter may lie within the  
 1574 canopy.

1575



1576

1577



1578

1579 Figure 3.8. Three iterations of the ground finding concept for  $L$ -km segments with canopy.

1580

### 1581 3.3 Top of Canopy Finding Filter

1582 Finding the top of the canopy surface uses the same methodology as finding  
1583 the ground surface, except now the de-trended data are “flipped” over. The “flip”  
1584 occurs by multiplying the photons heights by -1 and adding the mean of all the heights  
1585 back to the data. The same procedure used to find the ground surface can be used to  
1586 find the indices of the top of canopy points.

1587

1588 **3.4 Classifying the Photons**

1589           Once a composite ground surface is determined, photons falling within the  
1590 point spread function of the surface are labeled as ground photons. Based on the  
1591 expected performance of ATLAS, the point spread function should be approximately  
1592 35 cm rms. Signal photons that are not labeled as ground and are below the ground  
1593 surface (buffered with the point spread function) are considered noise, but keep the  
1594 signal label.

1595           The top of canopy photons that are identified can be used to generate an upper  
1596 canopy surface through a shape-preserving surface fitting method. All signal photons  
1597 that are not labeled ground and lie above the ground surface (buffered with the point  
1598 spread function) and below the upper canopy surface are considered to be canopy  
1599 photons (and thus labeled accordingly). Signal photons that lie above the top of  
1600 canopy surface are considered noise, but keep the signal label.

1601

1602           FLAGS,           0 = noise  
1603                               1 = ground  
1604                               2 = canopy  
1605                               3 = TOC (top of canopy)

1606

1607           The final ground and canopy classifications are flags 1 – 3. The full canopy is  
1608 the combination of flags 2 and 3.

1609

1610 **3.5 Refining the Photon Labels**

1611           During the first iteration of the algorithm, it is possible that some photons are  
1612 mislabeled; most likely this would be noise photons mislabeled as canopy. To reject  
1613 these mislabeled photons, we apply three criteria:

- 1614           a) If top of canopy photons are 2 standard deviations above a  
1615               smoothed median top of canopy surface  
1616           b) If there are less than 3 canopy indices within a 15m radius

1617 c) If, for 500 signal photon segments, the number of canopy photons  
1618 is < 5% of the total (when SNR > 1), or < 10% of the total (when SNR  
1619 <= 1). This minimum number of canopy indices criterion implies a  
1620 minimum amount of canopy cover within a region.

1621 There are also instances where the ground points will be redefined. This  
1622 reassigning of ground points is based on how the final ground surface is determined.  
1623 Following the “iterate” steps in the flowchart shown in Figure 3.4, if there are no  
1624 canopy indices identified for the *L-km* segment, the final ground surface is  
1625 interpolated from the identified ground photons and then will undergo a final round  
1626 of median filtering and smoothing.

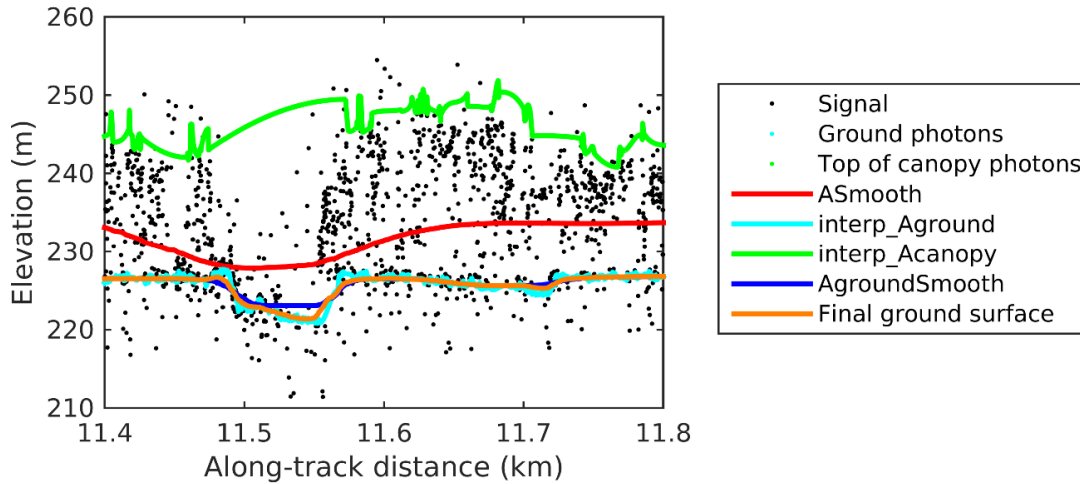
1627 If canopy photons are identified, the final ground surface is interpolated based  
1628 upon the level/amount of canopy at that location along the segment. The final ground  
1629 surface is a composite of various intermediate ground surfaces, defined thusly:

**ASmooth** heavily smoothed surface used to de-trend the signal data

**Interp\_Aground** interpolated ground surface based upon the identified ground photons

**AgroundSmooth** median filtered and smoothed version of Interp\_Aground

1630



1631

1632 Figure 3.9. Example of the intermediate ground and top of canopy surfaces calculated from  
 1633 MABEL flight data over Alaska during July 2014.

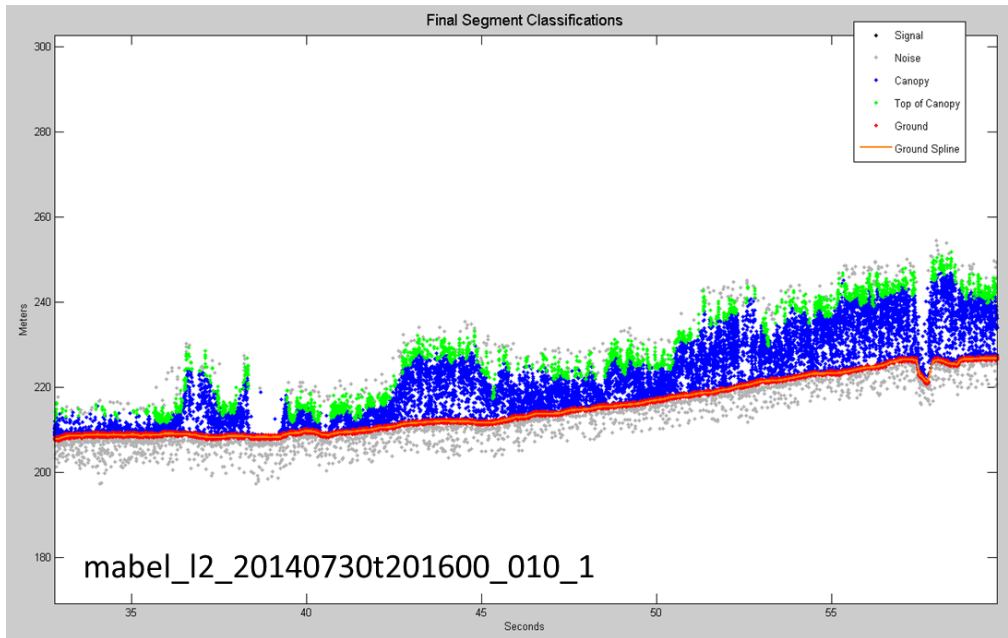
1634

1635 During the first round of ground surface refinement, where there are canopy  
 1636 photons identified in the segment, the ground surface at that location is defined by  
 1637 the smoothed ground surface (AgroundSmooth) value. Else, if there is a location  
 1638 along-track where the standard deviation of the ground-only photons is greater than  
 1639 the 75% quartile for all signal photon standard deviations (i.e., canopy level 3), then  
 1640 the ground surface at that location is a weighted average between the interpolated  
 1641 ground surface (Interp\_Aground\*1/3) and the smoothed interpolated ground surface  
 1642 (AgroundSmooth\*2/3). For all remaining locations long the segment, the ground  
 1643 surface is the average of the interpolated ground surface (Interp\_Aground) and the  
 1644 heavily smoothed surface (ASmooth).

1645 The second round of ground surface refinement is simpler than the first.  
 1646 Where there are canopy photons identified in the segment, the ground surface at that  
 1647 location is defined by the smoothed ground surface (AgroundSmooth) value again.  
 1648 For all other locations, the ground surface is defined by the interpolated ground  
 1649 surface (Interp\_Aground). This composite ground surface is run through the median  
 1650 and smoothing filters again.

1651 The pseudocode for this surface refining process can be found in section 4.10.

1652 Examples of the ground and canopy photons for several MABEL lines are  
1653 shown in Figures 3.10 – 3.12.



1654

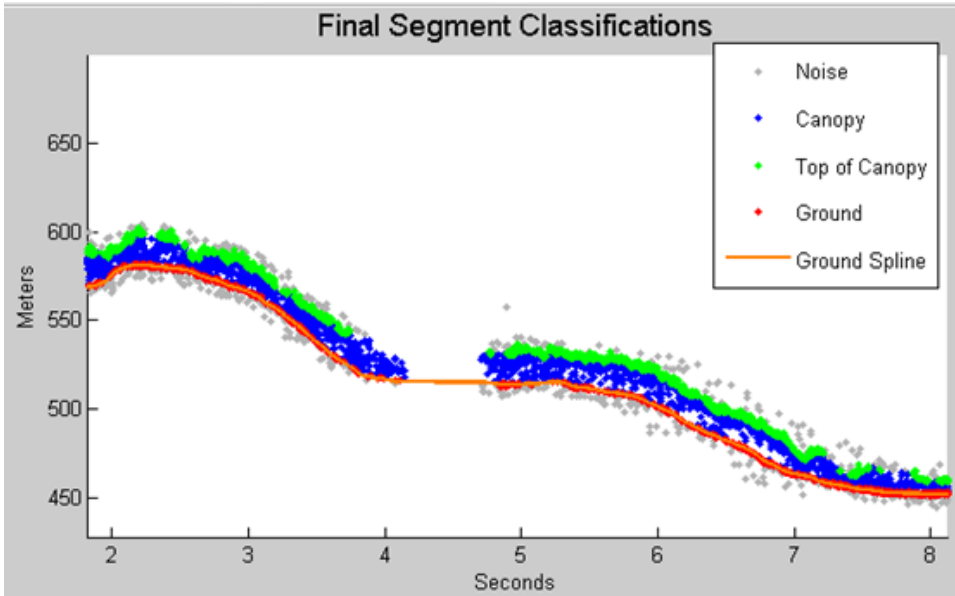
1655 Figure 3.10. Example of classified photons from MABEL data collected in Alaska 2014.

1656 Red photons are photons classified as terrain. Green photons are classified as top of canopy.

1657 Canopy photons (shown as blue) are considered as photons lying between the terrain

1658 surface and top of canopy.





1659

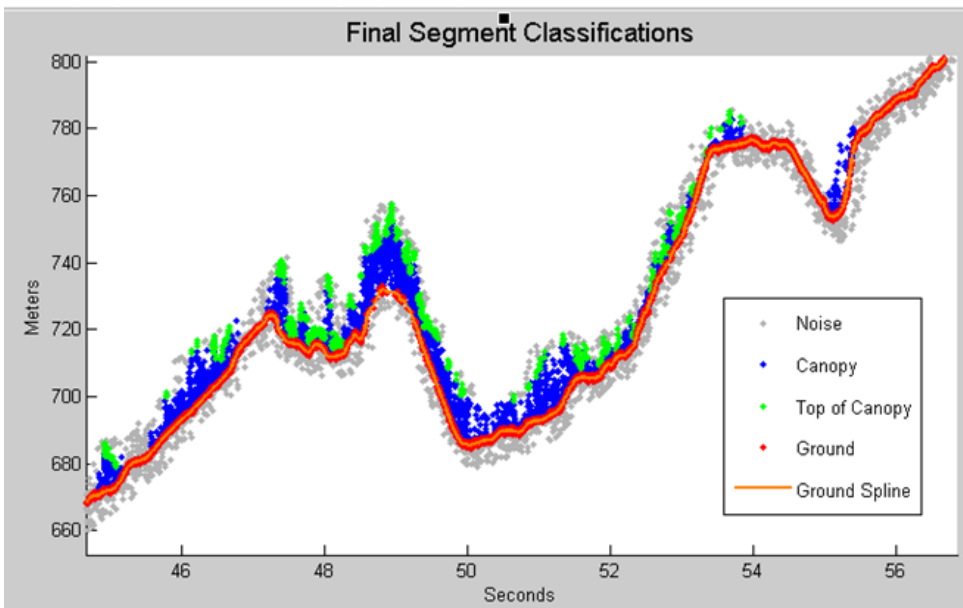
1660 Figure 3.11. Example of classified photons from MABEL data collected in Alaska 2014.

1661 Red photons are photons classified as terrain. Green photons are classified as top of canopy.

1662 Canopy photons (shown as blue) are considered as photons lying between the terrain

1663 surface and top of canopy.

1664



1665

1666 Figure 3.12. Example of classified photons from MABEL data collected in Alaska 2014.

1667 Red photons are photons classified as terrain. Green photons are classified as top of canopy.

1668 Canopy photons (shown as blue) are considered as photons lying between the terrain  
1669 surface and top of canopy.

1670

### 1671 **3.6 Canopy Height Determination**

1672 Once a final ground surface is determined, canopy heights for individual  
1673 photons are computed by removing the ground surface height for that photon's  
1674 latitude/longitude. These relative canopy height values will be used to compute the  
1675 canopy statistics on the ATL08 data product.

1676

### 1677 **3.7 Link Scale for Data products**

1678 The link scale for each segment within which values for vegetation parameters  
1679 will be derived will be defined over a fixed distance of 100 m. A fixed segment length  
1680 ensures that canopy and terrain metrics are consistent between segments, in addition  
1681 to increased ease of use of the final products. A size of 100 m was selected as it should  
1682 provide approximately 140 photons (a statistically sufficient number) from which to  
1683 make the calculations for terrain and canopy height.

1684

#### 1685 4. ALGORITHM IMPLEMENTATION

1686 Prior to running the surface finding algorithms used for ATL08 data products, the  
1687 superset of output from the GSFC medium-high confidence classed photons (ATL03  
1688 signal\_conf\_ph: flags 3-4) and the output from DRAGANN will be considered as the input  
1689 data set. ATL03 input data requirements include the along-track time, latitude, longitude,  
1690 height, and classification for each photon. The motivation behind combining the results  
1691 from two different noise filtering methods is to ensure that all of the potential signal  
1692 photons for land surfaces will be provided as input to the surface finding software. Prior to  
1693 running DRAGANN, reject telemetry bins that occur 150m above or below the reference  
1694 DEM. Rejection of these noise blocks will ensure a better parameterization of DRAGANN.

1695 Some additional quality checks are also described here prior to implementing the  
1696 ATL08 software. The first check utilizes the POD\_PPD flag on ATL03. In instances where  
1697 the satellite is maneuvering or the pointing/ranging solutions are suspect, ATL08 will not  
1698 use those data. Thus, data will only flow to the ATL08 algorithm when the POD\_PPD flag  
1699 is set to 0 which indicates ‘nominal’ conditions.

1700 A second quality check pertains to the flags set on the ATL03 photon quality flag  
1701 (quality\_ph). Currently, ATL03 quality\_ph flags are described as:

1702 0 = nominal conditions

1703 1 = possible after-pulse (this identifies the after pulses that occur between 2.3 and  
1704 5 m below the surface)

1705 2 = possible late impulse response effect (this flag identifies additional detector  
1706 effects 5 – 50 m below the surface).

1707 3 = possible TEP crossing.

1708 For this release of the software, we want to mention that there are cases of after-pulsing  
1709 that occur 0.5 – 2.3 m below the surface that are considered nominal with the quality\_ph  
1710 flag. The output from the DRAGANN algorithm (i.e. the DRAGANN flag) will be set to a

1711 value of 0 when ATL03 quality\_ph flags are greater than 0 such that they are ignored in  
 1712 the ATL08 algorithm.

1713

1714 A third quality check pertains to the signal photons (DRAGANN + ATL03 signal  
 1715 confidence photons) and whether those heights are near the surface heights. To pass this  
 1716 check, signal photons that lie 120 m above the reference DEM will be disregarded. Signal  
 1717 photons lying below the reference DEM will be allowed to continue for additional ATL08  
 1718 processing. The motivation for this quality check is to eliminate ICESat-2 photons that are  
 1719 reflecting from clouds rather than the true surface.

1720 Table 4.1. Input parameters to ATL08 classification algorithm.

Name	Data Type	Long Name	Units	Description	Source
<b>delta_time</b>	DOUBLE	GPS elapsed time	seconds	Elapsed GPS seconds since start of the granule for a given photon. Use the metadata attribute <code>granule_start_seconds</code> to compute full gps time.	ATL03
<b>lat_ph</b>	FLOAT	latitude of photon	degrees	Latitude of each received photon. Computed from the ECEF Cartesian coordinates of the bounce point.	ATL03
<b>lon_ph</b>	FLOAT	longitude of photon	degrees	Longitude of each received photon. Computed from the ECEF Cartesian coordinates of the bounce point.	ATL03
<b>h_ph</b>	FLOAT	height of photon	meters	Height of each received photon, relative to the WGS-84 ellipsoid.	ATL03
<b>sigma_h</b>	FLOAT	height uncertainty	m	Estimated height uncertainty (1-sigma) for the reference photon.	ATL03
<b>signal_conf_ph</b>	UINT_1_LE	photon signal confidence	counts	Confidence level associated with each photon event selected as signal (0-noise, 1- added to allow for buffer but algorithm classifies as background, 2-low, 3-med, 4-high).	ATL03
<b>segment_id</b>	UNIT_32	along-track segment ID number	unitless	A seven-digit number uniquely identifying each along-track segment. These are sequential, starting with one for the first	ATL03

				segment after an ascending equatorial crossing node.	
<b>cab_prof</b>	FLOAT	Calibrated Attenuated Backscatter	unitless	Calibrated Attenuated Backscatter from 20 to -1 km with vertical resolution of 30m	ATL09
<b>dem_h</b>	FLOAT	DEM Height	meters	Best available DEM (in priority of GIMP/ANTARCTIC/GMTED/MSS) value at the geolocation point. Height is in meters above the WGS84 Ellipsoid.	ATL09

1721

1722 Table 4.2. Additional external parameters referenced in ATL08 product.

Name	Data Type	Long Name	Units	Description	Source
<b>atlas_pa</b>				Off nadir pointing angle of the spacecraft	
<b>ground_track</b>				Ground track, as numbered from left to right: 1 = 1L, 2 = 1R, 3 = 2L, 4 = 2R, 5 = 3L, 6 = 3R	
<b>dem_h</b>				Reference DEM height	ANC06
<b>ref_azimuth</b>	FLOAT	azimuth	radians	Azimuth of the unit pointing vector for the reference photon in the local ENU frame in radians. The angle is measured from north and positive towards east.	ATL03
<b>ref_elev</b>	FLOAT	elevation	radians	Elevation of the unit pointing vector for the reference photon in the local ENU frame in radians. The angle is measured from east-north plane and positive towards up.	ATL03
<b>rgt</b>	INTEGER_2	reference ground track	unitless	The reference ground track (RGT) is the track on the Earth at which a specified unit vector within the observatory is pointed. Under nominal operating conditions, there will be no data collected along the RGT, as the RGT is spanned by GT2L and GT2R. During slews or off-pointing, it is possible that ground tracks	ATL03

				may intersect the RGT. The ICESat-2 mission has 1,387 RGTs.	
<b>sigma_along</b>	DOUBLE	along-track geolocation uncertainty	meters	Estimated Cartesian along-track uncertainty (1-sigma) for the reference photon.	ATL03
<b>sigma_across</b>	DOUBLE	across-track geolocation uncertainty	meters	Estimated Cartesian across-track uncertainty (1-sigma) for the reference photon.	ATL03
<b>surf_type</b>	INTEGER_1	surface type	unitless	Flags describing which surface types this interval is associated with. 0=not type, 1=is type. Order of array is land, ocean, sea ice, land ice, inland water.	ATL03 , Section 4
<b>layer_flag</b>	Integer	Consolidated cloud flag	unitless	Flag indicating the presence of clouds or blowing snow with good confidence	ATL09
<b>cloud_flag_asr</b>	Integer(3)	Cloud probability from ASR	unitless	Cloud confidence flag, from 0 to 5, indicating low, med, or high confidence of clear or cloudy sky	ATL09
<b>msw_flag</b>	Byte(3)	Multiple scattering warning flag	unitless	Flag with values from 0 to 5 indicating presence of multiple scattering, which may be due to blowing snow or cloud/aerosol layers.	ATL09
<b>asr</b>	Float(3)	Apparent surface reflectance	unitless	Surface reflectance as modified by atmospheric transmission	ATL09
<b>snow_ice</b>	INTEGER_1	Snow Ice Flag	unitless	NOAA snow-ice flag. 0=ice free water; 1=snow free land; 2=snow; 3=ice	ATL09

1723

#### 1724 **4.1 Cloud based filtering**

1725 It is possible for the presence of clouds to affect the number of surface photon  
1726 returns through signal attenuation, or to cause false positive classifications of  
1727 ground or canopy photons on low cloud returns. Either of these cases would reduce  
1728 the accuracy of the ATL08 product. To improve the performance of the ATL08  
1729 algorithm, ideally all clouds would be identified prior to processing through the  
1730 ATL08 algorithm. There will be instances, however, where low lying clouds (e.g.

1731 <800 m above the ground surface) may be difficult to identify. Currently, ATL08  
1732 provides an ATL09 derived cloud flag (layer\_flag) on its 100 m product and  
1733 encourages the user to make note of the presence of clouds when using ATL08  
1734 output. Unfortunately at present, a review of on-orbit data from ATL03 and ATL09  
1735 indicate that the cloud layer flag is not being set correctly in the ATL09 algorithm.  
1736 Ultimately, the final cloud based filtering process used in the ATL08 algorithm will  
1737 most likely be derived from parameters/flag on the ATL09 data product. Until the  
1738 ATL09 cloud flags are proven reliable, however, a preliminary cloud screening  
1739 method is presented below. This methodology utilizes the calibrated attenuated  
1740 backscatter on the ATL09 data product to identify (and subsequently remove for  
1741 processing) clouds or other problematic issues (i.e. incorrectly telemetered  
1742 windows). Using this new method, telemetered windows identified as having either  
1743 low or no surface signal due to the presence of clouds (likely above the telemetered  
1744 band), as well as photon returns suspected to be clouds instead of surface returns,  
1745 will be omitted from the ATL08 processing. This process, however, will not identify  
1746 the extremely low clouds (i.e. <800 m). The steps are as follows:

- 1747 1. Match up the ATL09 calibrated attenuated backscatter (cab\_prof) columns to  
1748 the ATL03 granule being processed using segment ID.
- 1749 2. Flip the matching cab\_prof vertical columns so that the elevation bins go  
1750 from low to high.
- 1751 3. For each of the matching ATL09 cab\_prof vertical columns, perform a cubic  
1752 Savitsky-Golay smoothing filter with a span size of 15 vertical bins. Call this  
1753 cab\_smooth.
- 1754 4. Perform the same smoothing filter on each horizontal row of the cab\_smooth  
1755 output, this time using a span size of 7 horizontal bins. Call this  
1756 cab\_smoother.
- 1757 5. Create a low\_signal logical array the length of the number of matching ATL09  
1758 columns and set to false.
- 1759 6. For each column of cab\_smoother:
  - 1760 a. Set any values below 0 to 0.

- 1761           b. Set a logical array of cab\_smoother bins that are below 15 km in  
1762           elevation to true. Call this cab15.
- 1763           c. Using the ATL09 dem\_h value for that column, find the ATL09  
1764           cab\_smoother bins that are 240 m above and 240 m below (~8 ATL09  
1765           vertical bins each direction) the dem\_h value. The bins found here that  
1766           are also within cab15 are designated as sfc\_bins.
- 1767           d. Find the maximum peak value of cab\_smoother within the sfc\_bins, if  
1768           any. This will represent the surface peak.
- 1769           e. Find the maximum value of cab\_smoother that is higher in elevation  
1770           than the sfc\_bins and within cab15, if any. This will represent the  
1771           cloud peak.
- 1772           f. If there is no surface peak, set the low\_signal flag to true.
- 1773           g. If there are both surface and cloud peak values returned, determine a  
1774           surface peak / cloud peak ratio. If that ratio is less than or equal to 0.4,  
1775           set low\_signal flag for that column to true.
- 1776        7. After each matching ATL09 column of cab\_smoother has been analyzed for  
1777        low signal, assign the low\_signal flag to an ATL03 photon resolution logical  
1778        array by matching up the ATL03 photon segment\_id values to the ATL09  
1779        range of segment IDs for each ATL09 cab\_prof column.
- 1780        8. For each ATL09 cab\_prof column where the low\_signal flag was not set, check  
1781        for any ATL03 photons greater than 800 meters (TBD) in elevation away  
1782        (higher or lower) from the ATL09 dem\_h value. Assign an ATL03 photon  
1783        resolution too\_far\_signal flag to true when this conditional is met.
- 1784        9. A logical array mask is created for any ATL03 photons that have either the  
1785        low\_signal flag or the too\_far\_signal flag set to true such that those photons  
1786        will not be further processed by the ATL08 function.

1787

#### 1788    **4.2 Preparing ATL03 data for input to ATL08 algorithm**

- 1789        1. At times, cloud attenuation will lead to a reduced L-km with a length that is  
1790        not a multiple of 100 meters. If the last 100m land segment of the L-km



1791 segment contains fewer than 5 ATL03 20m geosegments and the current L-  
1792 km segment is not the last one of the granule, do not report output for this  
1793 last 100m land segment. Retain the starting geosegment of this land segment  
1794 and begin the next L-km segment here.

1795 2. Break up data into *L-km* segments. Segments equivalent of 10 km in along-  
1796 track distance of an orbit would be appropriate.

1797 a. If the last portion of an ATL03 granule being processed would result  
1798 in an *L-km* segment with less than 3.4 km (170 geosegments) worth of  
1799 data, that last portion is added to the previous *L-km* processing  
1800 window to be processed together as one extended *L-km* processing  
1801 segment.

1802 i. The resulting **last\_seg\_extend** value would be reported as a  
1803 positive value of distance beyond 10 km that the ATL08  
1804 processing segment was extended by.

1805 b. If the last *L-km* segment would be less than 10 km but greater than 3.4  
1806 km, a portion extending from the start of current *L-km* processing  
1807 segment backwards into the previous *L-km* processing segment would  
1808 be added to the current ATL08 processing segment to make it 10 km  
1809 in length. Only new 100 m ATL08 segment products generated from  
1810 this backward extension would be reported.

1811 i. The distance of this backward data gathering would be  
1812 reported in **last\_seg\_extend** as a negative distance value.

1813 c. All other segments that are not extended will report a last\_seg\_extend  
1814 value of 0.

1815 3. Add a buffer of 200 m (or 10 segment\_id's) to both ends of each *L-km*  
1816 segment. The total processing segment length is ( $L\text{-km} + 2*\text{buffer}$ ), but will  
1817 be referred to as *L-km* segments for simplicity.

1818 a. The first *L-km* segment from an ATL03 granule would only have a  
1819 buffer at the end, and the last *L-km* segment from an ATL03 granule  
1820 would only have a buffer at the beginning.

1821 4. The input data for ATL08 algorithm is X, Y, Z, T (where T is time).

1822

### 1823 **4.3 Noise filtering via DRAGANN**

1824 DRAGANN will use ATLO3 photons with all signal classification flags (0-4). These  
1825 will include both signal and noise photons. This section give a broad overview of the  
1826 DRAGANN function. See Appendix A for more details.

- 1827 1. Determine the relative along-track time, ATT, of each geolocated photon  
1828 from the beginning of each *L-km* segment.
- 1829 2. Rescale the ATT with equal-time spacing between each data photon, keeping  
1830 the relative beginning and end time values the same.
- 1831 3. Normalize the height and rescaled ATT data from 0 – 1 for each *L-km*  
1832 segment based on the min/max of each field. So,  $\text{normtime} = (\text{time} -$   
1833  $\text{mintime})/(\text{maxtime} - \text{mintime})$ .
- 1834 4. Build a kd-tree based on normalized Z and normalized and rescaled ATT.
- 1835 5. Determine the search radius starting with Equation 3.1.  $P$ =[determined by  
1836 preprocessor; see Sec 4.3.1], and  $V_{\text{total}} = 1$ .  $N_{\text{total}}$  is the number of photons  
1837 within the data *L-km* segment. Solve for  $V$ .
- 1838 6. Now that you know  $V$ , determine the radius using Equation 3.2.
- 1839 7. Compute the number of neighbors for each photon using this search radius.
- 1840 8. Generate a histogram of the neighbor count distribution. As illustrated in  
1841 Figure 3.2, the noise peak is the first peak (usually with the highest  
1842 amplitude).
- 1843 9. Determine the 10 highest peaks of the histogram.
- 1844 10. Fit Gaussians to the 10 highest peaks. For each peak,
  - 1845 a. Compute the amplitude,  $a$ , which is located at peak position  $b$ .
  - 1846 b. Determine the width,  $c$ , by stepping one bin at a time away from  $b$  and  
1847 finding the last histogram value that is  $> \frac{1}{2}$  the amplitude,  $a$ .
  - 1848 c. Use the amplitude and width to fit a Gaussian to the peak of the  
1849 histogram, as described in Equation 3.3.
  - 1850 d. Subtract the Gaussian from the histogram, and move on to calculate  
1851 the next highest peak's Gaussian.

1852 e. Reject Gaussians that are too near ( $< 2$  standard deviations) and  
1853 amplitude too low ( $< 1/5$  previous amplitude) from the previous  
1854 signal Gaussian.

1855 11. Reject any of the returned Gaussians with imaginary components.

1856 12. Determine if there is a narrow noise Gaussian at the beginning of the  
1857 histogram. These typically occur when there is little noise, such as during  
1858 nighttime passes.

1859 a. Search for the Gaussian with the highest amplitude,  $a$ , in the first 5%  
1860 of the histogram

1861 b. Check if the highest amplitude is  $\geq 1/10$  of the maximum of all  
1862 Gaussian amplitudes

1863 c. Check if the width,  $c$ , of the Gaussian with the highest amplitude is  $\leq$   
1864 4 bins

1865 d. If these three conditions are met, save the  $[a,b,c]$  values as  $[a_0,b_0,c_0]$ .

1866 e. If the three conditions are not met, search again within the first 10%.  
1867 Repeat the process, incrementing the percentage of histogram  
1868 searched by 5% up to 30%. As soon as the conditions are met, save  
1869 the  $[a_0,b_0,c_0]$  values and break out of the percentage histogram search  
1870 loop.

1871 13. If a narrow noise peak was found, sort the remaining Gaussians from largest  
1872 to smallest area, estimated by  $a*c$ , then append  $[a_0,b_0,c_0]$  to the beginning of  
1873 the sorted  $[a,b,c]$  arrays. If a narrow noise peak was not found, sort all  
1874 Gaussians by largest to smallest area.

1875 a. If a narrow noise peak was not found, check in sorted order if one of  
1876 the Gaussians are in the first 10% of the histogram. If so, it becomes  
1877 the first Gaussian.

1878 b. Reject any Gaussians that are fully contained within another.

1879 c. Reject Gaussians whose centers are within 3 standard deviations of  
1880 another, unless only two Gaussians remain

1881 14. If there are two or more Gaussians remaining, they are referred to as  
1882 Gaussian 1 and Gaussian 2, assumed to be the noise and signal Gaussians.

- 1883 15. Determine the threshold value that will define the cutoff between noise and  
1884 signal.
- 1885 a. If the absolute difference of the two Gaussians becomes near zero,  
1886 defined as  $< 1e-8$ , set the first bin index where that occurs, past the  
1887 first Gaussian peak location, as the threshold. This would typically be  
1888 set if the two Gaussians are far away from each other.
- 1889 b. Else, the threshold value is the intersection of the two Gaussians,  
1890 which can be estimated as the first bin index past the first Gaussian  
1891 peak location and before the second Gaussian where there is a  
1892 minimum absolute difference between the two Gaussians.
- 1893 c. If there is only one Gaussian, it is assumed to be the noise Gaussian,  
1894 and the threshold is set to  $b + c$ .
- 1895 16. Label all photons having a neighbor count above the threshold as signal.
- 1896 17. Label all photons having a neighbor count below the threshold as noise.
- 1897 18. Reject noise photons.
- 1898 19. Retain signal photons for feeding into next step of processing.
- 1899 20. Use Logical OR to combine DRAGANN signal photons with ATL03 medium-  
1900 high confidence signal photons (flags 3-4) as ATL08 signal photons.
- 1901 21. Calculate a signal to noise ratio (SNR) for the  $L$ -km segment by dividing the  
1902 number of ATL08 signal photons by the number of noise (i.e., all – signal)  
1903 photons.

#### 1904 **4.3.1 DRAGANN Quality Assurance**

1905 Based upon on-orbit data, there are instances where only noise photons are selected  
1906 as signal photons following running through DRAGANN. These instances usually  
1907 occur to telemetered windows with low signal, signal attenuation near the surface  
1908 due to fog, haze (or other atmospheric properties). If any  $d\_flag$  results in the 10 km  
1909 = 1

- 1910 1. For each 20 m  $segment\_id$  that has a  $d\_flag = 1$ , build a histogram of 5 m  
1911 height bins using the height of only the DRAGANN-flagged photons  
1912 ( $d\_flag=1$ )

- 1913 2. If the number of bins indicates that all d\_flag photons fall within the same  
1914 vertical 60 m, do nothing and move to the next geosegment.
- 1915 3. If the d\_flag photons fall outside of 60 m, calculate the median and  
1916 standard deviation of the histogram counts.
- 1917 4. If the maximum value of the histogram counts is greater than the median  
1918 + 3\*standard deviation, a surface peak has been detected based on the  
1919 relative photon density within the 5 meter steps. Else, set all d\_flag = 0  
1920 for this geosegment.
- 1921 5. Set all d\_flag = 0 from 3 height bins below the detected peak to the bottom  
1922 of the telemetry window.
- 1923 6. Starting with the peak count bin (surface), step upwards bin by bin and  
1924 check if 12 bin counts (60 meters of height bins) above surface are less  
1925 than 0.5 \* histogram median. If so, for all photons above current height in  
1926 loop + 60 meters, set all d\_flag = 0 and exit bin-by-bin loop.
- 1927 7. Starting with one bin above the peak count bin (surface), again step  
1928 upwards bin by bin. For each iteration, calculate the standard deviation of  
1929 the bin counts including only the current bin to the highest height bin and  
1930 call this noise standard deviation. If all remaining vertical height bins  
1931 from current bin to highest height bin are less than 2\* histogram  
1932 standard deviation, or if the noise standard deviation is less than 1.0, or if  
1933 this bin and the next 2 higher bins each have counts less than the peak bin  
1934 count (entire histogram) - 3\*histogram standard deviation, then set all  
1935 d\_flag = 0 for all heights above this level and exit bin-by-bin loop
- 1936 8. For a final check, construct a new histogram, with median and standard  
1937 deviation, using the corrected d\_flag results and only where d\_flag = 1. If  
1938 the histogram median is greater than 0.0 and the standard deviation is  
1939 greater than 0.75\*median, set all d\_flag in this geosegment = 0. This  
1940 indicates results not well constrained about a detectible surface.  
1941

### 4.3.2 Preprocessing to dynamically determine a DRAGANN parameter

While a default value of  $P=20$  was found to work well when testing with MABEL flight data, further testing with simulated data showed that  $P=20$  is not sufficient in cases of very low or very high noise. Additional testing with real ATL03 data have shown the ground signal to be much stronger, and the canopy signal to be much weaker, than originally anticipated. Therefore, a preprocessing step for dynamically calculating  $P$  and running the core DRAGANN function is described in this subsection. This assumes  $L$ -km to be 10 km (with additional  $L$ -km buffering).

1. Define a DRAGANN processing window of 170 segments ( $\sim 3.4$  km), and a buffer of 10 segments ( $\sim 200$  m).
2. The buffer is applied to both sides of each DRAGANN processing window to create buffered DRAGANN processing windows (referenced as “buffered window” for the rest of this section) that will overlap the DRAGANN processing windows next to them.
3. For each buffered window within the  $L$ -km segment, calculate a histogram of points with 1 m elevation bins.
4. For each buffered window histogram, calculate the median counts.
5. Bins with counts below the buffered window median count value are estimated to be noise. Calculate the mean count of noise bins.
6. Bins with counts above the buffered window median count value are estimated to be signal. Calculate the mean count of signal bins.
7. Determine the time elapsed over the buffered window.
8. Calculate estimated noise and signal rates for each buffered window by multiplying each window’s mean counts of noise bins and signal bins, determined from steps 5 and 6 above, by  $1/(\text{elapsed time})$  to return the rates in terms of points/meter[elevation]/second[across].
9. Calculate a noise ratio for each window by dividing the noise rate by the signal rate.
10. If, for all the buffered windows in the  $L$ -km segment, the noise rate is less than 20 and the noise ratio is less than 0.15; OR any noise rate is

1972 0; OR any signal rate is greater than 1000: re-calculate steps 3-9  
1973 using the entire *L-km* segment. Continue with the following steps  
1974 using results from the one *L-km* window (instead of multiple buffered  
1975 windows).

1976 11. Now, determine the DRAGANN parameter, P, for each buffered  
1977 window based on the following conditionals:

1978 a. If the signal rate is NaN (i.e., an invalid value), set the signal  
1979 index array to empty and move on to the next buffered  
1980 window.

1981 b. If noise rate < 20 || noise ratio < 0.15:  
1982 P = signal rate  
1983 If signal rate is < 5, P = 5; if signal rate > 20, P = 20

1984 c. Else P = 20.

1985 12. Run DRAGANN on the buffered window points using the calculated P.  
1986 13. If DRAGANN fails to find a signal (i.e., only one Gaussian found), run  
1987 DRAGANN again with P = 10.  
1988 14. If DRAGANN still fails to find a signal, try to determine P a second time  
1989 using the following conditionals:

1990 a. If (noise rate >= 20) ...  
1991 && (signal rate > 100) ...  
1992 && (signal rate < 250),  
1993 P = (signal rate)/2

1994 b. Else if signal rate >= 250,  
1995 if noise rate >= 250,  
1996 P = (noise rate)\*1.1  
1997 else,  
1998 P = 250

1999 c. Else, P = mean(noise rate, signal rate)

2000 15. Run DRAGANN on the buffered window points using the newly  
2001 calculated P.

2002 a. If still no signal points are found, set a dragannError flag.

2003 16. If signal points were found by DRAGANN, for each buffered window  
2004 calculate a signal check by dividing the number of signal points found  
2005 via DRAGANN by the number of total points in the buffered window.

2006 17. If dragannError has been set, or there are suspect signal statistics, the  
2007 following snippet of pseudocode will check those conditionals and try  
2008 to iteratively find a better P value to run DRAGANN with:  
2009  
2010 try\_count = 0  
2011  
2012 While dragannError ...  
2013 || ( (noise rate >= 30) ...  
2014 && (signal check > noise ratio) ...  
2015 && (noise ratio >= 0.15) ) ...  
2016 || (signal check < 0.001):  
2017  
2018 if P < 3,  
2019 break  
2020 else,  
2021 P = P\*0.75  
2022 end  
2023  
2024 if try\_count < 2  
2025 Clear out signal index results from previous DRAGANN run  
2026 Re-run DRAGANN with new P value  
2027 Recalculate the signal check  
2028 end  
2029  
2030 if no signal index results are returned  
2031 P = P\*0.75  
2032 end  
2033  
2034 try\_count = try\_count + 1  
2035  
2036 end

2037  
2038 18. If no signal photons are found by DRAGANN because only one  
2039 Gaussian was found, set the threshold as b+c (i.e., one standard  
2040 deviation away from the Gaussian peak location) for a final DRAGANN  
2041 run. Otherwise, set the signal index array to empty and move on to the  
2042 next buffered window.



- 2043 19. Assign the signal values found from DRAGANN for each buffered  
 2044 window to the original DRAGANN processing window range of points.  
 2045 20. Combine signal points from each DRAGANN processing window back  
 2046 into one  $L$ -km array of signal points for further processing.

2047

### 2048 4.3.3 Iterative DRAGANN processing

2049 It is possible in processing segments with high noise rates that DRAGANN will  
 2050 incorrectly identify clusters of noise as signal. One way to reduce these false positive  
 2051 noise clusters is to run the alternative DRAGANN process (Sec 4.3.1) again with the  
 2052 input being the signal output photons from the first run through alternative  
 2053 DRAGANN. Note that this methodology is still being tested, so by default this option  
 2054 should not be set.

- 2055 1. If  $SNR < 1$  (TBD) from alternative DRAGANN run, run alternative DRAGANN  
 2056 process again using the output signal photons from first DRAGANN run as the  
 2057 input to the second DRAGANN run.  
 2058 2. Recalculate SNR based on output of second DRAGANN run.

2059

2060

### 2061 4.4 Compute Filtering Window

- 2062 1. Next step is to run a surface filter with a variable window size (variable in  
 2063 that it will change from  $L$ -km segment to  $L$ -km segment). The window-size is  
 2064 denoted as Window.  
 2065 2.  $Sspan = ceil[5 + 46 * (1 - e^{-a*length})]$ , where  $length$  is the number of  
 2066 photons in the segment.  
 2067 3.  $a = \frac{\log\left(1 - \frac{21}{51-5}\right)}{-28114} \approx 21 \times 10^{-6}$ , where  $a$  is the shape parameter for the window  
 2068 span.  
 2069

2070 **4.5 De-trend Data**

2071 In this first phase of the ATL08 process, we will utilize signal photons identified by  
2072 DRAGANN and the ATL03 classification (signal\_conf\_ph) values of 3 and 4 as well as  
2073 the YAPC photon weights on the ATL03 data product. In lieu of the steps presented in  
2074 4.5.2 through 4.5.3, we are now using the photon weights from the YAPC algorithm  
2075 provided on the ATL03 data product as a better initial estimate of the ground surface. Early  
2076 results indicate that the highest 5-10% of photon weights correspond to the ground surface  
2077 except in areas of dense vegetation. We have found that in areas of high topographic  
2078 change, the utilization of the yapc photons weights out-performs the previous approach of  
2079 iterative filtering to estimate the initial ground line.

2080 For each 20m segment, develop a mask of likely ground photons to use for limiting those  
2081 returned by YAPC analysis by:

- 2082 a) Build histograms of heights of all photons with 0.5m bin size
- 2083 b) If fewer than 3 bins, skip to next segment
- 2084 c) Using only the 0.5m bin size histograms, determine noise bin count via 25th  
2085 percentile of lowest 10% of bin count
- 2086 d) If the above doesn't produce a valid number, such as in the case of few histogram  
2087 bins, recalculate via median of lowest 10% of bin count
- 2088 e) Enforce a minimum noise count of 1
- 2089 f) If max histogram count is less than  $3 * \text{noise count}$ , cycle, add 0.5m to bin size,  
2090 cycle back to start of histograms, to a maximum bin size of 6m
- 2091 g) If maximum histogram count  $\leq \text{noise count} * 3$ , assume no well-captured surface,  
2092 expand bin size by 0.5 and cycle to back to building histograms
- 2093 h) Starting at lowest histogram step through bins, lowest to DEM+10m, until the  
2094 sum of 2 bin counts exceeds noise count
- 2095 i) If any DRAGANN/signal\_conf photons are present, set only those photons with  
2096 heights within the 2 height bins as initial ground "guess"
- 2097 j) If no DRAGANN/signal\_conf photons are present, set all photons within the 2  
2098 height bins as initial ground "guess"

2099  
2100 Evaluate YAPC weights, inclusive of DEM, DRAGANN, signal\_conf, and initial  
2101 ground "guess" via:

- 2102 k) Normalize YAPC weights for each segment via ATL03 YAPC  
2103  $\text{weight} * \sqrt{\text{segment\_ph\_cnt}}$ , while setting zero for any photons beyond 3.0m  
2104 above DEM elevation. Divide these values by the 95th percentile value of the  
2105 same for normalization. Limit to a maximum value of 1.0
- 2106 l) Normalize weight for the entire 10km processing window by ATL03 YAPC  
2107  $\text{photon weight} * \sqrt{\text{count of all photons}} / 95\text{th percentile of the same}$

2108 For each 20m segment:

2109 m) If no photons in the segment provide weight from 10km normalization  $\geq 0.3$ ,  
2110 assume a noise segment and cycle segments loop  
2111 n) Track all photons in the segment included in initial ground “guess”, with  
2112 normalized weights  $\geq 0.4$ , and photon height  $\leq \text{DEM}+3.0\text{m}$   
2113 o) If less than 2 photons result in any 20m segment, track photons that are  
2114 DRAGANN/signal\_conf positive, with normalized weights  $\geq 0.4$ , and photon  
2115 height  $\leq \text{DEM}+3.0\text{m}$   
2116 p) If still less than 2 photons present, track photons that are DRAGANN/signal\_conf  
2117 positive and photon height  $\leq \text{DEM}+3.0\text{m}$   
2118 q) These photons are provided to ATL08 filtering, smoothing functions for initial  
2119 ground surface finding  
2120

2121 The output of these steps is a set of masked photons referred to here as  
2122 Asmooth\_yapc\_weights.

2123

- 2124 1. The input data are the signal photons identified by DRAGANN and the ATL03  
2125 classification (signal\_conf\_ph) values of 3-4.
- 2126 2. Generate a rough surface by connecting all photons to each other. Let’s call this  
2127 surface interp\_A.
- 2128 3. Run a median filter through Asmooth\_yapc\_weights using the window size set by  
2129 the software. Output = Asmooth.
- 2130 4. Define a reference DEM limit (ref\_dem\_limit) as 120 m (TBD).
- 2131 5. Remove any Asmooth values further than the ref\_dem\_limit threshold from the  
2132 reference DEM, and interpolate the Asmooth surface based on the remaining  
2133 Asmooth values. The interpolation method to use is the shape preserving  
2134 piecewise cubic Hermite interpolating polynomial – hereafter labeled as “pchip”  
2135 (Fritsch & Carlson, 1980).
- 2136 6. Compute the approximate relief of the  $L$ -km segment using the 95<sup>th</sup> - 5<sup>th</sup>  
2137 percentile heights of the signal photons. We are going to filter Asmooth again  
2138 and the smoothing is a function of the relief.
- 2139 7. Define the SmoothSize using the conditional statements below. The SmoothSize  
2140 will be used to detrend the data as well as to create an interpolated ground  
2141 surface later.

2142 SmoothSize = 2 \* Window

2143 • If relief >= 900, SmoothSize = round(SmoothSize/4)

2144 • If relief >= 400 && <= 900, SmoothSize = round(SmoothSize/3)

2145 • If relief >= 200 && <= 400, SmoothSize = round(SmoothSize/2)

2146 8. Greatly smooth Asmooth by first running Asmooth 10 times through a median  
2147 filter then a smoothing filter with a moving average method on the result. Both  
2148 the median filter and the smoothing filter use a window size of SmoothSize.

2149 9. Create a second smooth line (Asmooth2) that roughly follows the ground and  
2150 Asmooth2 will be used only for detrending data during initial ground  
2151 estimation. Asmooth2 is created by running five iterations of a median filter  
2152 and smoothing using SmoothSize defined in 4.6.7. The threshold for removing  
2153 photons is 1 m above each iteration.

#### 2154 **4.6 Filter outlier noise from signal**

2155 1. If there are any signal data that are 150 meters above Asmooth\_yapc, remove  
2156 them from the signal data set.

2157 2. If the standard deviation of the detrended signal is greater than 10 meters,  
2158 remove any signal value from the signal data set that is 2 times the standard  
2159 deviation of the detrended signal below Asmooth\_yapc or Asmooth2.

2160 3. Calculate a new Asmooth surface by interpolating (pchip method) a surface  
2161 from the remaining signal photons and median filtering using the Window  
2162 size, then median filter and smooth (moving average method) 10 times again  
2163 using the SmoothSize.

2164 4. Calculate a new Asmooth2 surface by interpolating a surface from remaining  
2165 signal photons and repeat **step 4.6**.

2166 5. Detrend the signal photons by subtracting the signal height values from the  
2167 Asmooth2 surface height values. Use the Asmooth2 detrended heights for the  
2168 initial ground estimate surface finding.

2169 6. Other calculations for canopy and ground finding will utilize detrended from  
2170 the original Asmooth.

2171

#### 2172 **4.7 Finding the initial ground estimate**

- 2173 1. At this point, the initial signal photons have been noise filtered and de-trended  
2174 and should have the following format: X, Y, detrended Z, T (T=time). From this,  
2175 the input data into the ground finding will be the ATD (along track distance)  
2176 metric (such as time) and the detrended Z height values.
- 2177 2. Define a medianSpan as  $\text{round}(\text{Window} * 2/3)$ .
- 2178 3. Calculate the background neighbor density of the subsurface photons using ALL  
2179 available photons (the non-detrended data). This step is run on all photons  
2180 including noise photons. Histogram the photons in 1 m vertical bins and a 60 m  
2181 horizontal bin.
- 2182 4. To avoid including zero population bins in the histogram signal tracking process,  
2183 identify the bin with the maximum bin count among bins 2 – 4 (starting at the  
2184 lowest height) across each 60 m within the 10-km processing window.
- 2185 5. Calculate the mean of those maximum bin values to represent the noise count for  
2186 the 10-km window.
- 2187 6. The following steps are run on the detrended signal photons.
- 2188 7. Calculate the brightness of the surface for each 60 m to be histogrammed via the  
2189 calculation in Section 2.4.21. If a bright surface is detected, skip steps 8 and 9
- 2190 8. Determine the lowest 1 m histogram height bin for each 60 m along track, in the  
2191 detrended heights where:
  - 2192 a. The neighbor density is 10 x greater than the background density or
  - 2193 b. The neighbor density is greater than the histogram population median  
2194 plus 1/3 of the population standard deviation.
- 2195 9. The photons with detrended heights above this bin are masked from  
2196 consideration in the initial ground height estimate. Detrended signal photons  
2197 implies that the d\_flag photons.
- 2198 10. Identifying the ground surface is an iterative process. Start by assuming that all  
2199 the input signal height photons are the ground. The first goal is the cut out the  
2200 lower height excess photons in order to find a lower bound for potential ground

2201 photons. This process is done 5 times and an offset of 4 meters is subtracted  
2202 from the resulting lower bound. The smoothing filter uses a moving average  
2203 again:

```
2204     for j=1:5
2205         cutOff = median filter (ground, medianSpan)
2206         cutOff = smooth filter (cutOff, Window)
2207         ground = ground( (cutOff - ground) > -1 )
2208     end
2209     lowerbound = median filter (ground, medianSpan*3)
2210     middlebound = smooth filter (lowerbound, Window)
2211     lowerbound = smooth filter (lowerbound, Window) - 4
2212 end;
```

2213 11. Create a linearly interpolated surface along the lower bound points and only  
2214 keep input photons above that line as potential ground points:

```
2215     top = input( input > interp(lowerbound) )
```

2216 12. The next goal is to cut out excess higher elevation photons in order to find an  
2217 upper bound to the ground photons. This process is done 3 times and an offset of  
2218 1 meter is added to the resulting upper bound. The smoothing filter uses a  
2219 moving average:

```
2220     for j = 1:3
2221         cutOff = median filter (top, medianSpan)
2222         cutOff = smooth filter (cutOff, Window)
2223         top = top( (cutOff - top) > -1 )
2224     end
2225     upperbound = median filter (top, medianSpan)
2226     upperbound = smooth filter (upperbound, Window) + 1
```

2227 13. Create a linearly interpolated surface along the upper bound points and extract  
2228 the points between the upper and lower bounds as potential ground points:

```

2229         ground = input( ( input > interp(lowerbound) ) & ...
2230             ( input < interp(upperbound) ) )

2231 14. Refine the extracted ground points to cut out more canopy, again using the
2232     moving average smoothing:

2233     For j = 1:2
2234         cutOff = median filter (ground, medianSpan)
2235         cutOff = smooth filter (cutOff, Window)
2236         ground = ground( (cutOff - ground) > -1 )
2237     end

2238 15. Run the ground output once more through a median filter using window side
2239     medianSpan and a smoothing filter using window size Window, but this time
2240     with the Savitzky-Golay method.

2241 16. Finally, linearly interpolate a surface from the ground points.

2242 17. The first estimate of canopy points are those indices of points that are between 2
2243     and 150 meters above the estimated ground surface. Save these indices for the
2244     next section on finding the top of canopy.

2245 18. The output from the final iteration of ground points is temp_interpA - an
2246     interpolated ground estimate.

2247 19. Find ground indices that lie within 10 m below and 0.5 m above of
2248     temp_interpA . Now, find ground indices that lie <=6 m above the refDEM

2249 20. Apply the ground indices to the original heights (i.e., not the de-trended data) to
2250     label ground photons.

2251 21. Interpolate a ground surface using the pchip method based on the ground
2252     photons. Output is interp_Aground.

2253 22. All initial ground results (interp_Aground) must lie within 6m or below the
2254     reference DEM height.

2255

```

2256 **4.8 Find the top of the canopy**

- 2257 1. The input are the ATD metric (i.e., time), and the de-trended Z values indexed  
2258 by the canopy indices extracted from step 4.7(17).
- 2259 2. Flip this data over so that we can find a canopy “surface” by multiplying the  
2260 de-trended canopy heights by -1.0 and adding the mean(heights).
- 2261 3. Finding the top of canopy is also an iterative process. Follow the same steps  
2262 described in 4.7(2) – 4.7(16), but use the canopy indexed and flipped Z  
2263 values in place of the ground input.
- 2264 4. Final retained photons are considered top of canopy photons. Use the indices  
2265 of these photons to define top of canopy photons in the original (not de-  
2266 trended) Z values.
- 2267 5. Build a kd-tree on canopy indices using elevation data detrended with  
2268 Asmooth.
- 2269 6. If there are less than three canopy indices within a 100m radius, reassign  
2270 these photons to noise photons. Initially, a value of 15 m was used for the  
2271 search radius. In Release 004 of the algorithm, this value was increased to  
2272 100 m to include more top of canopy photons that were not captured in the  
2273 initial canopy spline estimate.

2274

2275 **4.9 Compute statistics on de-trended (Asmooth) data**

- 2276 1. The input data have been noise filtered and de-trended (Asmooth) and  
2277 should have the following input format: X, Y, detrended Z, T.
- 2278 2. The input data will contain signal photons as well as a few noise photons  
2279 near the surface.
- 2280 3. Compute statistics of heights in the along-track direction using a sliding  
2281 window. Using the window size (window), compute height statistics for all  
2282 photons that fall within each window. These include max height, median  
2283 height, mean height, min height, and standard deviation of all photon heights.  
2284 Additionally, in each window compute the median height and standard



2285 deviation of just the initially classified top of canopy photons, and the  
2286 standard deviation of just the initially classified ground photon heights.  
2287 Currently only the median top of canopy, and all STD variables are being  
2288 utilized, but it's possible that other statistics may be incorporated as  
2289 changes/improvements are made to the code.

- 2290 4. Slide the window  $\frac{1}{4}$  of the window span and recompute statistics along the  
2291 entire  $L$ - $km$  segment. This results in one value for each statistic for each  
2292 window.
- 2293 5. Determine canopy index categories for each window based upon the total  
2294 distribution of STD values for all signal photons along the  $L$ - $km$  segment  
2295 based on STD quartiles.
- 2296 6. Open canopy have STD values falling within the 1<sup>st</sup> quartile.
- 2297 7. Canopy Level 1 has STD values falling from 1<sup>st</sup> quartile to median STD value.
- 2298 8. Canopy Level 2 has STD values falling from median STD value to 3<sup>rd</sup> quartile.
- 2299 9. Canopy Level 3 has STD values falling from 3<sup>rd</sup> quartile to max STD.
- 2300 10. Linearly interpolate the window STD values (both for all photons and  
2301 ground-only photons) back to the native along-track resolution and calculate  
2302 the interpolated all-photon STD quartiles to create an interpolated canopy  
2303 level index. This will be used later for interpolating a ground surface.  
2304

#### 2305 **4.10 Refine Ground Estimates**

- 2306 1. Detrend the interpolated ground surface using Asmooth. Smooth the  
2307 detrended interpolated ground surface 10 times. All further ground surface  
2308 smoothing use the moving average method:

2309 For j= 1:10

2310           AgroundSmooth = median filter (interp\_Aground, SmoothSize\*3)

2311           AgroundSmooth = smooth filter (AgroundSmooth, SmoothSize)

2312 End

2313

2314 2. This output (AgroundSmooth) from the filtering/smoothing function is an

2315 intermediate ground solution and it will be used to estimate the final

2316 solution.

2317 3. If there are **no canopy indices** identified along the entire segment AND relief

2318 >400 m

2319           FINALGROUND = median filter (ASmooth, SmoothSize)

2320           FINALGROUND = smooth filter (FINALGROUND, SmoothSize)

2321       Else

2322           FINALGROUND = AgroundSmooth

2323       end

2324 4. If there are **canopy indices** identified along the segment:

2325 If there is a canopy photon identified at a location along-track above the

2326 ground surface, then at that location along-track

2327           FINALGROUND = AgroundSmooth

2328 else if there is a location along-track where the interpolated ground STD has

2329 an interpolated canopy level  $\geq 3$

2330           FINALGROUND =  $\text{Interp\_Aground} * 1/3 + \text{AgroundSmooth} * 2/3$

2331 else

2332           FINALGROUND =  $\text{Interp\_Aground} * 1/2 + \text{ASmooth} * 1/2$

2333 end

2334 5. Smooth the resulting interpolated ground surface (FINALGROUND) once

2335 using a median filter with window size of 9 then a smoothing filter twice with

2336 window size of 9. Select ground photons that lie within the point spread

2337 function (PSF) of FINALGROUND.

2338 6. PSF is determined by sigma\_atlas\_land (Eq. 1.2) calculated at the photon

2339 resolution and thresholded between 0.5 to 1 m.

- 2340 a. Estimate the terrain slope by taking the gradient of FINALGROUND.  
 2341 Gradient is reported at the center of  $((\text{finalground}(n+1)-$   
 2342  $\text{finalground}(n-1))/(\text{dist}_x(n+1)-\text{dist}_x(n-1)))/2$   
 2343 b. Linearly interpolate the sigma\_h values to the photon resolution.  
 2344 c. Calculate sigma\_topo (Eq. 1.3) at the photon resolution.  
 2345 d. Calculate sigma\_atlas\_land at the photon resolution using the sigma\_h  
 2346 and sigma\_topo values at the photon resolution.  
 2347 e. Set PSF equal to sigma\_atlas\_land.  
 2348 i. Any PSF < 0.5 m is set to 0.5 m as the minimum PSF.  
 2349 ii. Any PSF > 1 m is set to 1 m as the maximum PSF. Set psf\_flag to  
 2350 true.

2351

#### 2352 **4.11 Canopy Photon Filtering**

- 2353 1. The first canopy filter will remove photons classified as top of canopy that  
 2354 are significantly above a smoothed median top of canopy surface. To  
 2355 calculate the smoothed median top of canopy surface:  
 2356 a. Linearly interpolate the median and standard deviation canopy  
 2357 window statistics, calculated from 4.9 (3), to the top of canopy photon  
 2358 resolution. Output variables: interpMedianC, interpStdC.  
 2359 b. Calculate a canopy window size using Eq. 3.4, where *length* = number  
 2360 of top of canopy photons. Output variable: winC.  
 2361 c. Create the median filtered and smoothed top of canopy surface,  
 2362 smoothedC, using a locally weighted linear regression smoothing  
 2363 method, “lowess” (Cleveland, 1979):

2364  $\text{smoothedC} = \text{median filter} (\text{interpMedianC}, \text{winC})$

2365

2366 if SNR > 1, canopySmoothSpan = winC\*2;

2367 else, canopySmoothSpan = smoothSpan;

2368

2369  $\text{smoothedC} = \text{smooth filter} (\text{smoothedC}, \text{canopySmoothSpan} )$

2370 d. Add the detrended heights back into the smoothedC surface:

2371  $\text{smoothedC} = \text{smoothedC} + \text{Asmooth}$

2372 2. Set canopy height thresholds based on the interpolated top of canopy STD:

2373 If  $\text{SNR} > 1$ ,  $\text{canopySTDthresh} = 3$ ; else,  $\text{canopySTDthresh} = 2$ ;

2374  $\text{canopy\_height\_thresh} = \text{canopySTDthresh} * \text{interpStdC}$

2375  $\text{high\_cStd} = \text{canopy\_height\_thresh} > 10$

2376  $\text{low\_cStd} = \text{canopy\_height\_thresh} < 3$

2377  $\text{canopy\_height\_thresh}(\text{high\_cStd}) =$

2378  $\text{canopy\_height\_thresh}(\text{high\_cStd})/2$

2379  $\text{canopy\_height\_thresh}(\text{low\_cStd}) = 3$

2380 3. Relabel as noise any top of canopy photons that are higher than smoothedC +

2381  $\text{canopy\_height\_thresh}$ .

2382 4. Next, interpolate a top of canopy surface using the remaining top of canopy

2383 photons (here we are trying to create an upper bound on canopy points). The

2384 interpolation method used is pchip. This output is named  $\text{interp\_Acanopy}$ .

2385 5. Photons falling below  $\text{interp\_Acanopy}$  and above  $\text{FINALGROUND} + \text{PSF}$  are

2386 labeled as canopy points.

2387 6. For 500 signal photon segments, if number of all canopy photons (i.e., canopy

2388 and top of canopy) is:

2389  $< 5\%$  of the total (when  $\text{SNR} > 1$ ), OR

2390  $< 10\%$  of the total (when  $\text{SNR} \leq 1$ ),

2391 relabel the canopy photons as noise.

2392 7. Interpolate, using the pchip method, a new top of canopy surface from the

2393 filtered top of canopy photons. This output is again named  $\text{interp\_Acanopy}$ .

- 2394 8. Again, label photons that lie between `interp_Acanopy` and  
2395 `FINALGROUND+PSF` as canopy photons.
- 2396 9. Since the canopy points have been relabeled, we need to do a final  
2397 refinement of the ground surface:
- 2398 If canopy is present at any location along-track
- 2399 `FINALGROUND = AgroundSmooth` (at that location)
- 2400 Else if canopy is not present at a location along-track
- 2401 `FINALGROUND = interp_Aground`
- 2402 Smooth the resulting interpolated ground surface (`FINALGROUND`) once  
2403 using a median filter with window size of `SmoothSize` (`SmoothSize = 9`), then  
2404 a moving average smoothing filter twice with window size of `SmoothSize`  
2405 (`SmoothSize = 9`)
- 2406 10. Relabel ground photons based on this new (and last) `FINALGROUND` solution  
2407 +/- a recalculated PSF (via steps in 4.10 (6)). Points falling below the buffer  
2408 are labeled as noise.
- 2409 11. Using `Interp_Acanopy` and this last `FINALGROUND` solution + PSF buffer,  
2410 label all photons that lie between the two as canopy photons.
- 2411 12. Repeat the canopy cover filtering: For 500 signal photon segments, if  
2412 number of all canopy photons (i.e., canopy and top of canopy) is:  
2413 < 5% of the total (when `SNR > 1`), OR  
2414 < 10% of the total (when `SNR <= 1`),  
2415 relabel the canopy photons as noise. This is the last canopy labeling step.

2416

#### 2417 ***4.12 Compute individual Canopy Heights***

- 2418 1. At this point, each photon will have its final label assigned in  
2419 **`classed_pc_flag`**: 0 = noise, 1 = ground, 2 = canopy, 3 = top of canopy.

- 2420 2. For each individual photon labeled as canopy or top of canopy, subtract the Z  
2421 height value from the interpolated terrain surface, FINALGROUND, at that  
2422 particular position in the along-track direction.
- 2423 3. The relative height for each individual canopy or top of canopy photon will  
2424 be used to calculate canopy products described in Section 4.15. Additional  
2425 canopy products will be calculated using the absolute heights, as described in  
2426 Section 4.15.1.  
2427

#### 2428 **4.13 Final photon classification QA check**

- 2429 1. Find any ground, canopy, or top of canopy photons that have elevations  
2430 further than the ref\_dem\_limit from the reference DEM elevation value.  
2431 Convert these to the noise classification.
- 2432 2. Find any relative heights of canopy or top of canopy photons that are greater  
2433 than 150 m above the interpolated ground surface, FINALGROUND. Convert  
2434 these to the noise classification.
- 2435 3. Find any FINALGROUND elevations that are further than the ref\_dem\_limit  
2436 from the reference DEM elevation value. Convert those FINALGROUND  
2437 elevations to an invalid value, and convert any classified photons at the same  
2438 indices to noise.
- 2439 4. If more than 50% of photons are removed in a segment, set ph\_removal\_flag  
2440 to true.

2441

#### 2442 **4.14 Compute segment parameters for the Land Products**

- 2443 1. For each 100 m segment, determine the classed photons (photons classified  
2444 as ground, canopy, or top of canopy).
- 2445 a. If there are fewer than 50 classed photons in a 100 m segment, do not  
2446 calculate land or canopy products.
- 2447 b. If there are 50 or more classed photons in a 100 m segment, extract  
2448 the ground photons to create the land products.

- 2449 2. If the number of ground photons > 5% of the total number of classed photons  
2450 within the segment (this control value of 5% can be modified once on orbit):  
2451 a. Compute statistics on the ground photons: mean, median, min, max,  
2452 standard deviation, mode, and skew. These heights will be reported  
2453 on the product as **h\_te\_mean**, **h\_te\_median**, **h\_te\_min**, **h\_te\_max**,  
2454 **h\_te\_mode**, and **h\_te\_skew** respectively described in Table 2.1.  
2455 b. Compute the standard deviation of the ground photons about the  
2456 interpolated terrain surface, FINALGROUND. This value is reported as  
2457 **h\_te\_std** in Table 2.1.  
2458 c. Compute the residuals of the ground photon Z heights about the  
2459 interpolated terrain surface, FINALGROUND. The product is the root  
2460 sum of squares of the ground photon residuals combined with the  
2461 **sigma\_atlas\_land** term in Table 2.5 as described in Equation 1.4. This  
2462 parameter reported as **h\_te\_uncertainty** in Table 2.1.  
2463 d. Compute a linear fit on the ground photons and report the slope. This  
2464 parameter is **terrain\_slope** in Table 2.1.  
2465 e. Calculate a best fit terrain elevation at the mid-point location of the  
2466 100 m segment:  
2467 i. Calculate each terrain photon's distance along-track into the  
2468 100 m segment using the corresponding ATL03 20 m products  
2469 segment\_length and dist\_ph\_along, and determine the mid-  
2470 segment distance (expected to be 50 m ± 0.5 m).  
2471 1. Use the mid-segment distance to linearly interpolate a  
2472 mid-segment time (**delta\_time** in Table 2.4). Use the  
2473 mid-segment time to linearly interpolate other mid-  
2474 segment parameters: interpolated terrain surface,  
2475 FINALGROUND, as **h\_te\_interp** (Table 2.1); **latitude**  
2476 and **longitude** (Table 2.4).  
2477 ii. Calculate a linear fit, as well as 3<sup>rd</sup> and 4<sup>th</sup> order polynomial fits  
2478 to the terrain photons in the segment.

- 2479                   iii. Create a slope-adjusted and weighted mid-segment variable,  
2480                   weightedZ, from the linear fit: Use terrain\_slope to apply a  
2481                   slope correction to each terrain photon by subtracting the  
2482                   terrain photon heights from the linear fit. Determine the mid-  
2483                   segment location of the linear fit, and add that height to the  
2484                   slope corrected terrain photons. Apply a linear weighting to  
2485                   each photon based on its distance to the mid-segment location:  
2486                    $1 / \sqrt{(\text{photon distance along} - \text{mid-segment distance})^2}$  ).  
2487                   Calculate the weighted mid-segment terrain height, weightedZ:  
2488                    $\text{sum}(\text{each adjusted terrain height} * \text{its weight}) / \text{sum}(\text{all}$   
2489                   weights).
- 2490                   iv. Determine which of the three fits is best by calculating the  
2491                   mean and standard deviation of the fit errors. If one of the fits  
2492                   has both the smallest mean and standard deviations, use that  
2493                   fit. Else, use the fit with the smallest standard deviation. If  
2494                   more than one fit has the same smallest mean and/or standard  
2495                   deviation, use the fit with the higher polynomial.
- 2496                   v. Use the best fit to define the mid-segment elevation. This  
2497                   parameter is **h\_te\_best\_fit** in Table 2.1.
- 2498                               1. If h\_te\_best\_fit is farther than 3 m from h\_te\_interp (best  
2499                               fit diff threshold), check if: there are terrain photons on  
2500                               both sides of the mid-segment location; or the elevation  
2501                               difference between weightedZ and h\_te\_interp is  
2502                               greater than the best fit diff threshold; or the number of  
2503                               ground photons in the segment is  $\leq 5\%$  of total  
2504                               number of classified photons per segment. If any of  
2505                               those cases are present, use h\_te\_interp as the corrected  
2506                               h\_te\_best\_fit. Otherwise use weightedZ as the corrected  
2507                               h\_te\_best\_fit.
- 2508                   f. Compute the difference of the median ground height from the  
2509                   reference DTM height. This parameter is **h\_dif\_ref** in Table 2.4.



2510  
2511  
2512  
2513  
2514  
2515  
2516  
2517  
2518  
2519  
2520  
2521  
2522  
2523

3. If the number of ground photons in the segment  $\leq 5\%$  of total number of classified photons per segment,
  - a. Report an invalid value for terrain products: **h\_te\_mean**, **h\_te\_median**, **h\_te\_min**, **h\_te\_max**, **h\_te\_mode**, **h\_te\_skew**, **h\_te\_std**, and **h\_te\_uncertainty** respectively as described in Table 2.1.
  - b. If the number of ground photons in the segment is  $\leq 5\%$  of total number of classified photons in the segment, compute **terrain\_slope** via a linear fit of the interpolated ground surface, FINALGROUND, instead of the ground photons.
  - c. Report the mid-segment interpolated terrain surface, FinalGround, as **h\_te\_interp** as described in Table 2.1, and report **h\_te\_best\_fit** as the h\_te\_interp value.

#### 2524 **4.15 Compute segment parameters for the Canopy Products**

- 2525 1. For each 100 m segment, determine the classed photons (photons classified as  
2526 ground, canopy, or top of canopy).
  - 2527 a) If there are fewer than 50 classed photons in a 100 m segment, do not  
2528 calculate land or canopy products.
  - 2529 b) If there are 50 or more classed photons in a 100 m segment, extract all  
2530 canopy photons (i.e., canopy and top of canopy; henceforth referred to  
2531 as “canopy” unless otherwise noted) to create the canopy products.
- 2532 2. Only compute canopy height products if the number of canopy photons is  $>$   
2533  $5\%$  of the total number of classed photons within the segment (this control  
2534 value of  $5\%$  can be modified once on orbit).
  - 2535 a) If the number of ground photons is also  $> 5\%$  of the total number of  
2536 classed photons within the segment, set **canopy\_rh\_conf** to 2.
  - 2537 b) If the number of ground photons is  $< 5\%$  of the total number of classed  
2538 photons within the segment, continue with the relative canopy height  
2539 calculations, but set canopy\_rh\_conf to 1.

- 2540 c) If the number of canopy photons is < 5% of the total number of classed  
 2541 photons within the segment, regardless of ground percentage, set  
 2542 canopy\_rh\_conf to 0 and report an invalid value for each canopy height  
 2543 variable.
- 2544 d) Considering adding in a QC check for the absolute canopy height. If the  
 2545 height is below the reference DEM, disregard this ATL08 segment.
- 2546 3. Again, the relative heights (height above the interpolated ground surface,  
 2547 FINALGROUND) have been computed already. All parameters derived in the  
 2548 section are based on relative heights.
- 2549 4. Sort the heights and compute a cumulative distribution of the heights. Select  
 2550 the height associated with the 98% maximum height. This value is **h\_canopy**  
 2551 listed in Table 2.2.
- 2552 5. Compute statistics on the relative canopy heights. Min, Mean, Median, Max and  
 2553 standard deviation. These values are reported on the product as  
 2554 **h\_min\_canopy, h\_mean\_canopy, h\_max\_canopy, and canopy\_openness**  
 2555 respectively in Table 2.2.
- 2556 6. Using the cumulative distribution of relative canopy heights, select the heights  
 2557 associated with the **canopy\_h\_metrics** percentile distributions (10, 15, 20, 25,  
 2558 30, 35, 40, 45, 50, 55, 60, 65, 70, 75, 80, 85, 90, 95), and report as listed in Table  
 2559 2.2.
- 2560 7. Compute the difference between h\_canopy and canopy\_h\_metrics(50). This  
 2561 parameter is **h\_dif\_canopy** reported in Table 2.2 and represents an amount of  
 2562 canopy depth.
- 2563 8. Compute the standard deviation of all photons that were labeled as Top of  
 2564 Canopy (flag 3) in the photon labeling portion. This value is reported on the  
 2565 data product as **toc\_roughness** listed in Table 2.2.
- 2566 9. The quadratic mean height, **h\_canopy\_quad** is computed by

2567 
$$qmh = \sqrt{\frac{\sum_{i=1}^{Nca} h_i^2}{Nca}}$$

2568 where  $N_{ca}$  is the number of canopy photons in the segment and  $h_i$  are the  
2569 individual canopy heights.

2570

#### 2571 **4.15.1 Canopy Products calculated with absolute heights**

- 2572 1. The absolute canopy height products are calculated if the number of canopy  
2573 photons is > 5% of the total number of classed photons within the segment.  
2574 No number of ground photons threshold is applied for these. Absolute  
2575 canopy heights are first determined as the relative heights of individual  
2576 photons above the estimated terrain surface. Once those cumulative  
2577 distribution is made, the absolute heights are the relative heights plus the  
2578 best fit terrain height ( $h_{te\_bestfit}$ ).
- 2579 2. The **centroid\_height** parameter in Table 2.2 is represented by all the classed  
2580 photons for the segment (canopy & ground). To determine the centroid  
2581 height, compute a cumulative distribution of all absolute classified heights  
2582 and select the median height.
- 2583 3. Calculate **h\_canopy\_abs**, the 98<sup>th</sup> percentile of the absolute canopy heights.
- 2584 4. Compute statistics on the absolute canopy heights: Min, Mean, Median, and  
2585 Max. These values are reported on the product as **h\_min\_canopy\_abs**,  
2586 **h\_mean\_canopy\_abs**, and **h\_max\_canopy\_abs**, respectively, as described in  
2587 Table 2.2.
- 2588 5. Again, using the cumulative distribution of relative canopy heights, select the  
2589 heights associated with the **canopy\_h\_metrics\_abs** percentile distributions  
2590 (10, 15, 20, 25, 30, 35, 40, 45, 50, 55, 60, 65, 70, 75, 80, 85, 90, 95) and then  
2591 added to the  $h_{te\_bestfit}$ , and report as listed in Table 2.2.

#### 2592 **4.16 Segment Quality Check**

- 2593 1. Quality check is based on the radiometry rates,  $te\_photon\_rate$  and  
2594  $can\_photon\_rate$ . For the strong beams, if the  $total\_photon\_rate$   
2595 ( $te\_photon\_rate + can\_photon\_rate$ ) has a value of 16 or higher, reject all  
2596 parameters in this ATL08 segment as invalid and reassign any labeled

2597 photons back to noise unless the saturation flag is on. For the weak beams, if  
 2598 the total\_photon\_rate (te\_photon\_rate + can\_photon\_rate) has a value of 4 or  
 2599 higher, reject all parameters in this ATL08 segment as invalid and reassign  
 2600 any labeled photons back to noise unless the saturation flag is on.

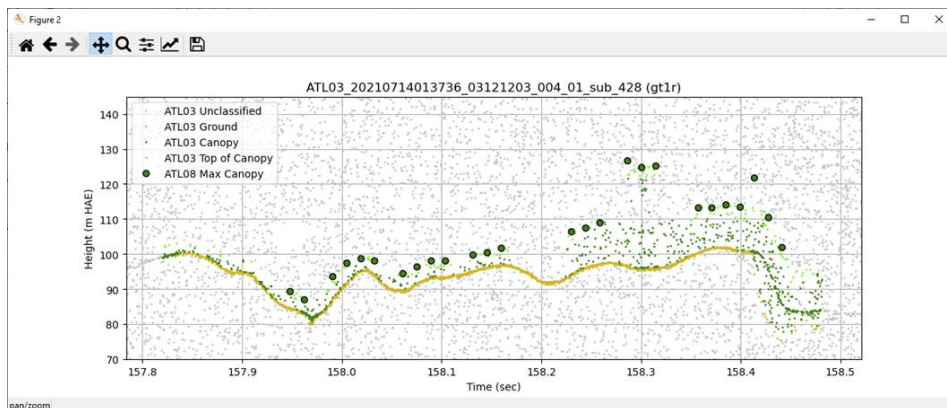
2601 2. If  $h\_canopy\_abs + 50 < ref\_dem$ , reject all parameters in this ATL08 segment  
 2602 as these height are likely noise points that were mislabeled. Reassign any  
 2603 labeled (ground or canopy) photons back to noise.

2604 3. Canopy Photon Background Rate QA check. The objective of this QA check is  
 2605 to utilize the calculated background noise and the calculated noise reduced  
 2606 canopy photon rate (photon\_rate\_can\_nr ) within each 100 m geosegment to  
 2607 relabel noise photons that may have incorrectly been labeled as canopy  
 2608 photons (see example below). The methodology for this step is as follows:

2609 a. For acquisitions where the solar\_elev>20 degrees, if canopy photons  
 2610 are within 1 m of the final interpolated ground line, ignore those  
 2611 canopy photons in this special canopy test. Thus, count only the  
 2612 canopy photons higher than 1 m above the final interpolated ground  
 2613 line.

2614 b. Divide the special canopy count by the unique delta times to  
 2615 determine a special canopy rate.

2616 c. If the background noise rate is >99.5% of the special canopy photon  
 2617 rate, reassign the canopy photons as noise (label value of  
 2618 0).



2619

2620

2621 **4.17 Record final product without buffer**

2622 1. Now that all products have be determined via processing of the *L-km*  
2623 segment with the buffer included, remove the products that lie within the  
2624 buffer zone on each end of the *L-km* segment.

2625 2. Record the final *L-km* products and move on to process the next *L-km*  
2626 segment.

2627

2628

2629 **5 DATA PRODUCT VALIDATION STRATEGY**

2630 Although there are no Level-1 requirements related to the accuracy and precision  
2631 of the ATL08 data products, we are presenting a methodology for validating terrain  
2632 height, canopy height, and canopy cover once ATL08 data products are created.  
2633 Parameters for the terrain and canopy will be provided at a fixed size of 100 m along  
2634 the ground track referred to as a segment. Validation of the data parameters should  
2635 occur at the 100 m segment scale and residuals of uncertainties are quantified (i.e.  
2636 averaged) at the 5-km scale. This 5-km length scale will allow for quantification of  
2637 errors and uncertainties at a local scale which should reflect uncertainties as a  
2638 function of surface type and topography.

2639

2640 **5.1 Validation Data**

2641 Swath mapping airborne lidar is the preferred source of validation data for the  
2642 ICESat-2 mission due to the fact that it is widely available and the errors associated  
2643 with most small-footprint, discrete return data sets are well understood and  
2644 quantified. Profiling airborne lidar systems (such as MABEL) are more challenging to  
2645 use for validation due to the low probability of exact overlap of flightlines between  
2646 two profiling systems (e.g. ICESat-2 and MABEL). In order for the ICESat-2 validation  
2647 exercise to be statistically relevant, the airborne data should meet the requirements  
2648 listed in Table 5.1. Validation data sets should preferably have a minimum average  
2649 point density of 5 pts/m<sup>2</sup>. In some instances, however, validation data sets with a  
2650 lower point density that still meet the requirements in Table 5.1 may be utilized for  
2651 validation to provide sufficient spatial coverage.

2652 Table 5.1. Airborne lidar data vertical height (*Z* accuracy) requirements for validation data.

ICESat-2 ATL08 Parameter	Airborne lidar (rms)
Terrain height	<0.3 m over open ground (vertical) <0.5 m (horizontal)

---

Canopy height	<2 m temperate forest, < 3 m tropical forest
Canopy cover	n/a

---

2653

2654 Terrain and canopy heights will be validated by computing the residuals between the  
2655 ATL08 terrain and canopy height value, respectively, for a given 100 m segment and  
2656 the terrain height (or canopy height) of the validation data for that same  
2657 representative distance. Canopy cover on the ATL08 data product shall be validated  
2658 by computing the relative canopy cover ( $cc = \text{canopy returns}/\text{total returns}$ ) for the  
2659 same representative distance in the airborne lidar data.

2660 It is recommended that the validation process include the use of ancillary data sets  
2661 (i.e. Landsat-derived annual forest change maps) to ensure that the validation results  
2662 are not errantly biased due to non-equivalent content between the data sets.

2663 Using a synergistic approach, we present two options for acquiring the required  
2664 validation airborne lidar data sets.

2665

2666 **Option 1:**

2667 We will identify and utilize freely available, open source airborne lidar data as the  
2668 validation data. Potential repositories of this data include OpenTopo (a NSF  
2669 repository or airborne lidar data), NEON (a NSF repository of ecological monitoring  
2670 in the United States), and NASA GSFC (repository of G-LiHT data). In addition to  
2671 small-footprint lidar data sets, NASA Mission data (i.e. ICESat and GEDI) can also be  
2672 used in a validation effort for large scale calculations.

2673

2674 **Option 2:**

2675 Option 2 will include Option 1 as well as the acquisition of additional airborne lidar  
2676 data that will benefit multiple NASA efforts.

2677 GEDI: With the launch of the Global Ecosystems Dynamic Investigation  
2678 (GEDI) mission in 2018, there are tremendous synergistic activities for  
2679 data validation between both the ICESat-2 and GEDI missions. Since the  
2680 GEDI mission, housed on the International Space Station, has a  
2681 maximum latitude of 51.6 degrees, much of the Boreal zone will not be  
2682 mapped by GEDI. The density of GEDI data will increase as latitude  
2683 increases north to 51.6 degrees. Since the data density for GEDI would  
2684 be at its highest near 51.6 degrees, we would propose to acquire  
2685 airborne lidar data in a “GEDI overlap zone” that would ample  
2686 opportunity to have sufficient coverage of benefit to both ICESat-2 and  
2687 GEDI for calibration and validation.

2688 We recommend the acquisition of new airborne lidar collections that will meet our  
2689 requirements to best validate ICESat-2 as well as be beneficial for the GEDI mission.  
2690 In particular, we would like to obtain data over the following two areas:

- 2691 1) Boreal forest (as this forest type will NOT be mapped with GEDI)
- 2692 2) GEDI high density zone (between 50 to 51.6 degrees N). Airborne lidar data  
2693 in the GEDI/ICESat-2 overlap zone will ensure cross-calibration between  
2694 these two critical datasets which will allow for the creation of a global,  
2695 seamless terrain, canopy height, and canopy cover product for the  
2696 ecosystem community.

2697 In both cases, we would fly data with the following scenario:

2698 Small-footprint, full-waveform, dual wavelength (green and NIR), high point density  
2699 (>20 pts/m<sup>2</sup>) and, over low and high relief locations. In addition, the newly acquired  
2700 lidar data must meet the error accuracies listed in Table 5.1.

2701 Potential candidate acquisition areas include: Southern Canadian Rocky Mountains  
2702 (near Banff), Pacific Northwest mountains (Olympic National Park, Mt. Baker-  
2703 Snoqualmie National Forest), and Sweden/Norway. It is recommended that the



2704 airborne lidar acquisitions occur during the summer months to avoid snow cover in  
 2705 either 2016 or 2017 prior to launch of ICESat-2.

2706

2707 **5.2 Internal QC Monitoring**

2708 In addition to the data product validation, internal monitoring of data  
 2709 parameters and variables is required to ensure that the final ATL08 data quality  
 2710 output is trustworthy. Table 5.2 lists a few of the computed parameters that should  
 2711 provide insight into the performance of the surface finding algorithm within the  
 2712 ATL08 processing chain.

2713 Table 5.2. ATL08 parameter monitoring.

Group	Description	Source	Monitor	Validate in Field
<b>h_te_median</b>	Median terrain height for segment	computed		Yes against airborne lidar data. The airborne lidar data should have an absolute accuracy of <30 cm rms.
<b>n_te_photons</b> <b>n_ca_photons</b> <b>n_toc_photons</b>	Number of classed (sum of terrain, canopy, and top of canopy) photons in a 100 m segment	computed	Yes. Build an internal counter for the number of segments in a row where there aren't enough photons (currently a minimum of 50 photons	

---

<b>h_te_interp</b>	Interpolated terrain surface height, FINALGROUND	computed	per 100 m segment is used) Difference h_te_interp and h_te_median and determine if the value is > a specified threshold. 2 m is suggested as the threshold value. This is an internal check to evaluate whether the median elevation for a segment is roughly the same as the interpolated surface height.	
<b>h_dif_ref</b>	Difference between h_te_median and ref_dem	computed	This value will be computed and flagged if the difference is > 25 m. The reference DEM is the onboard DEM.	
<b>h_canopy</b>	95% height of individual canopy heights for segment	computed	Yes, > a specified threshold (e.g. 60 m)	Yes against airborne lidar data. The

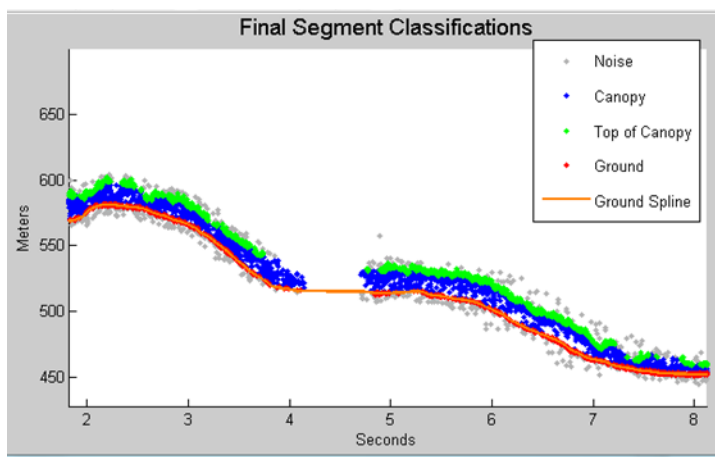
---

---

				canopy heights derived from airborne lidar data should have a relative accuracy <2 m in temperate forest, <3 m in tropical forest
<b>h_dif_canopy</b>	Difference between h_canopy and canopy_h_metrics(50)	computed	Yes, this is an internal check to make sure the calculations on canopy height are not suspect	
<b>psf_flag</b>	Flag is set if computed PSF exceeds 1m	computed	Yes, this is an internal check to make sure the calculations are not suspect	
<b>ph_removal_flag</b>	Flag is set if more than 50% of classified photons in a segment is removed during final QA check	computed		
<b>dem_removal_flag</b>	Flag is set if more than 20% of classified photons in a segment is removed due to a large distance from the reference DEM	computed	Yes, this will check if bad results are due to bad DEM values or because too much noise was labeled as signal	

---

2715 In addition to the monitoring parameters listed in Table 5.2, a plot such as what is  
2716 shown in Figure 5.1 would be helpful for internal monitoring and quality  
2717 assessment of the ATL08 data product. Figure 5.1 illustrates in graphical form what  
2718 the input point cloud look like in the along-track direction, the classifications of each  
2719 photon, and the estimated ground surface (FINALGROUND).



2720

2721 Figure 5.1. Example of *L-km* segment classifications and interpolated ground surface.

2722

2723 The following parameters are to be calculated and placed in the QA/QC group on the  
 2724 HDF5 data file, based on Table 5.2 of the ATL08 ATBD. Statistics shall be computed  
 2725 on a per-granule basis and reported on the data product. If any parameter meets the  
 2726 QA trigger conditional, an alert will be sent to the ATL08 ATBD team for product  
 2727 review.

2728 Table 5.3. QA/QC trending and triggers.

QA/QC trending description	QA trigger conditional
Percentage of segments with > 50 classed photons	None
Max, median, and mean of the number of contiguous segments with < 50 classed photons	None
Number and percentage of segments with difference in $h_{te\_interp} - h_{te\_median}$ is greater than a specified threshold (2 m TBD)	> 50 segments in a row
Max, median, and mean of $h_{diff\_ref}$ over all segments	None
Percentage of segments where $h_{diff\_ref} > 25$ m	Percentage > 75%
Percentage of segments where the $h_{canopy}$ is > 60m	None
Max, median, and mean of $h_{diff}$	None
Percentage of segments where $psf\_flag$ is set	Percentage > 75%
Percentage of classified photons removed in a segment during final photon QA check	Percentage > 50% (i.e., $ph\_removal\_flag$ is set to true)
Percentage of classified photons removed in a segment during the reference DEM threshold removal process	Percentage > 20% (i.e., $dem\_removal\_flag$ is set to true)

2729

2730

2731 **6 REFERENCES**

2732

2733 Carroll, M. L., Townshend, J. R., DiMiceli, C. M., Noojipady, P., & Sohlberg, R. A.  
2734 (2009). A new global raster water mask at 250 m resolution. *International Journal of*  
2735 *Digital Earth*, 2(4), 291–308. <http://doi.org/10.1080/17538940902951401>

2736 Channan, S., K. Collins, and W. R. Emanuel (2014). Global mosaics of the standard  
2737 MODIS land cover type data. University of Maryland and the Pacific Northwest  
2738 National Laboratory, College Park, Maryland, USA.

2739 Chauve, Adrien, et al. (2008). Processing full-waveform lidar data: modelling raw  
2740 signals. *International archives of photogrammetry, remote sensing and spatial*  
2741 *information sciences 2007*, 102-107.

2742 Cleveland, W. S. (1979). Robust Locally Weighted Regression and Smoothing  
2743 Scatterplots. *Journal of the American Statistical Association*, 74(368), 829–836.  
2744 <http://doi.org/10.2307/2286407>

2745 Friedl, M.A., D. Sulla-Menashe, B. Tan, A. Schneider, N. Ramankutty, A. Sibley and X.  
2746 Huang (2010). MODIS Collection 5 global land cover: Algorithm refinements and  
2747 characterization of new datasets, 2001-2012, Collection 5.1 IGBP Land Cover,  
2748 Boston University, Boston, MA, USA.

2749 Fritsch, F.N., and Carlson, R.E. (1980). Monotone Piecewise Cubic Interpolation.  
2750 *SIAM Journal on Numerical Analysis*, 17(2), 238–246.  
2751 <http://doi.org/10.1137/0717021>

2752 Goshtasby, A., and O'Neill, W.D. (1994). Curve fitting by a Sum of Gaussians.  
2753 *Graphical Models and Image Processing*, 56(4), 281-288.

2754 Goetz and Dubayah (2011). Advances in remote sensing technology and  
2755 implications for measuring and monitoring forest carbon stocks and change. *Carbon*  
2756 *Management*, 2(3), 231-244. doi:10.4155/cmt.11.18

2757 Hall, F.G., Bergen, K., Blair, J.B., Dubayah, R., Houghton, R., Hurtt, G., Kellndorfer, J.,  
2758 Lefsky, M., Ranson, J., Saatchi, S., Shugart, H., Wickland, D. (2011). Characterizing 3D  
2759 vegetation structure from space: Mission requirements. *Remote sensing of*  
2760 *environment*, 115(11), 2753-2775

2761 Harding, D.J., (2009). Pulsed laser altimeter ranging techniques and implications for  
2762 terrain mapping, in *Topographic Laser Ranging and Scanning: Principles and*  
2763 *Processing*, Jie Shan and Charles Toth, eds., CRC Press, Taylor & Francis Group, 173-  
2764 194.

2765 Neuenschwander, A.L. and Magruder, L.A. (2016). The potential impact of vertical  
2766 sampling uncertainty on ICESat-2/ATLAS terrain and canopy height retrievals for  
2767 multiple ecosystems. *Remote Sensing*, 8, 1039; doi:10.3390/rs8121039

2768 Neuenschwander, A.L. and Pitts, K. (2019). The ATL08 Land and Vegetation Product  
2769 for the ICESat-2 Mission. *Remote Sensing of Environment*, 221, 247-259.  
2770 <https://doi.org/10.1016/j.rse.2018.11.005>

2771 Neumann, T., Brenner, A., Hancock, D., Robbins, J., Saba, J., Harbeck, K. (2018). ICE,  
2772 CLOUD, and Land Elevation Satellite – 2 (ICESat-2) Project Algorithm Theoretical  
2773 Basis Document (ATBD) for Global Geolocated Photons (ATL03).

2774 Olson, D. M., Dinerstein, E., Wikramanayake, E. D., Burgess, N. D., Powell, G. V. N.,  
2775 Underwood, E. C., D'Amico, J. A., Itoua, I., Strand, H. E., Morrison, J. C., Loucks, C. J.,  
2776 Allnutt, T. F., Ricketts, T. H., Kura, Y., Lamoreux, J. F., Wettengel, W. W., Hedao, P.,  
2777 Kassem, K. R. (2001). Terrestrial ecoregions of the world: a new map of life on Earth.  
2778 *Bioscience*, 51(11), 933-938.

2779



2780 **Appendix A**

2781 **DRAGANN Gaussian Deconstruction**

2782 John Robbins

2783 20151021

2784

2785 Updates made by Katherine Pitts:

2786 20170808

2787 20181218

2788

2789 **Introduction**

2790 This document provides a verbal description of how the DRAGANN (Differential,  
2791 Regressive, and Gaussian Adaptive Nearest Neighbor) filtering system deconstructs  
2792 a histogram into Gaussian components, which can also be called *iteratively fitting a*  
2793 *sum of Gaussian Curves*. The purpose is to provide enough detail for ASAS to create  
2794 operational ICESat-2 code required for the production of the ATL08, Land and  
2795 Vegetation product. This document covers the following Matlab functions within  
2796 DRAGANN:

- 2797 • mainGaussian\_dragann
- 2798 • findpeaks\_dragann
- 2799 • peakWidth\_dragann
- 2800 • checkFit\_dragann

2801

2802 Components of the k-d tree nearest-neighbor search processing and histogram  
2803 creation were covered in the document, *DRAGANN k-d Tree Investigations*, and have  
2804 been determined to function consistently with UTexas DRAGANN Matlab software.

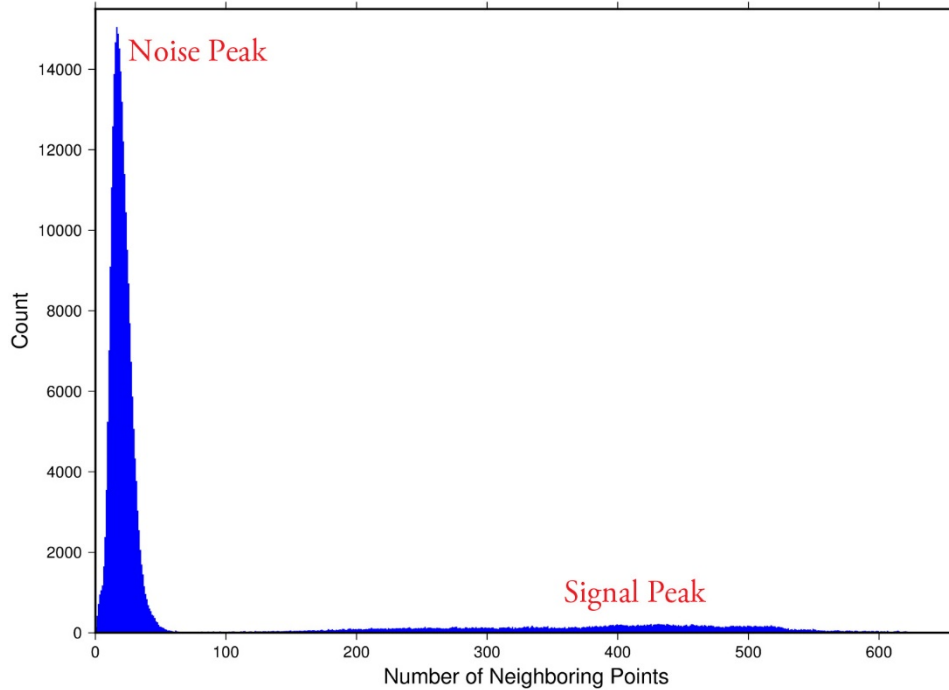
2805

2806 **Histogram Creation**

2807 Steps to produce a histogram of nearest-neighbor counts from a normalized photon  
2808 cloud segment have been completed and confirmed. Figure A.1 provides an example  
2809 of such a histogram. The development, below, is specific to the two-dimensional  
2810 case and is provided as a review.

2811 The histogram represents the frequency (count) of the number of nearby photons  
2812 within a specified radius, as ascertained for each point within the photon cloud. The  
2813 radius,  $R$ , is established by first normalizing the photon cloud in time (x-axis) and in  
2814 height (y-axis), i.e., both sets of coordinates (time & height) run from 0 to 1; then an  
2815 average radius for finding 20 points is determined based on forming the ratio of 20  
2816 to the total number of the photons in the cloud ( $N_{total}$ ):  $20/N_{total}$ .

2817



2818

2819 **Figure A.1.** Histogram for Mabel data, channel 43 from SE-AK flight on July 30, 2014  
 2820 at 20:16.

2821 Given that the total area of the normalized photon cloud is, by definition, 1, then this  
 2822 ratio gives the average area,  $A$ , in which to find 20 points. A corresponding radius is  
 2823 found by the square root of  $A/\pi$ . A single equation describing the radius, as a  
 2824 function of the total number of photons in the cloud (remembering that this is done  
 2825 in the cloud normalized, two-dimensional space), is given by

2826 
$$R = \sqrt{\frac{20/N_{total}}{\pi}} \quad (A.1)$$

2827 For the example in Figure A.1,  $R$  was found to be 0.00447122. The number of  
 2828 photons falling into this radius, at each point in the photon cloud, is given along the  
 2829 x-axis; a count of their number (or frequency) is given along the y-axis.

2830

### 2831 **Gaussian Peak Removal**

2832

2833 At this point, the function, `mainGaussian_dragann`, is called, which passes the  
 2834 histogram and the number of peaks to detect (typically set to 10).

2835 This function essentially estimates (i.e., fits) a sequence of Gaussian curves, from  
 2836 larger to smaller. It determines a Gaussian fit for the highest histogram peak, then  
 2837 removes it before determining the fit for the next highest peak, etc. In concept, the  
 2838 process is an iterative sequential-removal of the ten largest Gaussian components  
 2839 within the histogram.

2840 In the process of *sequential least-squares*, parameters are re-estimated when input  
2841 data is incrementally increased and/or improved. The present problem operates in  
2842 a slightly reverse way: the data set is fixed (i.e., the histogram), but components  
2843 within the histogram (independent Gaussian curve fits) are removed sequentially  
2844 from the histogram. The paper by *Goshtasby & O'Neill* (1994) outlines the concepts.

2845 Recall that a Gaussian curve is typically written as

$$2846 \quad y = a \cdot \exp(-(x - b)^2 / 2c^2) \quad (\text{A.2})$$

2847 where  $a$  = the height of the peak;  $b$  = position of the peak; and  $c$  = width of the bell  
2848 curve.

2849 The function, `mainGaussian_dragann`, computes the  $[a, b, c]$  values for the ten  
2850 highest peaks found in the histogram. At initialization, these  $[a, b, c]$  values are set to  
2851 zero. The process begins by locating histogram peaks via the function,  
2852 `findpeaks_dragann`.

2853

## 2854 **Peak Finding**

2855 As input arguments, the `findpeaks_dragann` function receives the histogram and a  
2856 minimum peak size for consideration (typically set to zero, which means all peaks  
2857 will be found). An array of index numbers (i.e., the “number of neighboring points”,  
2858 values along x-axis of Figure A.1) for all peaks is returned and placed into the  
2859 variable `peaks`.

2860 The methodology for locating each peak goes like this: The function first computes  
2861 the derivatives of the histogram. In Matlab there is an intrinsic function, called `diff`,  
2862 which creates an array of the derivatives. `diff` essentially computes the differences  
2863 along sequential, neighboring values. “ $Y = \text{diff}(X)$  calculates differences between  
2864 adjacent elements of  $X$ .” [from Matlab Reference Guide] Once the derivatives are  
2865 computed, then `findpeaks_dragann` enters a loop that looks for changes in the sign  
2866 of the derivative (positive to negative). It skips any derivatives that equal zero.

2867 For the  $k$ th derivative, the “*next*” derivative is set to  $k+1$ . A test is made whereby if  
2868 the  $k+1$  derivative equals zero and  $k+1$  is less than the total number of histogram  
2869 values, then increment “*next*” to  $k+2$  (i.e., find the next negative derivative). The test  
2870 is iterated until the start of the “down side” of the peak is found (i.e., these iterations  
2871 handle cases when the peak has a flat top to it).

2872 When a sign change (positive to negative) is found, the function then computes an  
2873 approximate index location (variable *maximum*) of the peak via

$$2874 \quad \text{maximum} = \text{round} \left( \frac{\text{next} - k}{2} \right) + k \quad (\text{A.3})$$

2875 These values of *maximum* are retained in the peaks array (which can be *grown* in  
2876 Matlab) and returned to the function mainGaussian\_dragann.

2877 Next, back within mainGaussian\_dragann, there are two tests to determine whether  
2878 the first or last elements of the histogram are peaks. This is done since the  
2879 findpeaks\_dragann function will not detect peaks at the first or last elements, based  
2880 solely on derivatives. The tests are:

2881 If ( histogram(1) > histogram(2) && max(histogram)/histogram(1) < 20 ) then  
2882 insert a value of 1 to the very first element of the peaks array (again, Matlab can  
2883 easily “grow” arrays). Here, max(histogram) is the highest peak value across the  
2884 whole histogram.

2885 For the case of the last histogram value (say there are N-bins), we have

2886 If ( histogram(N) > histogram(N-1) && max(histogram)/histogram(N) < 4 ) then  
2887 insert a value of N to the very last element of the peaks array.

2888 One more test is made to determine whether there any peaks were actually found  
2889 for the whole histogram. If none were found, then the function,  
2890 mainGaussian\_dragann, merely exits.

2891

## 2892 **Identifying and Processing upon the Ten Highest Peaks**

2893 The function, mainGaussian\_dragann, now begins a loop to analyze the ten highest  
2894 peaks. It begins the  $n^{\text{th}}$  loop (where  $n$  goes from 1 to 10) by searching for the largest  
2895 peak among all remaining peaks. The index number, as well as the magnitude of the  
2896 peak, are retained in a variable, called maximum, with dimension 2.

2897 In each pass in the loop, the  $[a,b,c]$  values (see eq. 2) are retained as output of the  
2898 function. The values of  $a$  and  $b$  are set equal to the index number and peak  
2899 magnitude saved in maximum(1) and maximum(2), respectively. The  $c$ -value is  
2900 determined by calling the function, peakWidth\_dragann.

### 2901 *Determination of Gaussian Curve Width*

2902 The function, peakWidth\_dragann, receives the whole histogram and the index  
2903 number (maximum(1)) of the peak for which the value  $c$  is needed, as arguments.  
2904 For a specific peak, the function essentially searches for the point on the histogram  
2905 that is about  $\frac{1}{2}$  the size of the peak and that is furthest away from the peak being  
2906 investigated (left and right of the peak). If the two sides (left and right) are  
2907 equidistant from the peak, then the side with the smallest value is chosen ( $> \frac{1}{2}$   
2908 peak).

2909 Upon entry, it first initializes  $c$  to zero. Then it initializes the index values left, xL and  
2910 right, xR as index-1 and index+1, respectively (these will be used in a loop,

2911 described below). It next checks whether the  $n^{\text{th}}$  peak is the first or last value in the  
2912 histogram and treats it as a special case.

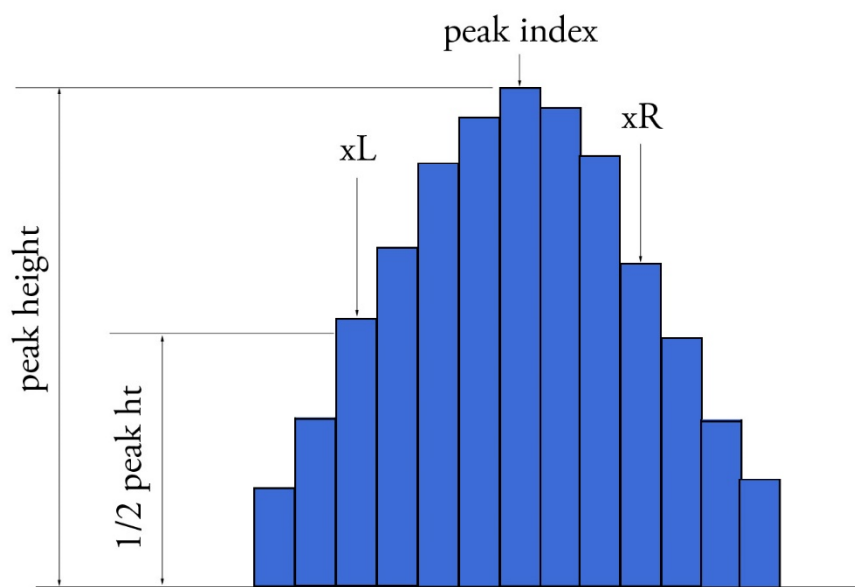
2913 At initialization, first and last histogram values are treated as follows:

2914 If first bin of histogram (peak = 1), set left = 1 and xL = 1.

2915 If last bin of histogram, set right =  $m$  and xR =  $m$ , where  $m$  is the final index of the  
2916 histogram.

2917 Next, a search is made to the left of the peak for a nearby value that is smaller than  
2918 the peak value, but larger than half of the peak value. A while-loop does this, with  
2919 the following conditions: (a) left > 0, (b) histogram value at left is  $\geq$  half of histo  
2920 value at peak and (c) histo value at left is  $\leq$  histo value at peak. When these  
2921 conditions are all true, then xL is set to left and left is decremented by 1, so that the  
2922 test can be made again. When the conditions are no longer met (i.e., we've moved to  
2923 a bin in the histogram where the value drops below half of the peak value), then the  
2924 program breaks out of the while loop.

2925 This is followed by a similar search made upon values to the right of the peak. When  
2926 these two while-loops are complete, we then have the index numbers from the  
2927 histogram representing bins that are above half the peak value. This is shown in  
2928 Figure A.2.



2929

2930 **Figure A.2.** Schematic representation of a histogram showing xL and xR parameters  
2931 determined by the function peakWidth\_dragann.

2932 A test is made to determine which of these is furthest from the middle of the peak. In  
2933 Figure A.2, xL is furthest away and the variable x is set to equal xL. The histogram

2934 “height” at  $x$ , which we call  $V_x$ , is used (as well as  $x$ ) in an inversion of Equation A.2  
2935 to solve for  $c$ :

$$2936 \quad c = \sqrt{\frac{-(x-b)^2}{2\ln\left(\frac{V_x}{a}\right)}} \quad (\text{A.4})$$

2937 The function, `peakWidth_dragann`, now returns the value of  $c$  and control returns to  
2938 the function, `mainGaussian_dragann`.

2939 The `mainGaussian_dragann` function then picks-up with a test on whether the  
2940 returned value of  $c$  is zero. If so, then use a value of 4, which is based on an *a priori*  
2941 understanding that  $c$  usually falls between 4 and 6. If the value of  $c$  is not zero, then  
2942 add 0.5 to  $c$ .

2943 At this point, we have the  $[a,b,c]$  values of the Gaussian for the  $n^{\text{th}}$  peak. Based on  
2944 these values, the Gaussian curve is computed (via Equation A.2) and it is removed  
2945 (subtracted) from the current histogram (and put into a new variable called  
2946 `newWave`).

2947 After a Gaussian curve is removed from the current histogram, the following peak  
2948 width calculations could potentially have a  $V_x$  value less than 1 from  $a$ . This would  
2949 cause the width,  $c$ , to be calculated as unrealistically large. Therefore, a check is put  
2950 in place to determine if  $a - V_x < 1$ . If so,  $V_x$  is set to a value of  $a - 1$ .

### 2951 *Numeric Optimization Steps*

2952 The first of the optimization steps utilizes a Full Width Half Max (*FWHM*) approach,  
2953 computed via

$$2954 \quad FWHM = 2c\sqrt{2\ln 2} \quad (\text{A.5})$$

2955 A left range,  $L_r$ , is computed by  $L_r = \text{round}(b - FWHM/2)$ . This tested to make sure it  
2956 doesn't go off the left edge of the histogram. If so, then it is set to 1.

2957 Similarly, a right range,  $R_r$ , is computed by  $R_r = \text{round}(b + FWHM/2)$ . This is also tested  
2958 to be sure that it doesn't go off the right edge of the histogram. If so, then it is set to  
2959 the index value for the right-most edge of the histogram.

2960 Using these new range values, create a temporary segment (between  $L_r$  and  $R_r$ ) of  
2961 the `newWave` histogram, this is called `errorWave`. Also, set three delta parameters  
2962 for further optimization:

2963  $\Delta C = 0.05;$        $\Delta B = 0.02;$        $\Delta A = 1$

2964 The temporary segment, `errorWave` is passed to the function `checkFit_dragann`,  
2965 along with a set of zero values having the same number of elements as `errorWave`,  
2966 the result, at this point, is saved into a variable called `oldError`. The function,  
2967 `checkFit_dragann`, computes the sum of the squares of the difference between two

2968 histogram segments (in this case, errorWave and zeros with the same number of  
2969 elements as errorWave). Hence, the result, oldError, is the sum of the squares of the  
2970 values of errorWave. This function is applied in optimization loops, to refine the  
2971 values of  $b$  and  $c$ , described below.

2972 *Optimization of the  $b$ -parameter.* The do-loop operates at a maximum of 1000 times.  
2973 It's purpose is to refine the value of  $b$ , in 0.02 increments. It increments the value of  
2974  $b$  by DeltaB, to the right, and computes a new Gaussian curve based on  $b+\Delta b$ , which  
2975 is then removed from the histogram with the result going into the variable  
2976 newWave. As before, checkFit\_dragann is called by passing the range-limited part of  
2977 newWave (errorWave) and returning a new estimate of the error (newError) which  
2978 is then checked against oldError to determine which is smaller. If newError is  $\geq$   
2979 oldError, then the value of  $b$  that produced oldError is retained, and the testing loop  
2980 is exited.

2981 *Optimization of the  $c$ -parameter.* Now the value of  $c$  is optimized, first to the left,  
2982 then to the right. It is performed independently of, but similarly, to the  $b$ -parameter,  
2983 using do-loops with a maximum of 1000 passes. These loops increment (to right) or  
2984 decrement (to left) by a value of 0.05 (DeltaC) and use checkFit\_dragann to, again,  
2985 check the quality of the fit. The loops (right and left) kick-out when the fit is found to  
2986 be smallest.

2987 The final, optimized Gaussian curve is now removed (subtracted) from the  
2988 histogram. After removal, a statement "corrects" any histogram values that may  
2989 drop below zero, by setting them to zero. This could happen due to any mis-fit of the  
2990 Gaussian.

2991 The  $n^{\text{th}}$  loop is concluded by examining the peaks remaining in the histogram  
2992 without the peak just processed by sending the  $n^{\text{th}}$ -residual histogram back into the  
2993 function findpeaks\_dragann. If the return of peak index numbers from  
2994 findpeaks\_dragann reveals more than 1 peak remaining, then the index numbers for  
2995 peaks that meet these three criteria are retained in an array variable called these:

- 2996 1. The peak must be located above  $b(n)-2*c(n)$ , and
- 2997 2. The peak must be located below  $b(n)+2*c(n)$ , and
- 2998 3. The height of the peak must be  $< a(n)/5$ .

2999

3000 The peaks meeting all three of these criteria are to be eliminated from further  
3001 consideration. What this accomplishes is eliminate the nearby peaks that have a size  
3002 lower than the peak just previously analyzed; thus, after their elimination, only  
3003 leaving peaks that are further away from the peak just processed and are  
3004 presumably "real" peaks. The  $n^{\text{th}}$  iteration ends here, and processing begins with the  
3005 revised histogram (after having removed the peak just analyzed).

3006

## 3007 **Gaussian Rejection**

3008 The function `mainGaussian_dragann` returns the  $[a,b,c]$  parameters for the ten  
3009 highest peaks from the original histogram. The remaining code in `dragann` examines  
3010 each of the ten Gaussian peaks and eliminates the ones that fail to meet a variety of  
3011 conditions. This section details how this is accomplished.

3012 First, an approximate area,  $area1=a*c$ , is computed for each found peak and  $b$ , for all  
3013 ten peaks, being the index of the peaks, are converted to an actual value via  
3014  $b+\min(\text{numptsinrad})-1$  (call this  $allb$ ).

3015 Next, a rejection is made for all peaks that have any component of  $[a,b,c]$  that are  
3016 imaginary (Matlab `isreal` function is used to confirm that all three components are  
3017 real, in which case it passes).

3018 To check for a narrow noise peak at the beginning of the histogram in cases of low  
3019 noise rates, such as during nighttime passes, a check is made to first determine if the  
3020 highest Gaussian amplitude,  $a$ , within the first 5% of the histogram is  $\geq 1/10 * \text{the}$   
3021 maximum amplitude of all Gaussians. If so, that peak's Gaussian width,  $c$ , is checked  
3022 to determine if it is  $\leq 4$  bins. If neither of those conditions are met in the first 5%,  
3023 the conditions are rechecked for the first 10% of the histogram. This process is  
3024 repeated up to 30% of the histogram, in 5% intervals. Once a narrow noise peak is  
3025 found, the process breaks out of the incremental 5% histogram checks, and the  
3026 noise peak values are returned as  $[a0, b0, c0]$ .

3027 If a narrow noise peak was found, the remaining peak area values,  $area1 (a*c)$ , then  
3028 pass through a descending sort; if no narrow noise peak was found, all peak areas go  
3029 through the descending sort. So now, the  $[a,allb,c]$ -values are sorted from largest  
3030 "area" to smallest, these are placed in arrays  $[a1, b1, c1]$ . If a narrow noise peak was  
3031 found, it is then appended to the beginning of the  $[a1, b1, c1]$  arrays, such that  $a1 =$   
3032  $[a0 a1]$ ,  $b1 = [b0 b1]$ ,  $c1 = [c0 c1]$ .

3033 In the case that a narrow noise peak was not found, a test is made to check that at  
3034 least one of the peaks is within the first 10% of the whole histogram. It is done  
3035 inside a loop that works from peak 1 to the number of peaks left at this point. This  
3036 loop first tests whether the first (sorted) peak is within the first 10% of the  
3037 histogram; if so, then it simply kicks out of the loop. If not, then it places the loop's  
3038 current peak into a holder (`ihold`) variable, increments the loop to the next peak and  
3039 runs the same test on the second peak, etc. Here's a Matlab code snippet:

```
3040     inds = 1:length(a1);  
3041     for i = 1:length(b1)  
3042         if b1(i) <= min(numptsinrad) + 1/10*max(numptsinrad)  
3043             if i==1  
3044                 break;  
3045             end  
3046             ihold = inds(i);  
3047             for j = i:-1:2  
3048                 inds(j) = inds(j-1);  
3049             end  
3050             inds(1) = ihold;
```



```

3051         break
3052     end
3053 end
3054

```

3055 The j-loop expression gives the `init_val:step_val:final_val`. The semi-colon at the end  
3056 of statements causes Matlab to execute the expression without printout to the user's  
3057 screen. When this loop is complete, then the indexes (`inds`) are re-ordered and  
3058 placed back into the `[a1,b1,c1]` and `area1` arrays.

3059 Next, are tests to reject any Gaussian peak that is entirely encompassed by another  
3060 peak. A Matlab code snippet helps to describe the processing.

```

3061 % reject any gaussian if it is fully contained within another
3062 isR = true(1,length(a1));
3063 for i = 1:length(a1)
3064     ai = a1(i);
3065     bi = b1(i);
3066     ci = c1(i);
3067     aset = (1-(c1/ci).^2);
3068     bset = ((c1/ci).^2*2*bi - 2*b1);
3069     cset = -(2*c1.^2.*log(a1/ai)-b1.^2+(c1/ci).^2*bi^2);
3070     realset = (bset.^2 - 4*aset.*cset >= 0) | (a1 > ai);
3071     isR = isR & realset;
3072 end
3073 a2 = a1(isR);
3074 b2 = b1(isR);
3075 c2 = c1(isR);
3076

```

3077 The logical array `isR` is initialized to all be true. The i-do-loop will run through all  
3078 peaks. The computations are done in array form with the variables `aset,bset,cset` all  
3079 being arrays of `length(a1)`. At the bottom of the loop, `isR` remains "true" when  
3080 either of the conditions in the expression for `realset` is met (the single "|" is a logical  
3081 "or"). Also, the nomenclature, "." and ".", denote element-by-element array  
3082 operations (not matrix operations). Upon exiting the i-loop, the array variables  
3083 `[a2,b2,c2]` are set to the `[a1,b1,c1]` that remain as "true." [At this point, in our test  
3084 case from channel 43 of East-AK Mable flight on 20140730 @ 20:16, six peaks are  
3085 still retained: 18, 433, 252, 33, 44.4 and 54.]

3086 Next, reject Gaussian peaks whose centers lay within  $3\sigma$  of another peak, unless only  
3087 two peaks remain. The code snippet looks like this:

```

3088 isR = true(1, length(a2));
3089 for i = 1:length(a2)
3090     ai = a2(i);
3091     bi = b2(i);
3092     ci = c2(i);
3093     realset = (b2 > bi+3*ci | b2 < bi-3*ci | b2 == bi);
3094     realset = realset | a2 > ai;
3095     isR = isR & realset;
3096 end
3097 if length(a2) == 2
3098     isR = true(1, 2);
3099 end
3100 a3 = a2(isR);

```

```
3101     b3 = b2(isR);  
3102     c3 = c2(isR);  
3103
```

3104 Once again, the isR array is initially set to “true.” Now, the array, realset, is tested  
3105 twice. In the first line, one of three conditions must be true. In the second line, if  
3106 realset is true or  $a2 > ai$ , then it remains true. At this point, we’ve pared down, from  
3107 ten Gaussian peaks, to two Gaussian peaks; one represents the noise part of the  
3108 histogram; the other represents the signal part.

3109 If there are less than two peaks left, a thresholding/histogram error message is  
3110 printed out. If the lastTryFlag is not set, DRAGANN ends its processing and an empty  
3111 IDX value is returned. The lastTryFlag is set in the preprocessing function which  
3112 calls DRAGANN, as multiple DRAGANN runs may be tried until sufficient signal is  
3113 found.

3114 If there are two peaks left, then set the array [a,b,c] to those two peaks. [At this  
3115 point, in our test case from channel 43 of East-AK Mable flight on 20140730 @  
3116 20:16, the two peaks are: 18 and 433.]

3117

### 3118 **Gaussian Thresholding**

3119 With the two Gaussian peaks identified as noise and signal, all that is left is to  
3120 compute the threshold value between the Gaussians.

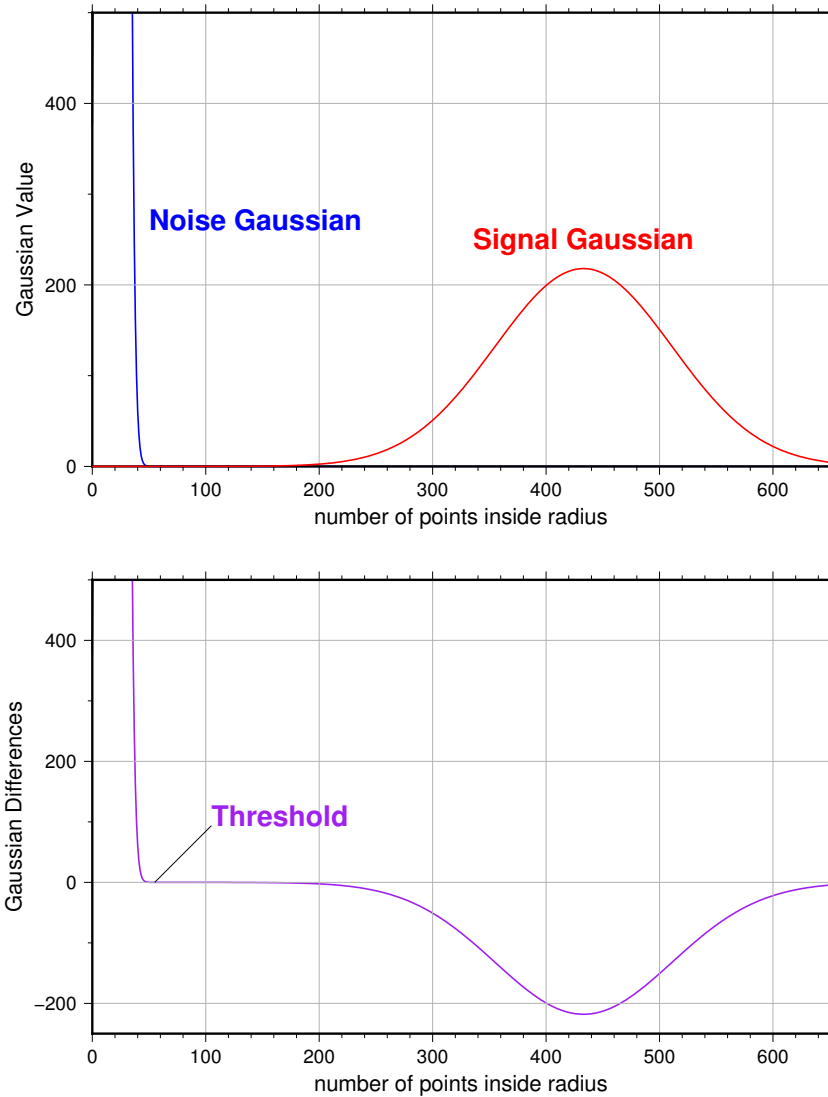
3121 An array of xvals is established running from  $\min(\text{numptsinrad})$  to  
3122  $\max(\text{numptsinrad})$ . In our example, xvals has indices between 0 and 653. For each  
3123 of these xvals, Gaussian curves (allGauss) are computed for the two Gaussian peaks  
3124 [a,b,c] determined at the end of the previous section. This computation is performed  
3125 via a function called gaussmaker which receives, as input, the xvals array and the  
3126 [a,b,c] parameters for the two Gaussian curves. An array of heights of the Gaussian  
3127 curves is returned by the function, computed with Equation A.2. In Matlab, the  
3128 allGauss array has dimension  $2 \times 654$ . An array, noiseGauss is set to be equal to the  
3129 1<sup>st</sup> column of allGauss.

3130 An if-statement checks whether the b array has more than 1 element (i.e., consisting  
3131 of two peaks), if so, then nextGauss is set to the 2<sup>nd</sup> column of allGauss, and a  
3132 difference, noiseGauss-nextGauss, is computed.

3133 The following steps are restricted to be between the two main peaks. First, the first  
3134 index of the absolute value of the difference that is near-zero (defined as  $1e-8$ ) is  
3135 found, if it exists, and put into the variable diffNearZero. This is expected to be found  
3136 if the two Gaussians are far away from each other in the histogram.

3137 Second, the point (i.e., index) is found of the minimum of the absolute value of the  
3138 difference; this index is put into variable, signchanges. This point is where the sign  
3139 changes from positive to negative as one moves left-to-right, up the Gaussian curve

3140 differences (noise minus next will be positive under the peak of the noise curve, and  
 3141 negative under the next (signal) curve). Figure A.3 (top) shows the two Gaussian  
 3142 curves. The bottom plot shows their differences.



3143

3144 **Figure A.3.** Top: two remaining Gaussian curves representing the noise (blue) and  
 3145 signal (red) portions of the histogram in F1gure A.1. Bottom: difference noise -  
 3146 signal of the two Gaussian curves. The threshold is defined as the point where the  
 3147 sign of the differences change.

3148 If there is any value stored in `diffNearZero`, that value is now saved into the variable  
 3149 `threshNN`. Else, the value of the threshold in `signchanges` is saved into `threshNN`,  
 3150 concluding the if-statement for `b` having more than 1 element.

3151 An else clause ( $b \neq 1$ ), merely sets threshNN to  $b+c$ , i.e., 1-standard deviation away  
3152 from mean of the (presumably) noise peak.

3153 The final step is mask the signal part of the histogram where all indices above the  
3154 threshNN index are set to logical 1 (true). This is applied to the numptsinrad array,  
3155 which represents the photon cloud. After application, dragann returns the cloud  
3156 with points in the cloud identified as “signal” points.

3157 The Matlab code has a few debug statements that follow, along with about 40 lines  
3158 for plotting.

3159

### 3160 **References**

3161 Goshtasby, A & W. D. O’Neill, Curve Fitting by a Sum of Gaussians, *CVGIP: Graphical*  
3162 *Models and Image Processing*, V. 56, No. 4, 281-288, 1994.